Titre: Title:	Dynamic Modeling and Intermittent Operation of a Flow-Through Microbial Electrolysis Cell
Auteur: Author:	Syed Azfar Hussain
Date:	2018
Type:	Mémoire ou thèse / Dissertation or Thesis
Référence: Citation:	Hussain, S. A. (2018). Dynamic Modeling and Intermittent Operation of a Flow-Through Microbial Electrolysis Cell [Thèse de doctorat, École Polytechnique de Montréal]. PolyPublie. https://publications.polymtl.ca/3168/

UNIVERSITÉ DE MONTRÉAL

DYNAMIC MODELING AND INTERMITTENT OPERATION OF A FLOW-THROUGH MICROBIAL ELECTROLYSIS CELL

SYED AZFAR HUSSAIN

DÉPARTEMENT DE GÉNIE CHIMIQUE

ÉCOLE POLYTECHNIQUE DE MONTRÉAL

THÈSE PRÉSENTÉE EN VUE DE L'OBTENTION

DU DIPLÔME DE PHILOSOPHIAE DOCTOR

(GÉNIE CHIMIQUE)

JUIN 2018

UNIVERSITÉ DE MONTRÉAL

ÉCOLE POLYTECHNIQUE DE MONTRÉAL

Cette thèse intitulée :

DYNAMIC MODELING AND INTERMITTENT OPERATION OF A FLOW-THROUGH MICROBIAL ELECTROLYSIS CELL

présentée par : HUSSAIN Syed Azfar

en vue de l'obtention du diplôme de : Philosophiae Doctor

a été dûment acceptée par le jury d'examen constitué de :

M. HENRY Olivier, Ph. D., président

M. PERRIER Michel, Ph. D., membre et directeur de recherche

M. TARTAKOVSKY Boris, Ph. D., membre et codirecteur de recherche

M. SRINIVASAN Bala, Ph. D., membre

M. BUDMAN Hector, Ph. D., membre externe

DEDICATION

This thesis is dedicated to

My mother, Dr. Nuzhat Zaidi, my wife Dr. Anny Fatima and my best friend & brother Mr. Jack Lasry.

ACKNOWLEDGEMENTS

I am extremely grateful to my Ph.D supervisors, Dr. Michel Perrier and Dr. Boris Tartakovsky. I have learnt a lot during my Ph.D studies. I am thankful to Michel for his able guidance throughout my studies. I also want to express my deep gratitude to Boris, for always being there to answer my questions and to motivate me.

I would also like to thank my colleagues at National Research Council, Didac, Jerome, Javier, Michelle, Fred and Fréderique for always being there to help me in the laboratory work and in computer programing.

It has been a beautiful journey and I have a lot of good memories to cherish throughout my life.

Thank you.

RÉSUMÉ

La pile microbienne électrolytique (MEC) représente une nouvelle technologie qui peut être appliquée pour le traitement des eaux usées combiné avec la production d'hydrogène ou de biogaz. La MEC est un dispositif bioélectrochimique, qui contient une anode et une cathode connectées à une alimentation externe. La modélisation dynamique et l'optimisation de réacteurs basés sur une MEC représentent plusieurs défis.

Cette thèse commence par la présentation de la MEC de type « circuit équivalent électrique » (EEC), qui fournit un outil pour la surveillance en temps réel et permet l'estimation des paramètres de la MEC. Lors du traitement des eaux usées, une surveillance en continue des MEC est essentielle pour assurer des performances adéquates, et à cet égard, le modèle EEC le permet. Le modèle EEC de base implique deux résistances (R_0 décrivant les pertes ohmiques et R_1 les pertes d'activation) connectées en série avec la force électromotrice interne (FEI). De plus, la croissance du biofilm est représentée par la capacitance (C) connectée en parallèle avec R_1. Ses paramètres électriques internes peuvent être estimés numériquement en minimisant la différence entre le courant théorique et mesuré de la MEC. De plus, les mêmes paramètres peuvent être estimés en utilisant une solution analytique du modèle EEC. Dans ce cas, la MEC doit être utilisée pendant une courte période (par exemple 1 à 2 minutes) avec une connexion intermittente de l'alimentation électrique. Une telle connexion est effectuée à des fréquences hautes et basses pour estimer R_0 (à haute fréquence) et R_1 et C (à basse fréquence). De plus, la FEI est estimée par la MEC dans des conditions de circuit ouvert. Pour démontrer l'approche proposée, des expériences ont été effectuées avec plusieurs concentrations de sources de carbone entrantes. Les paramètres électriques internes de la MEC ont été estimés à des intervalles de 6h. Le modèle EEC a permis de décrire avec succès la dynamique électrique de la MEC et de suivre les changements des paramètres électriques. Grâce à la simplicité du modèle, il peut être utilisé pour développer un système de surveillance et de diagnostic des MEC en temps réel. Un tel système de suivi en continu pourrait être essentiel au bon fonctionnement des systèmes de traitement des eaux usées à grande échelle basés sur les MEC. Les paramètres du modèle EEC fournissent un aperçu des performances des MEC soumises à diverses perturbations en temps réel. Cette thèse présente des résultats pour la surveillance en temps réel de MEC avec différentes concentrations influentes.

Avec l'augmentation de la concentration de l'influent, il y a une diminution subséquente de la résistance interne de la MEC et une augmentation de la C interne.

La thèse explique également en détail les performances à long terme de MEC sous connexion intermittente de l'alimentation électrique (mode marche/arrêt). Cette étude décrit une nouvelle approche pour atteindre une performance stable à long terme et maximiser l'élimination de la demande chimique en oxygène (DCO) dans une MEC. Dans l'approche proposée, la tension appliquée sur la MEC est périodiquement déconnectée, par exemple à une fréquence de 0,1 à 0,5 Hz et un rapport cyclique de 90 à 95%. Pour évaluer l'impact d'une telle intermittence de tension sur les performances de la MEC, des expériences ont été réalisées avec deux MEC à écoulement continu avec des électrodes de charbon activé granulaire. La stratégie d'exploitation d'une connexion intermittente a été appliquée à une MEC, tandis que l'autre a fonctionné à une tension fixe (MEC de contrôle). Un fonctionnement intermittent à long terme a entraîné une augmentation progressive de l'efficacité d'élimination de la DCO et du courant de la MEC avec le temps, tandis que la MEC de contrôle a montré des performances inférieures. De plus, en changeant la stratégie d'exploitation et en appliquant une connexion intermittente à la MEC de contrôle, ses performances ont été considérablement améliorées. L'amélioration des performances pendant la phase intermittente a été confirmée par la surveillance en continu de la résistance interne et de la C des MEC. Le mode de fonctionnement intermittent proposé peut être utilisé pour développer un système de traitement des eaux usées à haut débit basé sur les MEC.

Un modèle bioélectrochimique dynamique d'une MEC, dont les compartiments anodiques et cathodiques sont connectés en série, est également présenté dans cette thèse. Le modèle peut être utilisé pour estimer le courant circulant dans la MEC et la concentration du substrat de l'effluent. Les paramètres du modèle sont obtenus par une procédure d'estimation des paramètres numériques. Les résultats de la simulation correspondent assez bien aux données expérimentales. La thèse comprend également un modèle de biofilm une dimension (1D), qui décrit les changements de distribution de la source de carbone dans le biofilm électrochimiquement actif à l'anode. Le modèle est capable de prédire le courant obtenu dans une MEC ayant une tension intermittente.

ABSTRACT

Microbial electrolysis cell (MEC) represents a novel technology that can be applied for wastewater treatment combined with hydrogen or biogas production. MEC is a bioelectrochemical device, which houses anode and cathode connected to an external power supply. Dynamic modeling and optimization of a MEC-based reactor faces several challenges.

This thesis starts from presenting an equivalent electrical circuit (EEC) model of MEC, which provides a tool for online monitoring and parameter estimation of MEC. When treating wastewaters, continuous MEC monitoring is essential to ensure adequate performance, with this regard, the electrical equivalent circuit (EEC) model enables on-line parameter estimation and monitoring of a continuous flow MEC. Such simple EEC model involves two resistances (describing ohmic losses, R_0, and activation losses, R_1) connected in series with internal electromotive force (EMF). Also, biofilm growth is represented by capacitance (C) connected in parallel with R_1. These internal electrical parameters can be estimated numerically by minimizing the difference between the measured and predicted MEC current. Also, the same parameters can be estimated using an analytical solution of the EEC model. In this case, the MEC needs to be operated for a short time (e.g. 1-2 min) with intermittent connection to the power supply. Such intermittent connection is performed at high and low frequencies to estimate R_0 (at high frequency) and R_1 and C (at low frequency). Also, EMF is estimated by MEC under open circuit conditions. To demonstrate the proposed approach, experiments were carried out at several influent carbon source concentrations. MEC internal electrical parameters were estimated at 6h intervals. The EEC model successfully described electrical dynamics of the MEC and tracked changes in electrical parameters. Owing to the model simplicity, it can be used to develop a real-time MEC monitoring and diagnostics system. Such an on-line tracking system might be essential for successful operation of large scale MEC-based wastewater treatment systems. EEC model parameters provide an insight of MEC performance subjected to various perturbations in real time. This thesis presents results for online monitoring of MEC with different strength of influent concentrations. With the increase in influent concentration there is a subsequent decrease in internal resistance of MEC and increase in internal capacitance.

Furthermore, the thesis also explains in detail long term performance of MEC under intermittent connection/disconnection of power supply. This study describes a new approach for achieving stable long-term performance and maximizing removal of chemical oxygen demand (COD) in a Microbial Electrolysis Cell (MEC). In the proposed approach, the MEC applied voltage is periodically disconnected, e.g. at a frequency of 0.1 – 0.5 Hz and a duty cycle of 90-95%. To evaluate the impact of such periodic voltage disconnection (on/off mode) on MEC performance, experiments were carried out in two flow-through MECs with activated granular carbon electrodes. The on/off operating strategy was applied to one MEC, while the other one was operated at a fixed voltage (control MEC). Long-term on/off operation resulted in progressive increase in COD removal efficiency and MEC current over time, while the control MEC showed inferior performance. Furthermore, by changing the operating strategies and applying the on/off strategy to the control MEC, its performance was significantly improved. Performance improvement during on/off operation was confirmed by on-line monitoring of MFC internal resistance and capacitance. The proposed on/off mode of operation can be used to develop a high-rate MEC-based wastewater treatment system.

Dynamic bioelectrochemical model of MEC, which considers anodic and cathodic compartments connected in series, is also presented in this thesis. The model can be used to estimate current flowing through the MEC and effluent substrate concentration. Model parameters are estimated by numerical parameter estimation procedure. The simulation results provide a fairly good fit with the experimental data. Thesis also includes 1D biofilm model, which describes changes in carbon source distribution in the electrochemically active biofilm at anode under on/off operation of power supply. The model is able to predict current flowing through the MEC with periodic applied voltage.

TABLE OF CONTENTS

LIST OF TABLES

LIST OF FIGURES

LIST OF SYMBOLS AND ABBREVIATIONS

The list of symbols and abbreviations used in this thesis are presented below.

AD	Anaerobic digestion
ADM1	Anaerobic digester model 1
CCe	Cathodic columbic efficiency
COD	Chemical oxygen demand
D	Duty cycle
ECE	Electrical conversion efficiency
ECF	Electro counter force
EEC	Equivalent electrical circuit
EMF	Electromotive force
HRT	Hydraulic retention time
IWA	International water association
MFC	Microbial fuel cell
MEC	Microbial electrolysis cell
MPPT	Maximum power point tracking
MRT	Minimum resistance tracking
OCV	Open circuit voltage
OLR	Organic load rate
PEM-FC	Proton exchange membrane fuel cell
P/O	Perturbation Observation
sCOD	Soluble oxygen demand
SM	Synthetic medium
WW	Wastewater

LIST OF APPENDICES

CHAPTER 1 INTRODUCTION

Microbial Electrochemical Cell (MEC) represents a novel technology, which can be used for wastewater treatment and hydrogen or biogas (mostly methane) production. External electrical energy is provided to MEC in order to facilitate the electron transfer from anode to a cathode lacking oxygen.

MEC is a bioelectrochemical device, which oxidizes organic materials by utilizing an anode as a terminal electron acceptor and combines electrons and protons at the cathode to produce hydrogen or methane. Wastewater treatment in a MEC results in a net energy production as opposed to an energy consumption, which is the case in conventional aerobic (activated sludge) treatment systems. Unlike conventional anaerobic reactors, MEC can be used for treating wastewaters with low organic content, e.g. domestic wastewater.

Motivation

MECs can be seen as an extension of the anaerobic digestion (AD) technology. As mentioned above, a MEC degrades organic materials at one electrode (anode) with the production of hydrogen or methane at another electrode (cathode) if external electrical supply is provided to overcome thermodynamic limitations of this bioelectrochemical process. MEC can be used to treat wastewater as well as to produce biofuel (H_2 or CH_4) or even valuable chemical products. Unlike conventional anaerobic reactors, the flow-through MEC can be used for treating wastewaters with low organic content, e.g. domestic wastewater. Methanogenic microorganisms have low affinity to a carbon source. accordingly, anaerobic reactors require a wastewater concentration of at least 2 g/L for successful operation. electroactive (anodophilic) bacteria were shown to exhibit higher affinity to the carbon source as compared to the methanogens (Pinto et al. 2010). Anaerobic treatment needs an additional aerobic reactor to further reduce the effluent concentration to satisfy discharge norms (aerobic polishing), while MEC – based systems were shown to achieve low effluent chemical oxygen demand (COD) concentrations (Clauwaert et al. 2009). Since aerobic treatment requires significant amounts of electricity, anaerobic treatment followed by aerobic polishing is much less energy efficient than the MEC treatment, which combines both treatment steps and produces biogas. In addition, methane percentage in an

anaerbic digester off-gas is around 50-60% whereas in MEC it is 80-85% (Amro et al. 2017). While several existing studies demonstrated MECs application for wastewater treatment, there are very few attempts to model or control MEC-based systems .

Problem definition

The research related to modeling dynamics of MECs is still at the very beginning. Currently published works focus on the reactor sizing and the design of electrodes with different shapes, size and material of construction. MEC performance was studied by minimizing the ohmic resistance by different arrangements of anode in the cell (Liang et al. 2011). External voltage is applied in MEC to overcome the thermodynamic barrier for the transfer of electrons from anode to cathode. Performance of MEC in terms of biogas production and soluble chemical oxygen demand removal was studied under different applied voltages (Linji et al. 2013). In a similar study, optimum methane production was analyzed by operating MEC under different applied voltage conditions (Ding et al. 2016). In a different approach, sulfate removal efficiency in a MEC was studied with variable current applied to the reactor (Kia et al. 2017). Hydrogen production in MEC was studied at different concentrations of influent carbon source (Tartakovsky et al. 2012). Recently it has been demonstrated that the volumetric production of hydrogen has increased and expensive Pt-based cathode material in Proton Exchange Membrane (PEM) designs can be replaced with membraneless MECs with non-noble Me catalysts such as Ni, stainless steel, or tungsten carbide (Chae et al. 2008). These improvements have made the scale-up of MECs more realistic and pragmatic.

However, in order to maximize the MECs performance the behaviour of different electrical variables should be studied. In particular, intermittent connection/disconnection of the power supply to MEC has not been studied yet. The electrical equivalent circuit (EEC) model could help in understanding of different electrical variables. Also, it offers some insight on the fast dynamics linked to the electrical properties of MEC.

It is very important to study the fast dynamics of the system. By operating MEC under high power supply switching frequency, it might be possible to unveil internal parameters. It is also possible to expect that the efficiency of MEC could be improved. Such MEC tests were never performed. Recently, microbial fuel cells (MFCs) have been operated with pulse width

modulation of the external resistance connection. Significant positive effect on MFC power output was observed. By applying this approach to MEC, it might be possible to achieve similar improvements to the MEC performance.

Equivalent circuit model lacks the predictive capacity of bio-electrochemical models such as recently developed two-population bio-electrochemical MEC model. At the same time the bio-electrochemical models have the ability to predict the influence of various process inputs such as organic loading rate on MEC performance. Several recent studies demonstrated significant charge storage in electrochemical biofilms (Coronado et al 2012). Aiming to evaluate the impact of charge storage on MEC performance, the goal of this study is to couple the bio-electrochemical and electrical models and to develop a model suitable for practical applications, which require description of both fast and slow dynamics of MECs. The understanding of MEC dynamics is at its initial stages. In particular, fast electrical dynamics is not well understood and an electrical equivalent circuit has not been developed for MECs. There is no understanding about the effect of fast dynamics on MEC performance. And last but not the least, the dynamic model of MEC for reactor configuration in which the anodic and cathodic compartments connected in series has not been developed yet.

Objectives

The general objective of this thesis is to study the dynamic behavior and long term performance of MEC under intermittent connection/disconnection of the power supply.

Furthermore, dynamic modeling and online monitoring strategies of MEC are developed. The specific objectives are as indicated below:

1. Develop an Electrical equivalent circuit (EEC) model of a MEC and a procedure for online estimation of the model parameters.

2. Develop online monitoring strategies to monitor internal parameters of MEC under the influence of external disturbances.

3. Qualitatively study the long term effect of on/off operation of the power supply on MEC performance in terms of current, and chemical oxidation demand (COD) removal efficiency.

4. Develop one dimensional biofilm model of MEC, capable of describing the effect of on/off operation (variable duty cycles and cycle lengths) on MEC performance (in terms of current).

5. Present a global bioelectrochemical model of MEC with the anodic and cathodic compartments connected in series to estimate the current flowing through the MEC and effluent COD concentration.

Thesis structure

This document is divided into four main chapters. Chapter 1 presents thorough literature review related to the characterization and optimization of MEC, monitoring and optimal control of MEC biofilm modeling and dynamic models of bioelectrochemical system. Chapter 2 describes the EEC model development of MEC and procedure to estimate the model parameters. This chapter also explains the online monitoring procedure of MEC under different influent acetate feed perturbations. Chapter 3 presents the long term performance of MEC under intermittent connection of power supply. The performance of MEC is analyzed in terms of current flowing through the MEC and chemical oxidation demand (COD) removal from the influent carbon source. Chapter 4 consists of two parts, (i) presents global bioelectrochemical model of MEC. The model can be used to estimate the current flowing through the MEC and effluent concentration. The model is developed by assuming anodic and cathodic compartments of MEC connected in series. Model parameter are also estimated by comparing the model outputs and experimental results, and (ii) 1-D biofilm model of MEC. The model describes the effect of on/off operation of power supply on different model parameters across the biofilm depth.

Experimental setup, MEC design and operation, material and methods, and numerical calculations are presented separately in the chapters 2, 3 and 4.

CHAPTER 2 LITERATURE REVIEW

This chapter covers the two main aspects of the study. Firstly, approaches to performance characterization as well as optimization of MFC and MECs are reviewed. Secondly, a critical review concerning the existing models of MFCs, MECs, and biofilm systems is presented. The review includes bioectrochemial models as well as electrical equivalent circuit model recently developed for MFC monitoring. The similarities between MFCs and MECs are highlighted to justify the development of a similar MEC model for enhanced real-time process monitoring.

As far as reactor architecture is concerned, a typical MEC consists of two electrodes. The anodic compartment houses an electrode covered in a biofilm colonized by electricigenic bacteria able to release electrons and protons from the oxidation of organic matter. Because of the presence of electrical potential difference, the resulting electrons are transferred to the anode surface and then to the cathode. Simultaneously, protons migrate to the cathode in the liquid phase and are combined with the electrons at the surface of cathode A typical reaction occurring at the cathode of MEC is the production of hydrogen. However, carbon dioxide, which is also released at the anode, can be transported to the cathode. This leads to a bioreaction in which methane is formed. In fact, there are two pathways, by which methane can be produced in a MEC. In one pathway, acetate produced by the decomposition of organic wastes is converted into carbon dioxide, protons and electrons at the anode as represented by following equation (Logan et al. 2006).

$$CH_3COOH + 2H_2O \rightarrow 2CO_2 + 8H^+ + 8e^- \quad (1.1)$$

At the cathode, hydrogen is produced by the direct electron transfer as follows (Logan et al. 2006).

$$2H^+ + 2e^- \rightarrow H_2 \quad (1.2)$$

The hydrogenophilic methanogens combine hydrogen with carbon dioxide to release methane as described by the following reaction.

$$4H_2 + CO_2 \rightarrow CH_4 + 2H_2O \quad (1.3)$$

In the second pathway, protons and electrons are also produced at the anode according to the first equation, then methane is generated at the cathode by direct extracellular microbially catalyzed transfer of electrons where carbon dioxide reacts with electrons and protons to form methane. This reaction is not feasible without the catalyst because it requires energy to overcome the thermodynamic barrier, but presence of microorganisms can catalyze the reaction as given below.

$$CO_2 + 8e^- + 8H^+ \rightarrow CH_4 + 2H_2O \quad (1.4)$$

Recent advancements of MEC systems also demonstrated production of hydrogen peroxide and iso-butanol at the cathode (Rabaey et al. 2010).

2.1 Characterization and optimization

MECs present a technical challenge since their dynamics and internal mechanisms are poorly understood. Hence, dynamic modeling is a useful tool in order to better understand the system. The models of MECs have been prepared by using bio electrochemical tools that benefit from the knowledge of physics, biology and electrochemistry to represent the behavior at long term.

This approach is helpful in understanding the dynamics of the system at long term, but it lacks information on relationship between the electrochemical and electrical variables. Firstly, a critical review of existing biofilm models is presented followed by electrical equivalent circuit model of MFC and finally bio-electrochemical models of microbial cells are explained.

Approaches for Performance Optimization

A suitable technique to increase the efficiency of MEC is to increase the electron transfer from anode to cathode. MFC studies serve as a good example. Several studies have been done to increase the current generation in MFCs by operating with a pulse-width modulation at high frequency (Grondin, et al. 2012). The same principle can be applied to MECs.

2.1.1 Real time Optimization

Recent advancement in MEC research has resolved several limitations that are considered crucial for the development of an industrial MEC based process. For example, it has been demonstrated that the volumetric production of hydrogen can e substantially increased and an expensive Proton Exchange Membrane (PEM) design can be replaced with a membraneless MEC with non-noble

Me catalysts such as Ni, stainless steel, or tungsten carbide (Chae et al. 2008). These improvements have made the scale-up of MECs more realistic and pragmatic.

Also, it was demonstrated by Tartakovsky, Mehta et al. (2011) that the production of hydrogen gas can be maximized by real-time optimization of applied voltage. Real-time control system was found to efficiently track the changes in the operating conditions of a MEC, while keeping the production of H_2 at the maximum achievable level. The applied voltage (U_{app}) was periodically adjusted in order to minimize the apparent resistance (Ra) by using an online minimal resistance tracking (MRT) algorithm similar to the perturbation and observation (P/O) algorithm used previously to maximize the power output of a microbial fuel cell (Woodward, Perrier et al. 2010). Constant amplitude for each change of the applied voltage (ΔU) was pre-set and the direction of the applied voltage was dependent on the sign of the gradient, which is determined by using the finite difference method. The value of internal resistance was estimated at time t_i and it was compared with the pervious estimated value t_{i-1}. The algorithm is mathematically expressed by the following equation:

$$U(i) = U(i-1) + \Delta U \pm \left(\frac{R_{\text{int}}(i-1) - R_{\text{int}}(i-2)}{U(i-1) - U(i-2)} \right) \tag{1.5}$$

where ΔU represents the input perturbation and i is the iteration number. The applied voltage was restricted between the upper and lower bounds to avoid the operation of MECs outside of the bioelectrochemical mode of operation, i.e. above the threshold value of water electrolysis.

$$Umin \ \leq (i) \leq Umax \tag{1.6}$$

It was found that the hydrogen production increases with increase in U_{app} until it reaches a plateau. Simultaneously power consumption also increases with the increase in U_{app}. The multi-criteria optimization was formulated as:

$$\max_{U_{app}} J = \begin{bmatrix} F_{H_2} \\ -P \end{bmatrix} \tag{1.7}$$

where F_{H2} is the flow rate of hydrogen and P is the power consumption. Multi-criteria optimization was minimized to a simpler problem:

$$\min_{U_{app}} R_a$$

T imizing hydrogen production based on R_a minimization was tested by using d OD concentrations and different types of influent wastewater. The tests confirmed the robustness of the proposed algorithm.

Overall, MEC performance can be greatly improved by minimizing the internal resistance. Internal resistance of the MEC can be affected by many factors, including material of construction for anode (Cheng et al. 2007; Liu et al. 2010; Logan et al. 2008), space between the electrodes (Cheng and Logan, 2011), configuration of cathode and the use of catalysts (Call et al., 2009; Hu et al. 2009; Selembo et al., 2009).

2.1.2 Arrangements of electrodes

Another important factor that could influence the performance of MEC by reducing ohmic resistance is electrode arrangement. In one of the arrangements, MEC was constructed by using anode as the graphite felt and cathode as carbon cloth (Liang et al. 2011). Two different arrangements were studied in this work; (i) Two anodes were placed in the reactor on both sides of the cathode and, (ii) Anodes were connected together on the same side of cathode. Figure 1.1 presents arrangements of anode in two MEC (MEC #1 and MEC # 2) in order to minimize the ohmic losses in MEC.

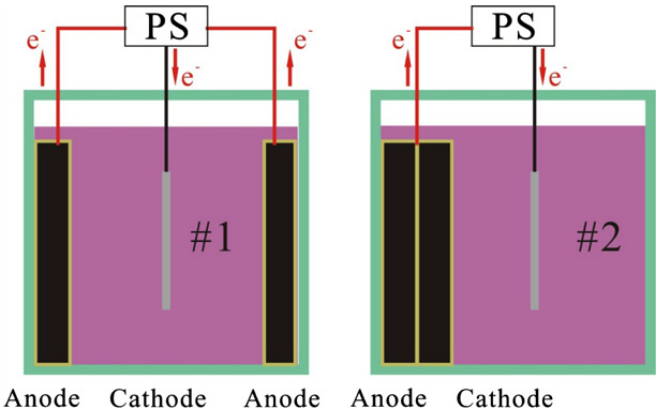

Figure 1.1: Schematic diagram of MECs with different electrode arrangements. Figures adopted from Liang et al. 2011.

It was observed that current was higher in MEC in which the anodes were placed separately on different sides of cathode as compared to the MEC which was constructed by placing anodes together on the same side of the cathode. Hydrogen production rate was also better for MEC#1. Internal resistance (solution resistance, polarization resistance and biofilm resistance) in MEC #1 were estimated by using EIS. Impedance analysis was carried out by an equivalent electrical circuit model of MEC with resistances and capacitance in parallel as shown in Figure 1.2.

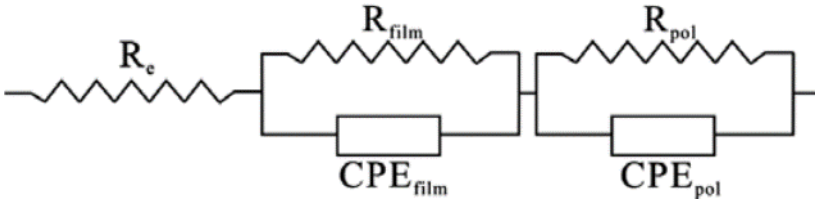

Figure 1.2: Electrical equivalent circuit of MEC for impedance data analysis (Liang et al. 2011)

Impedance test results have shown that anode arrangement as depicted in MEC#1 in Figure 1.1 was favourable in reducing the total internal resistance in MEC.

2.1.3 Biocathode

Performance of MEC is greatly affected by the material used as the cathode. Platinum has been used and have shown good results in reducing the overpotential in MEC but there have been many concerns associated with the use of platinum, being an expensive noble metal. It is also poisoned by the presence of CO and sulphur compounds. Study carried out by Tahereh et al. (2015); describes the use of alternative metal catalysts. In particular, biocathode utilizes microorganisms creating an environmental friendly and inexpensive electrode. In a biocathode MEC, electrode serves as an electron donor for electroactive microorganisms, which catalyse the reaction of hydrogen production (Tahereh et al. 2015).

Performance of bio-cathode based MEC was examined in three different types of MECs based on their construction: (i) half biological two-chambered biocathode MEC, (ii) full biological two-chambered biocathode MEC, and (iii) full biological single-chambered biocathode MEC. Maximum hydrogen production was achieved in half biological two-chambered MEC. It was also observed that when MEC is operated at higher current density, hydrogen loss through the membrane becomes less significant. Single-chambered MEC offers less resistance to the flow of electrons (Tahereh et al. 2015). Growth of microbial community on biocathode film is greatly influenced by the reactor design size and flow pattern.

2.1.4 Optimum Applied Voltage

External voltage is applied to overcome the thermodynamic barrier in MEC for the transfer of electrons from anode to cathode. A study carried out by Linji et al. (2013) analysed the effect of different applied voltage on soluble chemical oxygen demand (sCOD) removal efficiency and biogas production. Experiments were carried out by using activated municipal waste sludge and varying the applied voltage from 0.6 V to 1.2 V. It was observed that the soluble COD (sCOD) maximum removal efficiency took place at the applied voltage of 0.8 V with the maximum columbic efficiency at 98.9%. Figure 1.3 shows the sCOD removal efficiency and columbic efficiency and biogas production at different applied voltages.

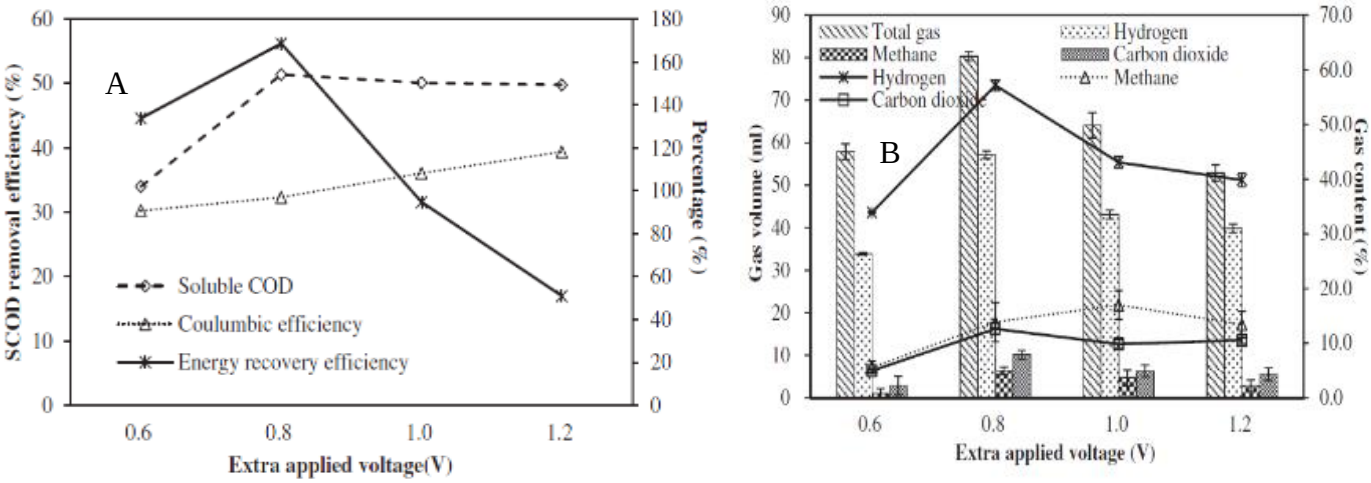

Figure 1.3: (a) sCOD removal at different applied voltage. (b) Gas volume at different applied voltage. Figure is taken from Linji et al. 2013.

These results indicate that maximum sCOD removal and biogas production occurs at an applied voltage of 0.8 V, while further increase in the applied voltage negatively affects the performance of MEC in terms of sCOD removal and biogas production.

Optimum applied voltage varies depending on the strength of influent concentration (organic loading rate, OLR) (Escapa et al. 2012). Different experiments were carried out by considering low and relatively high OLR, while operating the MEC reactor at different applied voltages to analyze the COD removal efficiency and hydrogen production. It was experimentally determined that the optimum applied voltage for treating low and high strength wastewater were 0.75 V and 0.85 V respectively. Hydrogen production displayed a Monod-type trend; it is highly dependent on influent carbon source concentration.

Another study carried out by Ding et al. 2016 determined optimum methane production at the applied voltage of 0.8 V. It was observed that further increase in the voltage decreases methane production as shown in Figure 1.4.

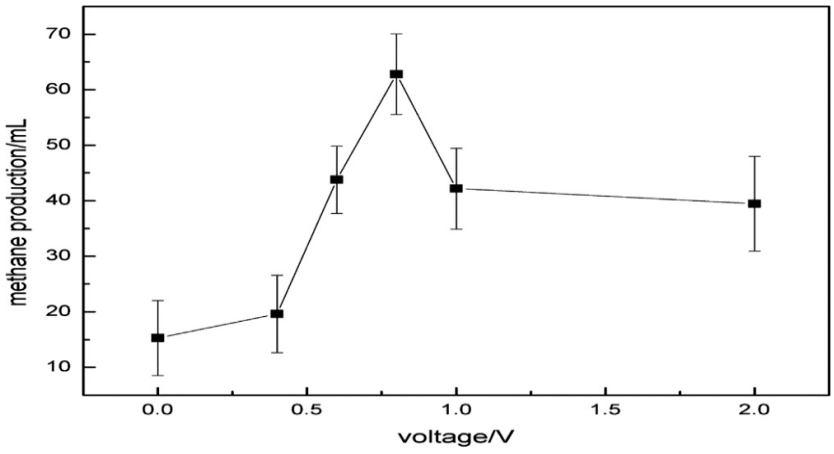

Figure 1.4: Methane production at different applied voltage. Figure taken from Ding et al. 2016

Dark fermentation effluent contains considerably high amounts of volatile fatty acids which needed to be treated before disposing it in the environment. The experiments carried out by Rivera et al. (2015) utilize dark fermentation effluent in two-chambered MEC for hydrogen production. MEC was operated at several COD concentrations (400 mg/L, 600 mg/L and 1200 mg/L) and at two different voltages (350 mV and 550 mV). Hydrogen production rate and COD effluent removal was studied under the above stated conditions. The robustness of MEC was evaluated by feeding the MEC with real effluent containing large amount of glucose. The substrate was composed of glucose, ethanol, acetate, propionate and butyrate with COD of 3700 mg/L. The reactor was operated under 350mV and 550 mV. The resulting biogas was mainly composed of methane and no hydrogen production was observed at the cathode chamber.

It was observed that MEC performs better when it was fed with dark fermentation effluent which contains VFAs. However, the performance of MEC in terms of hydrogen production was significantly decreased in the cathodic chamber, when substrate containing carbohydrates was used as the influent feed to MEC (Rivera et al. 2015).

2.1.5 Effect of Current on MEC Performance

Wastewater with high sulphate content is hazardous for the environment. MEC can be used to treat the sulphate-rich wastewater. In an experiment aimed at studying sulphate removal MEC was operated under different applied currents. It was observed that maximum sulphate removal occurs at 1.5 mA (Kia et al. 2017). As the applied current further increases the substrate consumption was observed to be decreased. High applied current also results in the cell membrane rupture. Following figure shows the removal of sulphate ions under different applied current values.

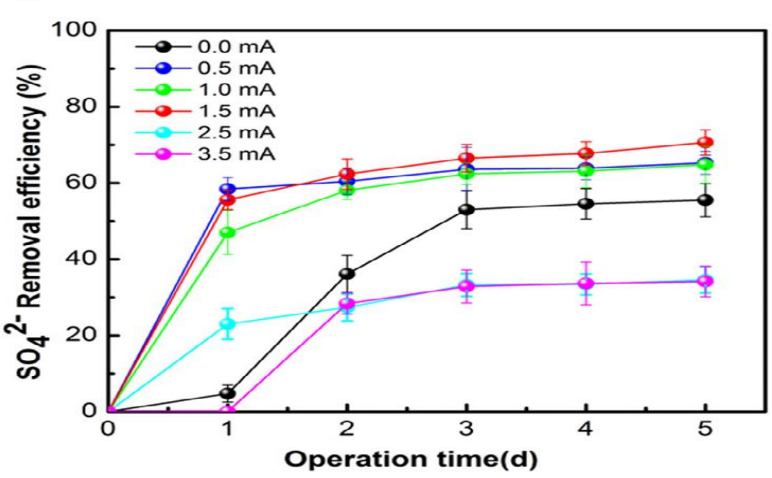

Figure 1.5: Rate of sulphate removal efficiency at different applied current. Figure taken from Kia et al. 2017

The results of this work indicate that there is an optimum value of the current (and corresponding voltage) in MEC. If the current is too high, it has detrimental effects on the biofilm formation, growth and metabolic activity of the microorganisms in MEC. However, the optimum current helps in the enrichment of the bacteria in the cathode film, consequently favouring the electron transfer to electrode (Kia et al. 2017).

Another study carried out by Tartakovsky et al. (2012) shows that the production of hydrogen gas in MEC is proportional to the strength of wastewater. The high strength wastewater led to higher rate of hydrogen production and vice versa. Another study carried out by Verea et al. (2014) focused on optimum production of hydrogen at low cost. The efficiency of hydrogen productivity was improved by the change in electrolyte conductivity and the electrode surface area/electrolyte volume ratio. It was observed that the hydrogen production rate was enhanced with the increase in electrolyte conductivity. Using this approach of maximizing hydrogen production through increased electrolyte conductivity and the optimization of electrode surface area/electrolyte volume ratio also improves cathodic reaction efficiency and columbic efficiency. It was observed that the hydrogen recovery rate was increased with the decrease in the volume of electrolyte when the electrode surface area was kept constant. The results obtained confirm that enrichment process of electroactive bacteria at anode is one of the important factors in improving hydrogen production in MEC (Verea at al. 2014).

2.1.6 Effect of external resistance on MFC performance

External resistance has a great influence on the power generation by MFCs. Maximum power can be harvested from MFCs when the external load (external resistance) equals to the internal

resistance (Logan 2008). Other factors such as temperature, pH and influent composition also affect the power generation by MFCs. Hence, a periodic adjustment of external load is required to maximize power production. The simplest way to operate the MFCs is to keep the external resistance constant, which results in severe power losses when the applied electrical load is not matched with the internal resistance (Logan 2008). Different electrical power sources like photovoltaic arrays and chemical fuel cells resolve this problem by online optimization of the electrical load. The electrical source is connected to a power converter and the duty cycle ratio or the current drawn by the converter is optimized by using a maximum power point tracking (MPPT) method (Esram and Chapman, 2007). The use of power convertor is out of the scope of this study, hence attention is paid to optimizing the electrical load.

2.1.7 Intermittent connection of external electrical load during MFC

In order to increase the power generation of an MFC (Grondin, et al. 2012) proposed to operate the MFC intermittently by alternating the value of external resistance from infinite (open circuit) to a fixed value. Internal MFC capacitance was exploited to develop novel power management methods (Fradler, et al. 2014). By periodically disconnecting the MFC from an electrical load, energy was internally stored and then released to enable a power output burst (Grondin, et al. 2012). Due to varying operating conditions and the process of biofilm growth and decay over time, significant changes of the total internal resistance over time can be expected. These changes result in a mismatch between the internal and the external resistance, even if the initial external resistance value was set close to optimal, hence decreasing MFC output (Grondin, et al. 2012). These mismatch can be reduced by adjusting the load (external resistance) connected to the MFC. This requires knowledge of internal resistance, which can be estimated by the polarization tests. This approach of controlling the equivalent resistance requires a detailed MFC characterization, since the growth rate of electricigenic microorganisms is unknown. In one attempt at optimizing MFC performance described in Pinto et al (2011), external resistance was connected periodically. The tests showed that by periodically connecting and disconnecting R_{ext}, even if R_{ext} is non-optimal, MFC can be operated without significant power losses.

Grondin, et al. (2012) compared the power output obtained by using the P/O method previously described with the periodic operation at values of the external resistance lower than its optimum. MFC can be operated without significant losses. The mismatch of R_{ext} and R_{int} was resolved operating MFC with periodic resistance connection, where connection and disconnection times were controlled based on voltage measurement. (Grondin et al. 2012). This approach of operating MFC resolves the problem of internal and external resistance mismatch and it also accounts for the variation in electrochemical characteristics due to varying operating conditions. No such periodic operation has been performed for MEC performance optimization. By varying external voltage, the internal and external mismatch in MECs can be also resolved and it gives the opportunity to study the yield and efficiency of MEC under varying operating conditions.

Periodic connection of external resistance can be also achieved by using pulse-width modulated mode of operation. This approach was recently demonstrated by Coronado et al (2013). In this work periodic connection of electrical load at frequencies ranging from 0.1-1000 Hz was studied. Experiments were performed using two membraneless MFCs. Pulse width modulated connection of the external resistance (R_{ext}) was established by the addition of an electronic switch. Figure 1.6 shows the experimental setup.

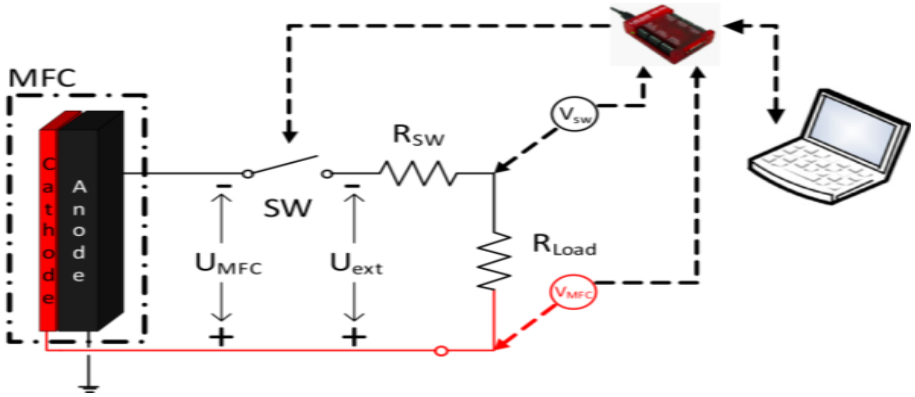

Figure 1.6: Schematic diagram of experimental setup and electric circuit. Figure adopted from Coronado et al. (2013).

As in the previous study, improved stability and higher power output was observed during pulse-width modulated mode of operation, even at lower than optimal external resistance values.

2.1.8 MEC performance on synthetic and real wastewaters

As mentioned earlier, MECs are mostly considered for hydrogen production. However, methane can also be considered as a reliable fuel produced from wastewater in a MEC. Experiments were conducted by Moreno et al. (2016) using synthetic medium and the real wastewater (WW) as the influents to MEC. It was observed that methane production was sharply decreased while using wastewater as the influent substrate because of low acetate concentration. The use of WW as the substrate also resulted in low cathodic conversion efficiency (CCe), it means that significant number of electrons at the cathode were not converted to methane. This loss is explained by the reduction of oxidized compounds such as nitrates and sulphates at the cathode, although these compounds are present in very small concentration in the WW, but their impact on CCe in MEC cannot be neglected. Figure 1.7 represents the comparisons between the CCe, COD removal and columbic efficiency in MEC with synthetic medium (SM) and wastewater (WW) as the influent feed.

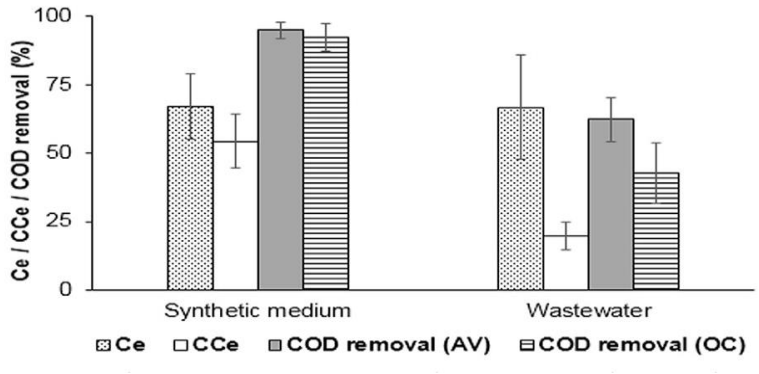

Figure 1.7: Columbic (Ce) and cathodic (CCe) efficiencies, and COD removal for SM and WW influent streams. Figure taken from Moreno et al. 2016

It was observed that MEC performed better while using synthetic media as compared to WW. The COD removal and CCe is much better while using SM. The methane production in MEC can also be improved by increasing the HRT. The experimental results show that MEC with WW as the influent generates more methane at higher HRT, where anode respiring bacteria have advantage over acetoclastic methanogens. Energy recovery is also favoured by higher HRT, which makes the process more cost effective. (Moreno et al. 2016).

2.1.9 Performance of Membraneless MEC

In order to improve the performance of MEC and to reduce ohmic losses, a study was carried out by constructing MEC without membrane and by eliminating metal catalyst on anode (Hyung et al. 2010). It was found that a single chamber membraneless MEC (operated at 1 V applied voltage) featured low ohmic resistance (losses). Also, single chamber MEC favours neutral pH due to ion exchange between the compartments. In turn, losses due to electrode overpotentials are also reduced. Energy-conversion efficiency (ECE) was calculated by following mathematical expressions.

$$ECE = \frac{E_{out,V}}{E_{in,V}} = \frac{V_{H_2}\Delta H_{c,H_2}\alpha}{I_V E_{app}/1000} = \frac{I_V \dfrac{CCE}{F}\Delta H_{c.H_2}\alpha}{I_V E_{app}/1000} = 0.815\frac{CCE}{E_{app}} \quad (1.8)$$

where $E_{out,v}$ is the output electrical energy from H_2-production per volume of MEC, $E_{in,v}$ represents the electrical energy supplied per volume of MEC (KJ/m^{3}s), V_{H2} is H_2-production rate per volume of MEC, $\Delta_{c,H2}$ is the heat of combustion of H_2 per electron equivalence (142.915 kJ/e_ eq of H_2), a is the energy-conversion parameter from heat energy of H_2 to electricity (0.55 in a hydrogen fuel cell) (Larminie et al. 2003), I_v is volumetric current density (A/m^3), 1000 is a units conversion factor (1000 J/kJ), *CCE* is cathodic conversion efficiency from coulombs to H_2 gas, and *F* is the Faraday constant (96,485 C/e_ eq).

In general, energy conversion efficiency of a MEC can be increased by lowering the anode and cathode activation losses and by decreasing the voltage applied to the MEC (Hyung at al. 2010). The maximum value of ECE was found at 0.6V of applied voltage. Study carried out by Tartakovsky et al. estimated ECE to be 81% with CE and CCE were very close to 100% with the voltage applied of 1V. In order to achieve more ECE > 100%, CCE must be greater than 80% and applied voltage less than 0.6V and by reducing the anode and cathode energy losses (Hyung et al. 2010).

2.2 Dynamic Modeling

Design of MEC systems presents a challenge since MEC dynamics is poorly understood. Hence, dynamic modeling is a useful tool in order to better understand the system. The models of MECs

have been developed by using bioelectrochemical reactions and the knowledge of physics, biology and electrochemistry to represent microbial and bioelectrochemical behavior of the system. This approach is helpful in understanding the slow dynamics of microbial transformations, but it lacks information on relationship between the electrochemical and electrical variables. Below, a critical review of existing MEC and MFC models is presented.

2.2.1 Biofilm Modeling

Microbial biofilms can be modeled using different approaches, sometimes resulting in rather complex models. A simplified dynamic one-dimensional multispecies model was presented by Wanner and Reichert (1996) where the biofilm growth and composition were combined into three main processes: (i) substrate conversion, (ii) volume expansion of biomass and (iii) substrate diffusion. The evolution of the biofilm thickness and dynamics, and spatial distribution of multiple microbial species and substrates can be predicted by the model derived from the mass conservation principle. This simplified approach to biofilm modeling was adopted in many biofilm studies, including modeling of bioelectrochemically active (anodophilic) biofilms.

Several anodophilic biofim models can be found in literature. One of the first models was proposed by Marcus et al. (2007). This model describes the anodic biofilm as a conductive solid matrix, which accepts electrons from a carbon source and transfers them to the anode. A diffusive non-conducting layer is considered between conductive matrix and the bulk anodic liquid. The model considers a hypothetical biofilm with electrical conduction property instead of exogenous mediators to explain the behaviour of biofilms in MFCs. This model does not take into account the reaction rate kinetics, diffusion limitations, overpotentials and the existence of several microbial populations competing for the same substrate. Later, Hamelers et al. (2011) described the kinetics of electricigenic bacteria by using Butler-Volmer- Monod expressions that produced better results when fitting the experimental polarization curves.

A one dimensional (1D) model is useful for analyzing the effects of current density and overpotential on biofilm thickness. Like in other biofilm-based biological reactors (such as anaerobic sludge blanket reactor, expanded granular sludge bed reactor, anaerobic biofilter, and anaerobic fluidized bed reactor), in an MFC bacteria are attached to the anode forming a biofilm (Saravanan, et al. 2006). This section discusses generalized one dimensional models developed in

Cartesian coordinates. A typical biofilm is composed of four compartments (Wanner, et al. 2006) namely: (i) the substratum where the biofilm grows, (ii) the biofilm itself, (iii) the bulk liquid around the biofilm, and (iv) mass transfer boundary layer between biofilm and bulk compartments that considers the resistance to mass transport. Each compartment contains components (such as biomass, substrate, etc.) that undergo various transformations.

Picioreanu, Head et al. (2007) described a multidimensional model of a MFC. This computational model includes parameters such as current produced, charge, power, voltage and consumption of substrates with suspended and attached biomass growth in the anode compartment under varying operating conditions. Electrochemical reactions occurring in the anode compartment are described using a redox mediator. Also, biochemical reactions corresponding to methanogenic and electricigenic species, formation of biofilm, mass transport and reactions occurring in biofilm and bulk liquid are considered. The modeling of biofilm was achieved by particle based approach developed by Picioreanu et al. (2004) was used to depict the dynamic mass balances in the bulk liquid for a CSTR which were used to determine substrate and suspended biomass concentration. In this biofilm model, microbial growth and biomass transport were represented by hard spherical particles and were combined with the diffusion reaction mass balances for chemical species.

The model of Picioreanu et al. (2007) requires large computational times of around 14 hours for a single 3D simulation. Later, the model was modified (Picioreanu, Katuri et al. (2008)) to describe degradation of wastewater. This modified model was based on International Water Association (IWA) anaerobic digestion model number 1 (ADM1) (Batstone et al. 2002). Picioreanu, et al. (2010) further extended the model and incorporated pH calculations and different electrode geometry. pH calculations were simulated by using Nernst-Planck fluxes of ions with ionic charge balance instead of molecular diffusion. The variations in electrode geometry were described by modeling mass transport by convection as the mediator that freely diffused in the biofilm and the bulk liquid. This study involved single-species electroactive biofilm on a planar and porous electrode and multi-species electroactive and fermentive biofilm on a planar electrode used to treat wastewater. However, the simulations obtained were not compared to any real data. The estimation from experimental data was impossible because of large amount of model parameters.

2.2.2 Multi-population models

A different approach for modeling of MFCs considers several microbial species, either in suspension or, more often, in a biofilm. Pinto et al. (2010) presented a two-population MFC model describing the competition of electricigenic and methanogenic microbial population for same substrate. It is important to consider multiple populations and the existence of biofilm if MFC is to be used for wastewater treatment applications. This model considers that methanogenic bacteria are competing with electricigenic bacteria for the same substrate. It is assumed that the methanogenic bacteria are present in the biofilm as well as suspended in the bulk liquid of the anodic compartment. The charge transfer mechanism assumes the presence of an intercellular mediator (e.g. NADP). Extracellular electron transfer is described by considering the electricigenic bacteria being attached to the anode surface. Also, growth-washout model (Tartakovsky, et al. 2008) is used to describe biofilm formation and retention. Model analysis was carried out by Fisher information matrix, which shows that only seven parameters of the model could be estimated by minimizing the weighted and normalized difference between the simulated and experimental values.

The model of Pinto et al (2010) established a link between external resistance, organic load and the coexistence of microbial populations. The model was further extended to simulate a microbial electrolysis cell for the production of hydrogen (Pinto et al. 2011). In this case the number of microbial populations was extended to include fermentative, electricigenic, methanogenic, acetoclastic, and methanogenic hydrogenophilic species.

In recent years significant progress has been made in MEC development. These improvements were mainly focused on enhancing hydrogen production by using better cathode materials, better electrode compartment design and optimizing operating conditions. Yet, the overall performance remains relatively low (Logan et al 2008). Modeling can significantly contribute to the process development effort. Pinto (2011) developed a model that solves the modeling complexity offered by MEC by presenting a simple dynamic model that simulate hydrogen production from wastewater. The model describes the influence of organic load and applied voltage on COD removal. The model was validated in an experimental setup with three membraneless MECs with 50 mL anodic and hydrogen collection compartments. Neutral pH was maintained and the

temperature was set to 30°C. The formation of anaerobic film was supported by three dimensional carbon felt anode. Electrochemical part of the MEC model considered ohmic, activation and concentration losses. The following equation described the electrochemical balance.

$$- E_{applied} = E_{CEF} - \eta_{ohm} - \eta_{conc} - \eta_{act} \quad (1.9)$$

where E_{CEF} represents the counter electromotive force for MEC, η_{ohm} is the ohmic losses, η_{conc} is the concentration overpotential and η_{act} is the activation overpotential.

Nernst equation is used to calculate the concentration losses at the anode, while the concentration losses at the cathode can be neglected due to small size of H_2 molecules resulting in a large diffusion coefficient of H_2 in a gas diffusion cathode. The concentration losses are given by the following equation, where M_{red} and M_{ox} are the reduced and oxidized forms of anodophilic intercellular mediator respectively. M_{total} is the sum of M_{red} and $M_{ox.}$

$$\eta_{conc} = \frac{RT}{mF} \ln\left(\frac{M_{total}}{M_{red}}\right) \quad (1.10)$$

The activation losses were calculated by Butler-Volmer equation approximation. The following equation describes the activation losses at cathode

$$\eta_{act} = \frac{BT}{\beta mF} Sinh^{-1}\left(\frac{I_{mec}}{2A_{sur,A} i_0}\right) \quad (1.11)$$

where i_0 represents the exchange current density in reference conditions, $A_{sur,A}$ is the anode surface area and β is either the reduction or the oxidation transfer coefficient. F is the Faraday's constant.

H_2 production was found to be maximum at an applied voltage of 1.2 V. Pinto and Srinivasan (2011) also demonstrated the effect of influent COD concentration and suggested that the high rate of H_2 production is possible with increasing the organic load. Less acetate is

produced at low concentration and consequently the shortage of electricigenic microorganisms results in decrease in the current and therefore less hydrogen flow.

The multipopulation model provides guidance with respect to MEC design and operation. The model is applicable for real-time processes control because of its simplicity. The model does not

provide information about the adjustment of electrical parameters that could be used to maximize the desired gas production while achieving a high degree of COD removal.

2.2.3 Electrical Equivalent Circuit Model

This section analyzes the electrical equivalent circuit models of MFCs that can be applied to MECs. In addition, the effect of change in external resistance with intermittent connection/disconnection of external resistance on the performance in MFCs is described to provide a basis for MEC modeling. Electrical circuit modeling is the strategy, which can be used in order to replace the highly complex multipopulation models of an MFC.

In electrochemical systems, the electrical charge is stored in the layer, which is at the interface between the electrode and the electrolyte. When current is manipulated, a sudden change in operating voltage occurs due to the internal resistance, which is followed by a gradual and slow transition to the final voltage equilibrium stage. This process is termed as double layer capacitance effect (Larminie, et al. 2003). An electrical equivalent circuit can model double layer capacitance if, the charged layer is represented by a capacitor. The electrical equivalent circuit modeling can be found in the literature of electrochemical systems such as lithium-ion batteries (Gao, et al. 2002), polymer electrolyte fuel cells (Wagner 2002) or lead acid batteries (Dür, et al. 2006). Even though this approach of modeling can be used in MFCs and MECs, however very few publications have been found on MFC modeling and none related to MEC modeling.

Proton exchange membrane fuel cell (PEM-FC) was characterized by using electrochemical impedance spectroscopy by Wagner (2002). The electrical equivalent circuit model includes ohmic (R) and capacitive (C) elements. The connection of the circuit elements in series represents the simultaneous occurring processes, while the connection in parallel depicts the subsequent processes. The following figure represents a simple equivalent electrical circuit of an MFC.

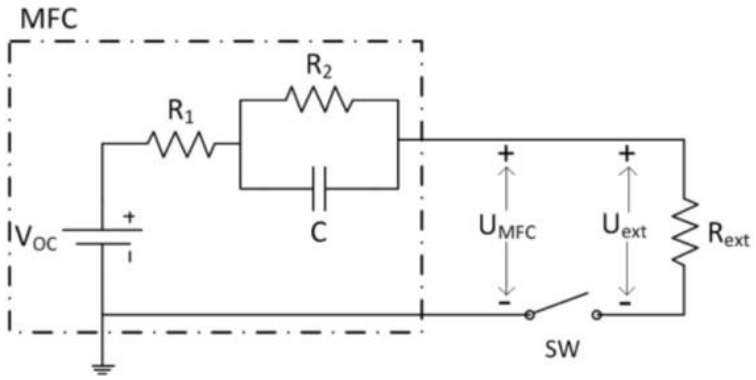

Figure 1.8: Electrical equivalent circuit of an MFC. Figure adopted from Coronado et al. (2013).

2.2.4 Long term dynamics of bioelectrochemical models

The relationship between the biochemical variables and the electrical properties are used to describe the long-term dynamics of bioelectrochemical models (Picioreanu et al. 2007). Generally, two mechanisms are accepted to describe the transport of electrons from biodegradable substance to the electrode (Schroder 2007): (i) The transfer of electrons through direct contact or by the presence of conducting nanowires, which helps in the conduction of electrons, and (ii) The transfer of electrons through a mediator; via exogenous redox mediators or via secondary metabolites.

This section describes the bioelectrochemical models of MFCs and MECs found in the literature.

Unified (MxC) Model

Modeling of biofilm formation is simplified by the division of biofilms into several distinct layers and the assumption of uniform distribution of microorganisms within each layer (Rauch et al. 1999). This approach was applied to develop a unified model capable of modeling both an MFC and MEC (hence an MxC model). In this model, the biofilm at the surface of anode is assumed to consist of anodophilic and acetoclastic methanogenic microorganisms. Here, anodophilic microorganisms are capable of utilizing the anode as terminal electron acceptor, while the acetoclastic microorganisms are capable of producing methane (Pinto et al. 2011). The transfer of charge from a carbon source towards anode is assumed to take place by intercellular mediator,

which is present in the reduced and oxidized forms (Pinto et al. 2010). The second biofilm layer consists of fermentative microorganisms, which transform large organic moleculaes into acetate. Also, it was also assumed that a biofilm layer is present at the cathode. This biofilm consists of hydrogenotrophic methanogens, which convert the hydrogen produced at the cathode into methane.

The carbon source (acetate) was assumed to be well distributed in the anodic chamber. The formation of the acetate gradient inside the biofilm is neglected. A constant pool of intercellular electron transfer mediator Finally, temperature and pressure are kept constant (Pinto et al. 2011). Main microbially catalyzed transformations are assumed as follows:

Andodophilic microorganisms:

$$C_2H_4O_2 + 2H_2O + 4M_{ox} \rightarrow 4M_{red} + 2CO_2 \quad (1.12)$$

$$4M_{red} \rightarrow 4M_{ox} + 8e^- + 8H^+ \quad (1.13)$$

where M_{red} and M_{ox} are the reduced and oxidized forms of anodophilic intercellular mediator respectively.

Acetoclastic methanogenic microorganisms:

$$C_2H_4O_2 \rightarrow CH_4 + CO_2 \quad (1.14)$$

Hydrogenotrophic methanogenic microorganisms:

$$CO_2 + 4H_2 \rightarrow CH_4 + 2H_2O \quad (1.15)$$

To collect data for model parameter estimation MEC was fed with acetate at three concentration levels: 1000, 1500 and 900 mg-A L^{-1}, while for model validation MEC was fed with acetate at either 1500 or 1900 mg-A L^{-1}, where A represents acetate concentration. In both conditions the temperature was kept constant at 30 °C and the voltage supplied was set to 1 V.

The model developed by Pinto et al; 2011 provided a simulation tool that can be used for design, optimization and control purposes.

Combined bioelectrochemical - electrical model of MFC

This section presents critical describes another modeling approach in which bio electrochemical MFC model was combined with an electrical equivalent circuit model to create a combined

bioelectrochemical--electrical (CBE) model of MFC. The model was developed by combining the equations describing microbial, carbon source and electron balances of the bioelectrochemical model developed by Pinto et al. (2012) with electrical equivalent circut equations developed by Coronado et al. (2013). Electrical model only accounts for the internal capacitance and resistance of the anode and it lacks biomass and carbon source material balances.

The CBE model of MFC proposed by Garrido, et al (2015) accounts for electricigenic (attached) and methanogenic (attached or suspended) microbial communities. Internal resistance (R_1) represents the electrolyte ohmic resistance, while a resistor/capacitor circuit is included to describe the internal capacitance (C) and the activation losses (R_2). The internal resistance (R_{int}) of MFC is described as the sum of activation and ohmic losses.

$$R_{\text{int}} = R_1 + R_2 \tag{1.16}$$

In addition to the mass balances, Garrido et al (2015) also describes the voltage at the internal capacitor C as follows:

$$\frac{dV_c}{dt} = \frac{I_{cell} - \frac{V_c}{R_2}}{C} \tag{1.17}$$

Where V_c is the voltage at cathode, I_{cell} represents current, C is the capacitance and R_2 is the resistance. The output electrical voltage and power were described by the following relations respectively,

$$V_{cell} = I_{cell} \times R_{ext} \tag{1.18}$$

$$P_{cell} = I_{cell} \times V_{cell} \tag{1.19}$$

In above equations, Voltage of the cell is denoted by V_{cell}, current passing through the cell is represented by I_{cell} and P_{cell} is the power of the cell.

The CBE model is capable of describing both fast and slow dynamics of MFC. The model was used to produce two distinct types of simulation: (i) conventional offline prediction approach with the help of model equations, and (ii) online version of the model where simulations are carried out co-currently with the experimental and empirical equations are used. The former

approach can be used to predict MFC output voltage, carbon source effluent concentration, and the distribution of microbial populations under varying operating conditions. The later approach used an on-line estimation procedure proposed by Coronado et al. (2013).

In order to simplify the model, sensitivity analysis was carried out to reduce the number of model parameters requiring identification. The norm of the sensitivity profiles for all parameters were computed and arranged from highest to lowest values. The highest norm is the indicator of the maximum impact of the parameter on the selected output. The confidence intervals were obtained from the Fisher information matrix. Consequently, the effect of all model parameters on the model outputs was evaluated and the parameters with the highest impact were selected for parameter identification. The sensitivity profiles were plotted by using the same inputs (influent acetate concentration and flow rate profiles) as those used in the experimental data for parameter estimation. Hence, the input substrate concentration was changed step-wise.

Garrido (2015) observed that the population of electricigenic bacteria decrease at low influent concentration. The CBE model provided an adequate description of the short-term output voltage during the pulse-width modulated connection of external resistance. It was also found that the concentration of oxidized mediator increased during the short-term closed circuit period and vice versa. This apparent behaviour occurs because during open circuit operation, the change in the concentration of the oxidized form of the intercellular mediator represents an accumulation of charge within the electricigenic bacteria (biofilm) in the anodic compartment. Overall, the “online” model was proved to be more accurate, particularly at higher values of the influent concentration.

CHAPTER 3 REAL-TIME MONITORING OF A MICROBIAL ELECTROLYSIS CELL USING AN ELECTRICAL EQUIVALENT CIRCUIT MODEL

This chapter describes a simple MEC equivalent electrical circuit (EEC) model and a parameter estimation procedure, which enable such real-time monitoring. The proposed approach involves MEC voltage and current measurements during its operation with periodic power supply connection/disconnection (on/off operation) followed by parameter estimation using either numerical or analytical solution of the model. The proposed monitoring approach is demonstrated using a membraneless MEC with flow-through porous electrodes. Laboratory tests showed that changes in the influent carbon source concentration and composition significantly affect MEC total internal resistance and capacitance estimated by the model. Fast response of these EEC model parameters to changes in operating conditions enables the development of a model-based approach for real-time monitoring and fault detection.

3.1 Analytical methods and media composition

Acetate concentrations were measured using an agilent 6890 gas chromatograph (agilent technologies inc, santa clara, ca, usa) equipped with a flame ionization detector. The off-gas composition was also measured by gas chromatography. Further details are provided in tartakovsky et al. 2008. Biogas production was measured using a miniature flip-flop gas meter (milligascounter, ritter apparatus, bochum, germany).

The stock solution of nutrients was composed of sodium acetate (40 g), yeast extract (0.83 g), ammonium chloride (18.7 g), potassium chloride (74.1 g), potassium phosphate dibasic (32 g) and potassium phosphate monobasic (20.4 g) dissolved in 1 l of distilled water. The feed solution was prepared by diluting the concentrated stock solution of nutrients to obtain the desired influent cod concentration (either 600-700 mg l^{-1} or 1300-1500 mg l^{-1}). The feed solution was maintained at a temperature of 4 °C.

3.2 MEC design, operation, and performance evaluation

Flow through membranless MEC reactors used in the laboratory tests differ from conventional MECs designed for hydrogen production. A typical MEC consists of anode and cathode compartments separated by a proton exchange membrane cathode as shown in Figure 2.1A (Ding et al., 2013). Only the anode compartment is fed with CODs, while the cathode compartment is used for H_2 production (Eq. 1.2). The recently proposed flow-through MEC also consists of anodic and cathodic compartments as shown in figure 2.1B. Here, the influent stream enters the reactor from anodic compartment, where degradation and hydrolysis of organic waste occurs, then wastewater flows through a porous non-conductive separator (e.g. geotextile cloth) to the cathode compartment where it undergoes further treatment. The treated water exits the cathode compartment. Biogas (mostly methane) is produced at the cathode due to hydrogentropic methanogenic activity that converts hydrogen to methane with carbon dioxide consumption (Eq. 1.3). The flow-through MEC used in the tests had granular activated carbon (GAC) as anode and cathode material. MEC was operated under somewhat higher applied voltage (1.4-1.5V) in order to overcome the ohmic and activation losses due to low conductivity of GAC granules.

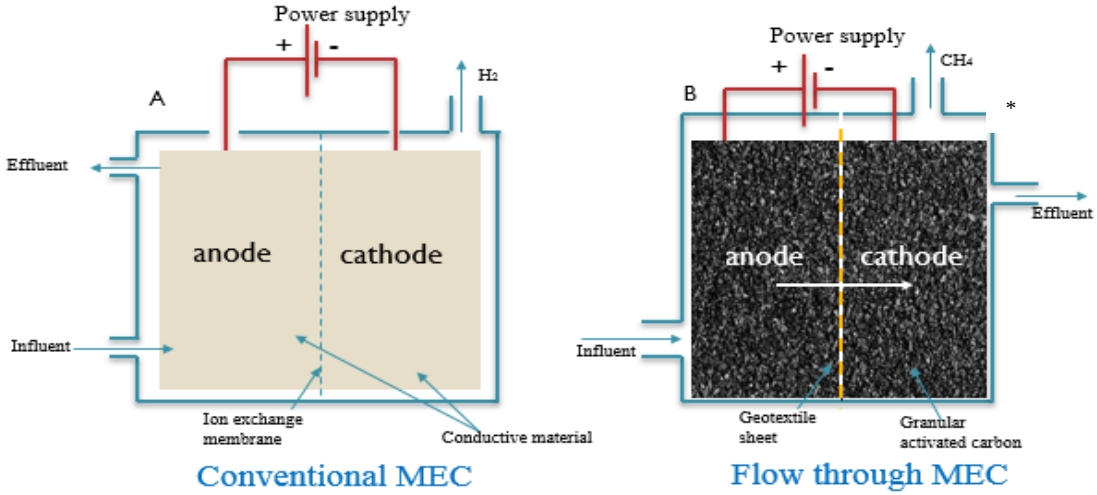

Figure 2.1: (A) Conventional MEC and (B) Flow through MEC.

* Image of granular activated carbon is taken from https://www.dreamstime.com/stock-photo-granular-activated-carbon-water-filter-texture-background-image50378304.

A vertical flow-through MEC (Figure 2.2) was constructed using a glass cylinder with a diameter of 5 cm, a length of 50 cm resulting in an empty bed volume of 1 L. Granular activated carbon (GAC) was used as both anode and cathode material. GAC was soaked in water for 1 day at room temperature and was incorporated into the MEC anodic and cathodic compartments. GAC was used due to its low corrodibility, high conductivity, high specific surface area porosity and it provides sustainable environment for the growth of microorganisms (Logan et al. 2008). The anode and cathode compartments had equal volumes of 500 mL and were separated with a 2 mm thick piece of geotextile cloth. Titanium wires were inserted into GAC electrodes and used to connect each electrode to a power supply. Marbles were used at the influent port of the reactor to disperse the fluid uniformly inside the reactor. A peristaltic pump was used to recirculate liquid between the effluent and influent ports, as shown in Figure 2.2. The flow rate of the recirculation pump was 9.6 mL min^{-1}. MEC was operated at a room temperature of 21-24ºC.

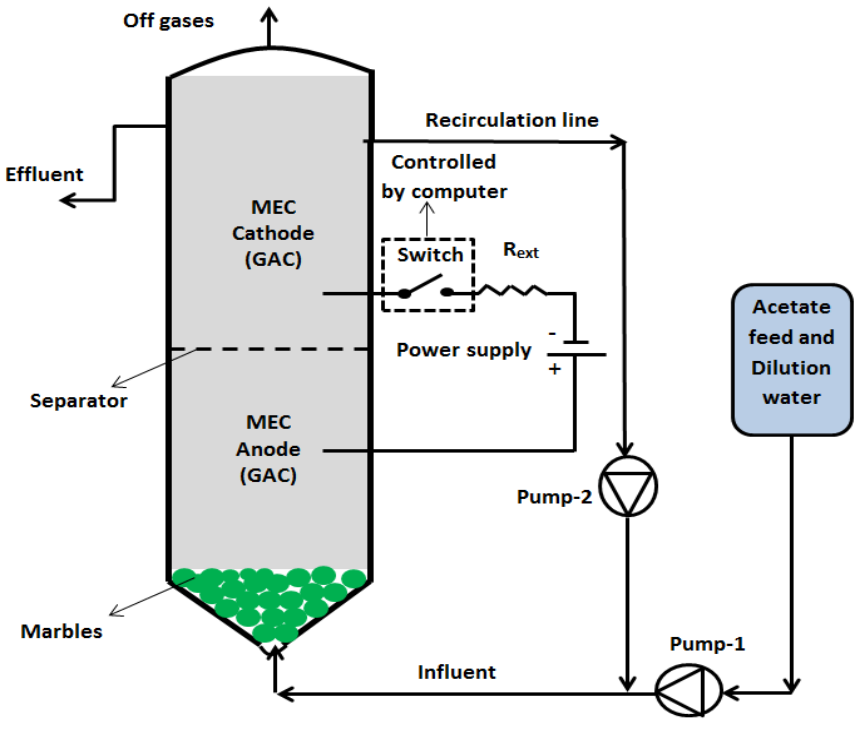

Figure 2.2: Experimental setup.

The MEC was inoculated with 10 mL of homogenized mesophilic anaerobic sludge (Lassonde Inc., Rougement, QC, Canada, which had a volatile suspended solids content of 22-25 g L^{-1}. Following inoculation, the MEC was continuously fed a solution of nutrients and acetate at a flow rate of 1 L d^{-1}. Typically, an influent COD concentration of 600-700 mg L^{-1} was maintained at a hydraulic retention time (HRT) of 1 day (based on an empty bed volume of 1 L). To test MEC performance at higher organic loads, an influent COD concentration of 1300-1500 mg L^{-1} was used between days 65-75 of the test.

Methane yield (L g^{-1}) was calculated according to the following equation:

$$Y_{CH4} = \frac{Q_g C_g / 100}{Q_l (S_{in} - S_{out})} \quad (2.1)$$

Where Q_g is the biogas flow rate (L d^{-1}), C_g is the percentage of methane in biogas (%), Q_l is the liquid flow to and from MEC (L d^{-1}), S_{in} and S_{out} are the influent and effluent acetate concentrations (g L^{-1} as COD).

Columbic efficiency (%) was calculated as

$$\eta_{CE} = \frac{I}{FnQ_l(S_{in} - S_{out})} 100\% \quad (2.2)$$

where I is the current (A), F is the = Faraday's Constant (F= 96480 C mol^{-1}), n is the number of electrons (n = 8 for acetate), Q_l is the liquid flow to and from MEC (L s^{-1}), S_{in} and S_{out} are the influent and effluent acetate concentrations measured (mol L^{-1} as COD) . Columbic efficiency was calculated based on the variables mentioned in Eq 2.2. Current (I), liquid flow to and from MEC (Q_l), effluent and influent acetate concentrations (S_{out} and S_{in}) were measured in the laboratory and values were incorporated in Eq 2.2 for the calculation of columbic efficiency.

3.3 Electrical measurements and numerical methods

The MEC was operated at an applied voltage of 1.4 V using a PW18-1.8AQ power supply (Kenwood Corp, Tokyo, Japan) interfaced with a computer. Current was measured with a 10 Ohm shunt resistance (R_{ext}) according to the diagram shown in Figure 2.1. MEC operation with periodic power supply connection/disconnection (on/off operation) was achieved using a

computer-controlled relay. LabJack U3-LV (LabJack Corp., Lakewood, CO, USA) data acquisition board was used to control the relay and record power supply voltage (V_s), and voltage measured across R_{ext} (V_R). MEC voltage (V_{MEC}) was calculated as the difference of V_R and V_S values. Software for on/off MEC operation and data acquisition was written in Matlab R2010a (Mathworks, Natick, MA, USA).

Numerical parameter estimation was carried out using *fminsearch* function of Matlab R2010a. Parameters were estimated by minimizing the difference between experimental data and model outputs. The following objective function (mean square error, MSE) was used:

$$MSE = \frac{1}{n}\sum_{i=1}^{n}\left(\frac{y_i^{exp} - y_i^{mod}}{\bar{Y}}\right)^2 \qquad (2.3)$$

where n is the number of measurements, y_i^{exp} is the i^{th} measured value, y_i^{mod} is the i^{th} model output, and $\bar{Y}$ is the average of all measured values.

Numerical solutions of the EEC models were obtained by solving first order differential equation of the model using *ode45* function of Matlab R2010a.

3.4 Results and discussion

3.4.1 COD removal in flow – through MEC

Owing to the concept simplicity, the recently developed MEC with porous flow-through electrodes can be conveniently used for treating wastewaters with a medium to high COD content (Tartakovsky et al. 2017). The flow-through design is based on microbially catalyzed electrochemical reactions in both anode and cathode electrode compartments, eliminating the need for a metal catalyst (e.g. Pt or Ni) at the cathode. While biocathode-based MECs require relatively long startup times, several studies have nevertheless demonstrated successful operation of these bioelectrochemical system (Jafary et al. 2015; Jeremiasse et al. 2010; Rozendal et al. 2008). In addition to featuring a biocathode, the membraneless design reduces ohmic resistance and ensures fast conversion of biocatalytically produced H_2 to CH_4. Indeed, in the absence of an ion exchange membrane, CO_2 produced at the anode is transported to the cathode, where hydrogenotrophic methanogens combine it with H_2. Increased CH_4 production in a MEC, as

compared to a conventional anaerobic digestion process, has been recently reported (Hou et al. 2015; Liu et al. 2016; Villano et al. 2011).

To facilitate the development of bioelectrochemically active biofilm, the flow-through MEC was operated at an initial fixed influent COD concentration of 600-700 mg L^{-1}. Once the observed current increased and stabilized at 4-6 mA (after about 20 days of operation), the influent COD concentration was increased to approximately 1300 mg L^{-1}. The rate of COD removal and methane yield were calculated based on the MEC performance between days 45 and 85 using acetate influent and effluent concentrations as well as biogas (methane) production. A summary of MEC performance over both moderate and high COD operational periods is shown in Figure 2.3. Notably, the experiment was carried out at a room temperature (22-24ºC) rather than at 35ºC, which would be optimal for anaerobic digestion. Nevertheless, an average CH_4 yield of 0.32 L g^{-1} (consumed COD) was estimated, which is sufficiently close to the stoichiometric value of 0.35 L g^{-1}.

Throughout MEC operation at an influent COD concentration of 600-700 mg L^{-1} the effluent concentration remained at 70-90 mg L^{-1} and only slightly increased to 120 - 150 mg L^{-1} during MEC operation at a higher influent COD concentration of 1300 mg L^{-1} (Figure 2.3A). These effluent concentrations corresponded to volumetric (per liter of reactor volume, L_R) COD removal rates of 0.56 and 1.10 g L_R^{-1} d^{-1}, respectively. Also, current was found to proportionally increase with the increased COD load (Figure 2.2B). A near doubling of the COD removal rate accompanied by a current increase implies that the maximum removal capacity of the reactor was not achieved, even at the highest organic load. Coulombic efficiency estimations according to Eq. 2.2 yielded relatively low values of 10-15%, i.e. a significant part of acetate was consumed by the methanogenic microorganisms, which competed with the anodophilic microorganisms for a common carbon source. Nevertheless, the anodophilic microorganisms provided an important contribution to the overall COD removal, as can be evidenced by the high values of methane yield given MEC operation at lower than optimal for anaerobic digestion temperature.

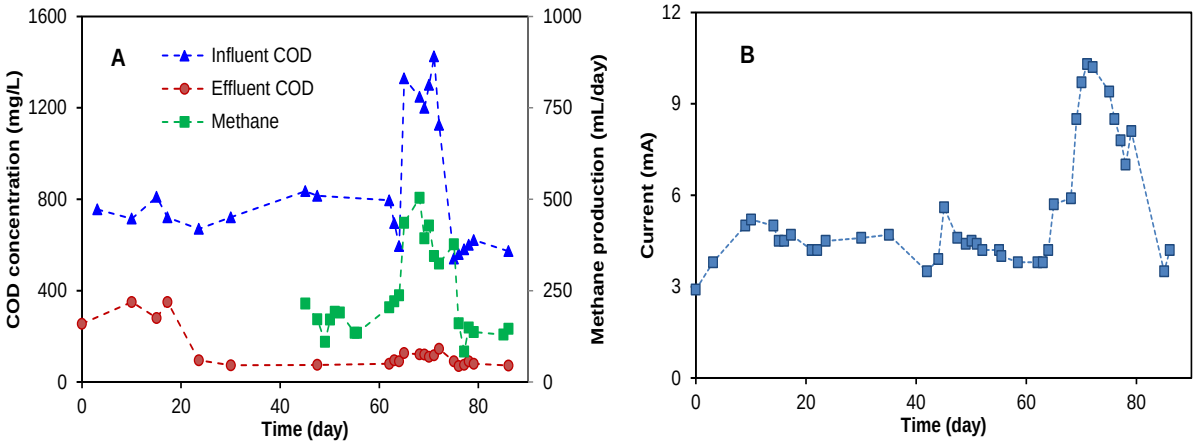

Figure 2.3: COD removal and methane production (A) and current (B) during MEC operation at moderate (700-800 mg L^{-1}) and high (1300-1500 mg L^{-1}) influent COD concentrations.

In addition to MEC performance characterization in terms of COD removal and biomethane production, a voltage scan test was carried out on day 69 of MEC operation (high organic load) and then repeated on day 107 (moderate organic load) to estimate total internal resistance. Based on the linear part of the voltage vs current plots, internal resistance values of 175 Ohm and 203 Ohm, respectively, were estimated, i.e. the total internal resistance was higher at a lower organic load. It might be mentioned that the open circuit voltage (OCV) observed at the beginning of each voltage scan did not decrease to zero as would be observed in a MEC without liquid exchange between the electrode compartments (Manuel et al. 2010). Instead, the voltage remained at around 0.30 V, as shown in Figure 2.4. This positive open OCV might be attributed to electrochemical processes occurring in a membraneless flow-through MEC.

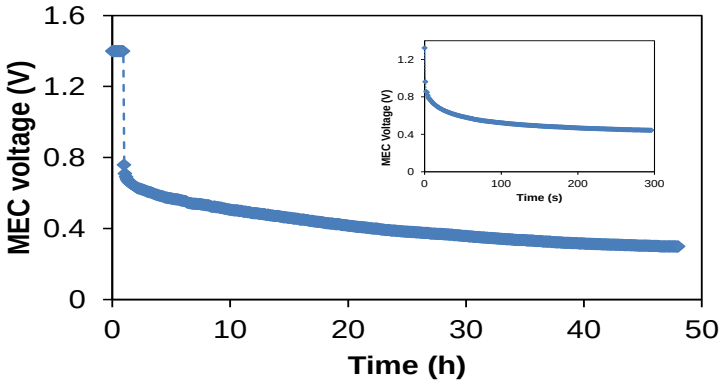

Figure 2.4: MEC voltage during the open circuit test. Inset shows first 300 s after power supply is disconnected.

3.4.2 EEC model development

Frequent variations in wastewater composition and strength necessitate thorough monitoring of MEC performance. In particular, internal resistance and capacitance of a MEC might be significantly affected (Martin et al. 2013; Meril et al. 2009). In addition to conventional measurements (COD concentrations, pH, biogas production), MEC performance can be followed by estimating parameters of an EEC model and interpreting these parameters for timely detection of changes in the activity of electrochemically active microorganisms and process faults. Owing to similarities between MFC and MEC anodic bioreactions, the EEC model describing electrical dynamics of a MEC might be similar to the recently developed MFC EEC model (Coronado et al. 2015). Thus, the proposed MEC EEC model consists of a resistance (R_0) in series with two R/C circuits (R_1/C_1 and R_2/C_2). Here, R_0 represents ohmic losses, while R_1 and R_2 are assumed to represent MEC activation losses (Yang et al. 2012). Also, C_1 and C_2 represent internal capacitance of a MEC. Notably, to account for the experimentally observed positive OCV values mentioned earlier (figure 2.4), the model considers an electromotive force (U_{EMF}). The resulting EEC model diagram is shown in figure 2.5. In addition to the EEC, the diagram shows shunt resistance (R_{ext}), power supply (PS) and a switch (SW), which was used for MEC operation in on/off mode (periodic PS connection).

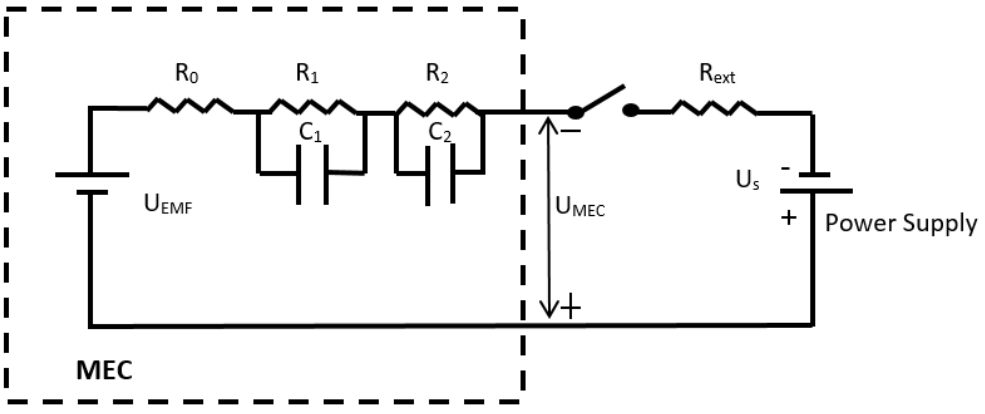

Figure 2.5: Diagram of an electrical equivalent circuit model with two R/C circuits. The diagram shows MEC connection to power supply using a switch (SW) to achieve on/off operation. R_{ext} is the shunt resistance used for current measurements.

The following first order differential equations can be written to describe voltage dynamics at C_1 and C_2 internal capacitors shown in figure 2.5.

$$\frac{dU_{C1}}{dt} = \frac{U_s + U_{emf}}{C_1(R_0 + R_{ext})} - \frac{U_{C1}(R_0 + R_1 + R_{ext})}{C_1 R_1 (R_0 + R_{ext})} - \frac{U_{C2}}{C_1(R_0 + R_{ext})} \tag{2.4}$$

$$\frac{dU_{C2}}{dt} = \frac{U_s + U_{emf}}{C_2(R_0 + R_{ext})} - \frac{U_{C2}(R_0 + R_2 + R_{ext})}{C_1 R_2 (R_0 + R_{ext})} - \frac{U_{C1}}{C_2(R_0 + R_{ext})} \tag{2.5}$$

where U_{C1} and U_{C2} are the voltages at internal capacitors C_1 and C_2, U_s is the power supply voltage, and U_{emf} is the electromotive force.

By applying Kirchhoff's voltage and current laws, the following equation describing MEC voltage (U_{MEC}) can be derived, as described in Appendix A (EEC Model #1):

$$U_{MEC} = U_s - (U_s - U_{C1} - U_{C2} - U_{emf}) \frac{R_{ext}}{R_0 + R_{ext}} \tag{2.6}$$

To simulate U_{MEC} dynamics, model equations (2.4-2.6) can be solved numerically.

A simpler EEC model, denoted as EEC model #2, can be derived by considering only one R/C circuit (e.g. $R_2 = 0$). In this case, the first-order differential equation describing voltage dynamics at the internal capacitor C_1 can be written as:

$$\frac{dU_{C1}}{dt} = \frac{U_s + U_{emf}}{C_1(R_0 + R_{ext})} - \frac{U_{C1}(R_0 + R_1 + R_{ext})}{C_1 R_1 (R_0 + R_{ext})} \tag{2.7}$$

Also, MEC voltage can be calculated as

$$U_{MEC} = U_s - (U_s - U_c - U_{emf}) \left(\frac{R_{ext}}{R_0 + R_{ext}} \right) \tag{2.8}$$

Notably, Eq (2.7) can be solved analytically leading to the following model equation:

$$U_{C1} = U_{final} + (U_0 - U_{final}) e^{-\frac{t - t_0}{\tau}} \tag{2.9}$$

where, U_{final} and τ (time constant) are model parameters defined as

$$U_{final} = \frac{(U_{emf} + U_s)R_1}{R_0 + R_1 + R_{ext}},\ \tau = \frac{CR_1(R_0 + R_{ext})}{R_0 + R_1 + R_{ext}} \quad (2.10)$$

As above, U_{MEC} can be calculated according to Eq. 2.8. Details of this analytical solution are provided in Appendix B.

Finally, the EEC model can be further simplified by assuming zero U_{emf}, in which case MEC voltage is calculated as

$$U_{MEC} = U_s - (U_s - U_{C1})\frac{R_{ext}}{R_0 + R_{ext}}, \quad (2.11)$$

where U_{C1} is defined in Eq (2.9). This model is referred to as EEC Model #3 in the following discussion.

3.4.3 Comparison of EEC models

The ability of the three EEC models to adequately describe MEC voltage dynamics was evaluated by estimating parameters of each model and then analyzing the discrepancies between the experimentally measured values and corresponding voltage outputs. To observe dynamics related to fast changes in applied voltage, the MEC was operated in the on/off mode by connecting and disconnecting the power supply at 5 s intervals (50% duty cycle) and measuring U_{MEC} at a frequency of 10 Hz. Parameters of all models described in the previous section were estimated by minimizing the objective function defined in Eq. 2.3. All models were solved numerically.

Figure 2.6 compares experimentally measured voltage profile with the outputs of the three models.

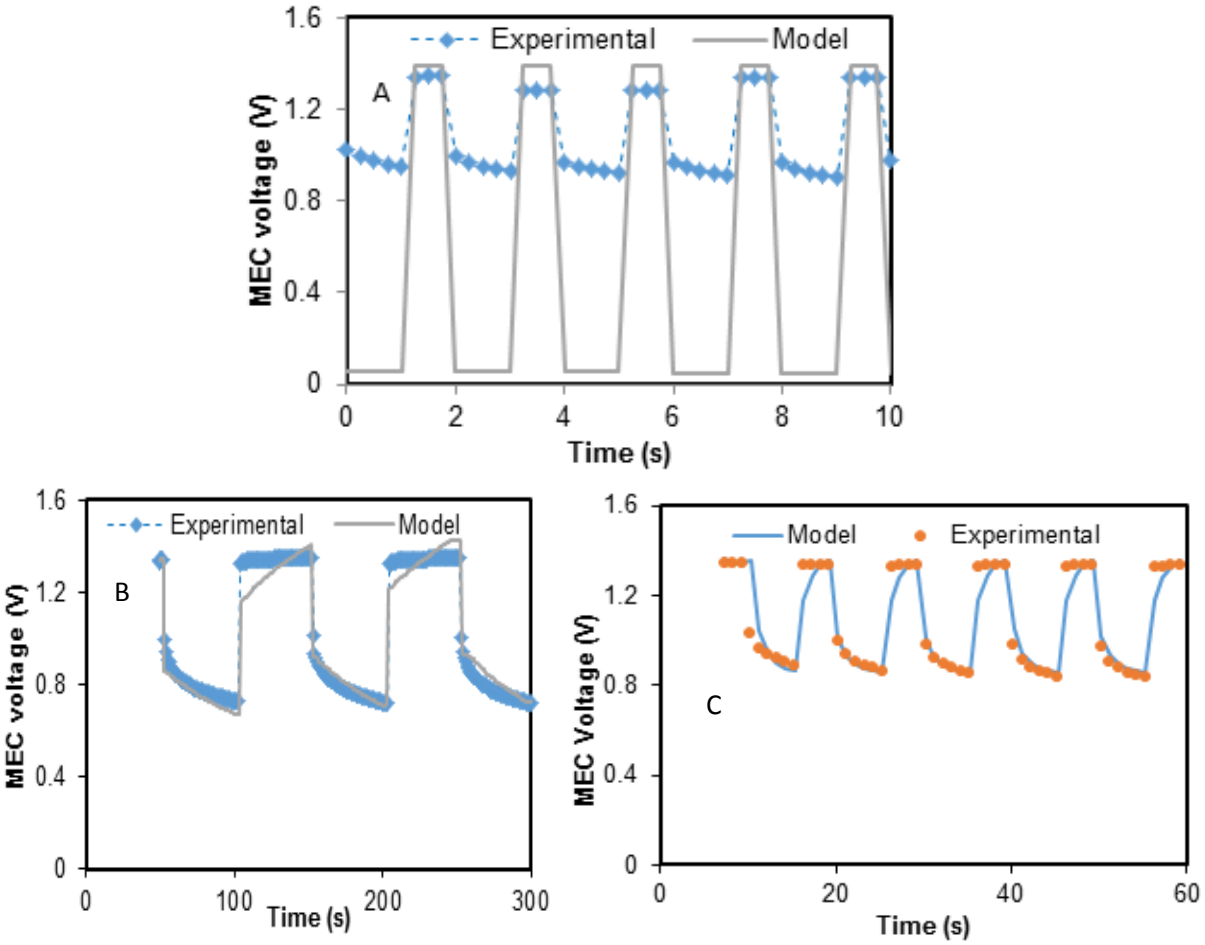

Figure 2.6**:** A comparison of experimental and calculated MEC voltage values for EEC models with (A) one R/C circuit & Uemf = 0; and (B) one R/C circuit & Uemf >0 and (C) two R/C circuits & Uemf >0.

The single R/C circuit model with U_{emf} = 0 (Model #3) was unable to adequately describe the observed voltage dynamics, as can be seen from the comparison of experimental and simulated voltage values (Figure 2.6 A). Clearly, when the power supply was disconnected (off part of each cycle), the existence of U_{emf} led to positive U_{MEC} voltage, while the model predicted zero values. A repeat of the parameter estimation procedure using U_{emf} as an additional model parameter (Model #2) led to a significantly better agreement between the experimentally measured and simulated values (Figure 2.6 B). Finally, when the parameter estimation procedure was repeated

to estimate Model #3 parameters (two R/C circuits), the modeling accuracy was marginally improved, as compared to Model #2 with the single R/C circuit model (Fig. 2.6 C).

Table 2.1 provides a summary of estimated model parameters and corresponding MSE values

Table 2.1: Parameter estimation results

Parameter	**Model**			
	Model 3 R-R/C; $U_{emf} = 0$	Model 1 R-R/C-R/C; $U_{emf} > 0$	Model 2 R-R/C; $U_{emf} > 0$	Model 2* R-R/C $U_{emf} > 0$
R_0 (Ω)	4	3	5.4	7
R_1 (Ω)	209	2	44	56
C_1 (F)	113	1	6	5
R_2 (Ω)	-	1.05	-	-
C_2 (F)	-	5	-	-
EMF (V)	-	0.3	0.42	0.35
MSE	0.02	0.017	0.002	0.01

* Analytical parameter estimation

A comparison of the parameter estimation results suggests that by including U_{emf} in the EEC model, the model accuracy is significantly improved, while the second R/C circuit only provides marginal improvement. Importantly, Model #2 can be solved analytically (Appendix B), while Model #1 requires numerical solution, which significantly increases computational time. Accordingly, Model #2 was used in the following test demonstrating on-line MEC monitoring.

3.4.4 Parameter estimation by analytical method

The simplicity of Model #2 (Eq 2.7-2.9) not only enables analytical solution, it also allows for the development of an analytical procedure for estimating model parameters. This parameter estimation (model calibration) procedure can be based on the approach proposed for estimating

parameters of the EEC model of an MFC (Coronado et al. 2015). In this approach a MFC is operated at high and low frequencies of R_{ext} connection/disconnection to sequentially estimate its internal resistances and capacitance.

Similarly, the MEC parameter estimation procedure can be started with U_{emf} estimation, e.g. during MEC operation with disconnected power supply. Next, the MEC is operated at a high frequency to estimate R_0 according to the following equation:

$$R_0 = \frac{U_h}{U_s - U_h} R_{ext}, \tag{2.12}$$

where U_h is the voltage across MEC corresponding to connected power supply. R_0 can be estimated since U_h, U_s and R_{ext} values are known.

At the low frequency (e.g. 0.01 Hz) of power supply connection/disconnection, the capacitive reactance increases and R_1 can be estimated according to

$$R_1 = \frac{U_L}{U_s - U_L} R_{ext} - R_0 \tag{2.13}$$

where U_L is the voltage across MEC when the power supply is connected while operating MEC at low frequency. R_1 can be estimated using Eq 2.13 since U_L, U_s ,R_{ext} and R_0 values are known.

Finally, internal capacitance (C_1) is estimated according to the following equation:

$$C_1 = \frac{\tau\left(R_0 + R_1 + R_{ext}\right)}{R_1(R_0 + R_{ext})} \tag{2.14}$$

Here, τ is defined as the time required to achieve 63% of the total voltage variation (Coronado et al. 2014) and can be calculated by a least squares method using values of U_{MEC} acquired during MEC operation with disconnected power supply.

To illustrate the proposed approach for estimating EEC model parameters, U_{MEC} voltage profiles were acquired during on/off mode of operation at two frequencies and model parameters were estimated. The following values were obtained using the analytical approach: R_0 = 7 Ω; R_1 = 56 Ω; C_1 = 5 F; U_{emf} = 0.35 V. These values can be compared to results of the numerical parameter

estimation provided in Table 1. Although the MSE value is higher with respect to the analytical estimation, it can be seen that the two methods provide similar estimations for R_0, R_1, and C_1.

3.4.5 Real-time MEC monitoring

The on-line procedure of estimating EEC model parameters described earlier can be used to achieve real-time monitoring of MEC performance. Indeed, previous studies have reported a significant impact of varying influent COD concentration and/or composition (organic load) on internal resistance and capacitance of bioelectrochemical systems (Pinto et al. 2011). Other external disturbances, such as variations in concentration of nutrients, pH, and temperature, may also affect MEC internal resistance and capacitance.

To demonstrate EEC model – based MEC monitoring, the flow-through MEC was operated at several influent acetate concentrations as described in Figure 2.7 A, while model parameters were estimated in real time using the numerical parameter estimation method described earlier. The test was carried out for a total of 55 days with the parameter estimation procedure repeated at 12 h intervals. Figure 2.7 B shows the impact of influent acetate concentration on MEC current, while results of parameter estimation representing changes in internal parameters are shown in Figure 2.7 C-F. Clearly, variations in influent COD (acetate) concentration affected the current and also were captured by the proposed monitoring method. In particular, the R_1 component of the internal resistance, which is associated with activation losses and therefore might be related to carbon source availability, was observed to increase during carbon source – deplete MEC operation, while R_0 remained almost unchanged. Generally, R_0 is associated with ohmic losses and therefore might be sensitive to solution conductivity. Considering that a decrease in influent acetate concentration did not lead to a significant change in the influent solution conductivity (only acetate concentration was changed, while the conductivity was kept constant), near constant R_0 values were expected. At the same time, R_1 abruptly increased during the acetate-deplete MEC operation, e.g. between days 21-25 when acetate feed was stopped and after day 50, when the influent acetate concentration was decreased.

Variations in internal capacitance and U_{emf} values were less pronounced, although the capacitance values were observed to increase over time, in particular at high acetate concentrations during days 26-50, suggesting biofilm growth under acetate-replete conditions

(Figure 2.7 E). Similar trends were observed in an MFC study (Martin et al. 2013). At the same time, the estimated U_{emf} values did not correlate well with carbon source concentrations showing slow decrease over the course of the experiment (Figure 2.7 F).

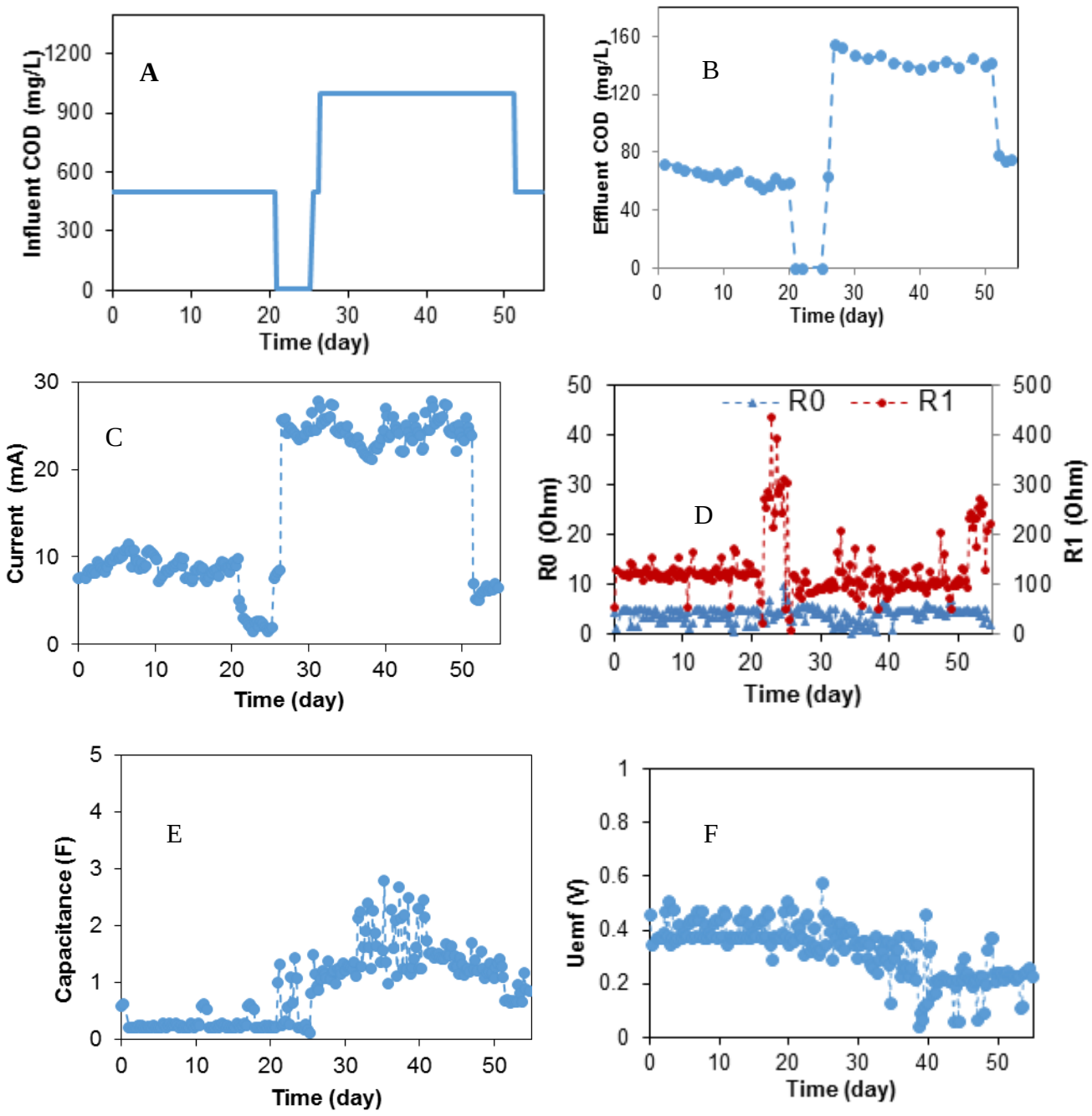

Figure 2.7: Results of long-term MEC monitoring using real-time numerical procedure of Model #2 parameter estimation. A – influent acetate concentration, B –Effluent acetate concentration, C-

measured MEC current, D- Variations of R_0 and R_1 components of the total internal resistance, E- Internal capacitance variations, F – U_{emf} variations.

In addition to long-term monitoring of MEC performance, the two approaches to estimating model parameters (analytical and numerical) were compared by calculating model parameters using both methods. For this test, MEC was once again operated at high and moderate influent acetate concentrations of 1000 mg L^{-1} and 500 mg L^{-1} respectively (target concentrations, actual concentrations were slightly different). The time-dependent profile of influent acetate concentration and the corresponding concentrations of acetate in the effluent are shown in Figure 2.8 A. For this test, model parameters were estimated every 3 h, while the test was carried out for 6 days.

Results of monitoring transitions from a high to lower influent acetate concentration (t = 2.7 day) and return to 1000 mg L^{-1} influent acetate concentration (t = 4.8 day) once again confirmed that the EEC model provides a convenient tool for MEC performance monitoring. A decrease in influent acetate concentration caused values of R_0 and R_1 to increase (i.e. total internal; resistance was increased). The increase in R_1 was more pronounced than in the previous test. R_1 estimation increased by approximately 20 Ohm as compared to a 2 Ohm increase in R_0 value. A change in internal capacitance estimation was more significant than during the previous test (Figure 2.8), with both estimation methods suggesting lower capacitance values under acetate-deplete conditions. This drop in capacitance corresponded to low effluent acetate concentrations between days 3-5, as can be seen from Figure 2.8 E. Hence, decrease in effluent concentration corresponds to lower capacitance.

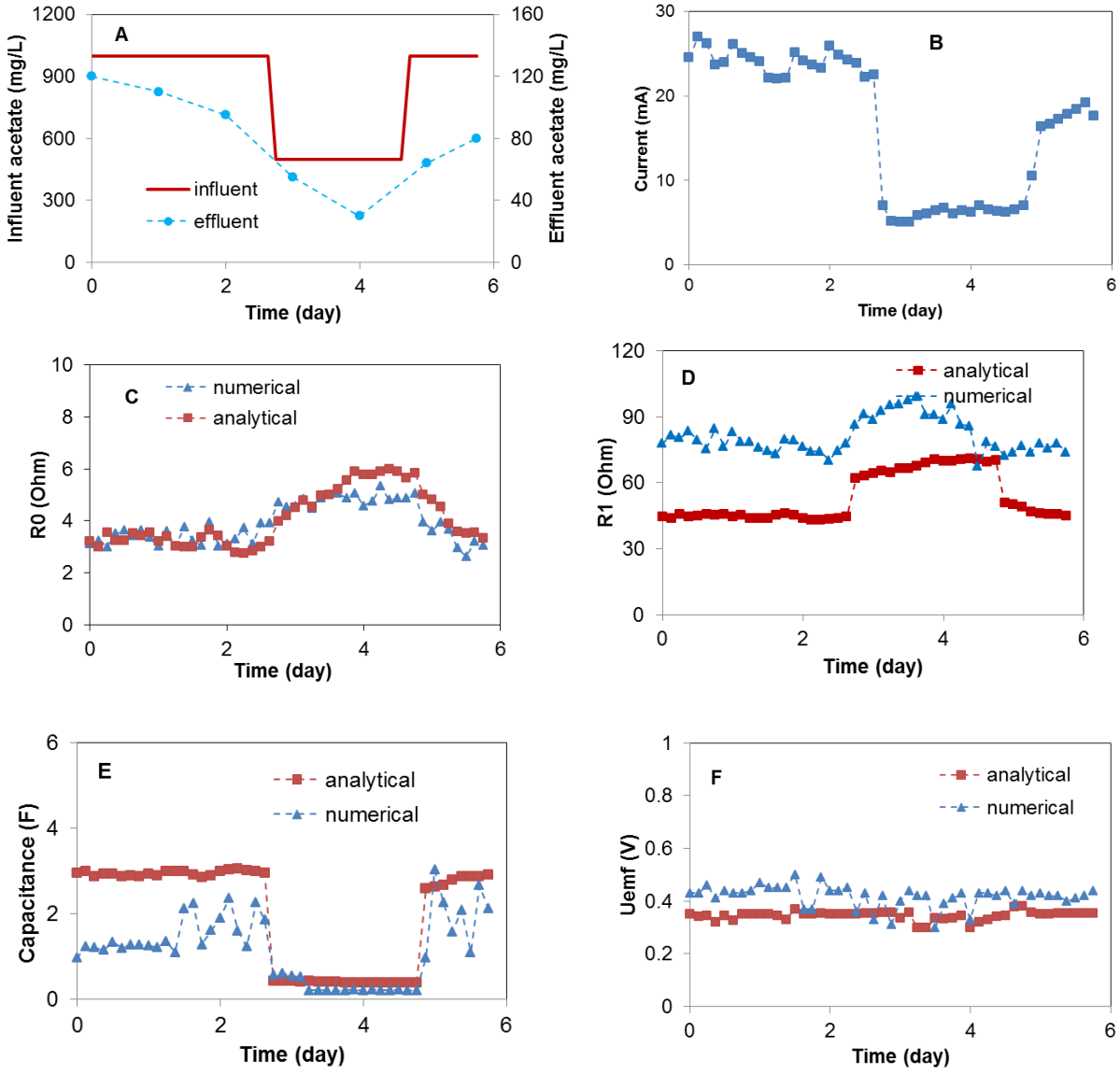

Figure 2.8: A comparison of numerical and analytical approaches for parameter estimation. (A) - Influent and effluent acetate concentrations during the test , (B) - observed MEC current, (C) – R_0 estimations, (D) – R_1 estimations, (E) – internal capacitance estimations, and (F) - U_{emf} estimations.

In another set of experiments influent acetate concentration was changed from 1334 mg/Ld to 667 mg/Ld and the its effect was observed on the internal electrical parameters of MEC. Results are presented in figure A.1 and figure A.2 in Appendix D.

Internal capacitance was also estimated by performing cyclic voltammetry was performed using an electrochemical analyzer CHI 601A (CH Instruments, Austin, TX). The anode was used as working and counter electrode while an Ag/AgCl electrode was employed as reference. Voltammetry was carried out at different scan rates between 10 and 0.5 mV/s, at amplitudes between –0.9 and 0.4V vs the Ag/AgCl electrode. The cyclic voltammetry test was performed on day 4 to estimate the double layer capacitance when the influent concentration was 500 mg/L. The estimated capacitance was 0.13 F. Results are presented in Appendix D (Fig A.4).

The internal resistance of the electrode pairs in MECs was estimated using a voltage scan technique (Escapa et al. 2012). Voltage scans were performed by changing the applied voltage between 0.3 and 1.5 V with 10-min intervals after each voltage change to allow the outputs to stabilize. The results were used to estimate MEC internal resistance as a slope of the linear part of voltage vs current curve. Total internal resistance was estimated to be 203 Ω and 175 Ω with influent acetate concentration of 500 mg/L and 1000 mg/L respectively. Voltage scan tests results are presented in Appendix D (Fig A.5).

Overall, a comparison of parameter values estimated by two methods showed that both approaches resulted in similar estimations. Parameters estimated by the numerical method were somewhat noisier, which can be expected for a numerical algorithm. Although both estimation methods can be used, the analytical solution might be preferable, as it requires less computational resources and can be implemented in a programmable logic controller (PLC).

3.5 Conclusion

This study demonstrated real time MEC monitoring using a simple equivalent electrical circuit model with a single R/C circuit. Owing to the model simplicity, its analytical solution was derived. Furthermore, an on-line analytical parameter estimation procedure was proposed based on MEC operation with periodic connection/disconnection of the applied voltage (on/off operation) in a sequence of high and low frequencies. This monitoring method was tested in a laboratory to achieve real-time monitoring of a flow-through MEC with granular activated carbon electrodes treating a synthetic (acetate-based) wastewater. Fast response of the EEC model parameters to changes in influent carbon source concentration was observed, thus validating the proposed monitoring approach.

CHAPTER 4 LONG-TERM PERFORMANCE OF A MICROBIAL ELECTROLYSIS CELL OPERATED WITH PERIODIC DISCONNECTION OF APPLIED VOLTAGE

Biodegradation of organic materials in a microbial electrolysis cell (MEC) can be used to develop a net energy-positive wastewater treatment process. Indeed, hydrogen production from wastewater in a MEC was one of the first proposed MEC applications (Ditzig et al., 2007). Methane production is often observed at the MEC cathode, either due to hydrogen conversion to methane by hydrogenotrophic methanogenic microorganisms, or by direct electromethanogenesis (Clauwaert and Verstraete, 2008, Villano et al., 2010, Villano et al., 2011, Wagner et al., 2009). A recently proposed MEC-based wastewater treatment technology takes advantage of fast conversion of hydrogen and carbon dioxide to methane by utilizing a flow-through membraneless MEC design, which combines electricigenic (anodophilic) and conventional anaerobic pathways of COD degradation (Tartakovsky et al., 2017). This technology is based on bioelectrodes made of granular activated carbon, which require relatively long startup times to develop an electrochemically active microbial biofilms at the anode and cathode. A strategy capable of accelerating this process, as well as providing a means for real-time MEC performance monitoring, is required for practical application of this MEC configuration.

Recently, several optimization approaches were proposed to enable real-time monitoring and optimization of Microbial Fuel Cells (MFCs). In particular, increased power production in a MFC operated with periodic disconnection of external resistance or using pulse width modulated (PWM) resistance connection was demonstrated (Coronado et al., 2013, Grondin et al., 2012). Furthermore, a simple equivalent electrical circuit (EEC) model of an MFC and a parameter estimation procedure adapted to the PWM mode of operation was developed and successfully used to achieve real time monitoring of MFC performance (Coronado et al., 2015).

So far, very few attempts were made to apply similar approaches to MEC optimization and/or monitoring. In one study, the production of hydrogen gas in a MEC was maximized by real-time optimization of applied voltage (Tartakovsky et al., 2011). Here, the applied voltage was modified in real time in order to minimize MEC apparent resistance by using a Perturb-and-Observe (P/O) algorithm. In a more recent study, an equivalent electrical circuit model of MEC was developed and used for real-time monitoring of internal resistance and capacitance (Hussain

et al., 2018). This approach was shown to be capable of successfully tracking changes in the operating conditions, including variations in the influent chemical oxygen demand (COD) concentration.

Constantly changing wastewater composition and COD concentration combined with a requirement of the treated effluent COD concentration to be below a certain regulatory threshold provides a limited number of controllable inputs in a wastewater treatment process. Since growth and metabolic activity of electroactive bacteria are directly proportional to the applied voltage, it could be expected to have significant impact on MEC performance.

This study attempts to adapt the approach of intermittent (on/off) MFC operation, which was shown to greatly improve MFC performance (Coronado et al., 2013) to operation of an MEC. Accordingly, experiments are carried out in MECs with flow-through porous bioelectrodes (Tartakovsky et al., 2017) to study the impact of operation with periodic disconnection of applied voltage. Additionally, changes in MEC internal parameters caused by such on/off operating strategy are monitored in real time with recently developed equivalent electrical circuit model (Hussain et al., 2018).

4.1 Media solutions and Analytical Methods

The stock solution of feed was either acetate-based (synthetic wastewater) or composed of brewery wastewater. Acetate stock solution was composed of (per L) anhydrous sodium acetate (40 g), yeast extract (0.83 g), ammonium chloride (18.7 g), potassium chloride (74.1 g), potassium phosphate dibasic (32.0 g) and potassium phosphate monobasic (20.4 g). The stock solution was diluted with deionized water to obtain the desired acetate concentration. Also, solution of trace metals was added to synthetic wastewater (1 mL per L) to provide essential microelements. The composition of the trace metal solution can be found elsewhere [4]. The resulting synthetic wastewater solution had a conductivity of 15-17 mS cm^{-1}. Brewery wastewater with an average total COD concentration of 6.7 g L^{-1} was obtained from Fleischmann's Yeast Ltd (Calgary, AB, Canada). It too was diluted with deionized water to obtain the desired influent COD concentration of 2000 mg L^{-1}. This solution had a conductivity of 5-7 mS cm^{-1}.

Biogas production was measured with the MilliGascounter (Ritter Apparatus, Bochum, Germany). Biogas composition was measured using an HP 6890 gas chromatograph (Hewlett Packard, Palo Alto, CA, USA). Acetate concentration was analyzed with a second Agilent 6890 gas chromatograph (Wilmington, DE, USA) equipped with a flame ionization detector.
details are provided elsewhere (Tartakovsky et al., 2008).

4.2 MEC design and operation

Two horizontal flow rectangular MECs (MEC-A and MEC-B) were constructed using Plexiglas plates. Each MEC had equally sized anode and cathode compartments separated by a piece of geotextile (non-conductive porous cloth). Granular activated carbon (GAC) was used both as the anode and cathode material. GAC bed occupied the entire volume of each electrode compartment. A total liquid volume of each MFC was 1.7 L, while headspace volume was 0.3 L. Each MEC was further equipped with off-gas exit, which collected biogas produced in both electrode compartments, and an external recirculation line to ensure adequate mixing. The recirculation rate was 9.6 mL min^{-1}. The MECs were operated as flow-through reactors, where the influent stream entered the anode compartment and the effluent was collected at the end of the cathode compartment as shown in Figure 3.1.

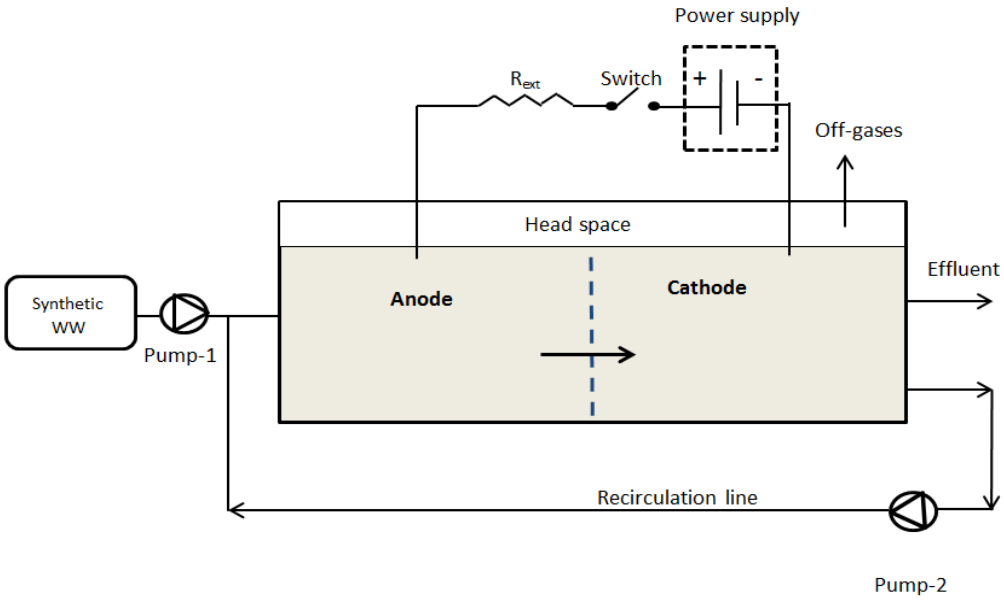

Figure 3.1: Experimental setup. Horizontal flow-through MEC with porous electrodes.

Each electrode compartment was inoculated with 20 mL of homogenized anaerobic sludge (Lassonde Inc., Rougement, QC, Canada), which had a volatile suspended solids content of 22-25 g L^{-1}. The MECs were operated at room temperature (22-24^{o}C). Initially the MECs were fed with synthetic (acetate-based) wastewater at a flow rate of 2 L d^{-1}, i.e. a hydraulic retention time (HRT) of 0.85 day was maintained, as calculated based on the total reactor volume. The stock acetate solution and the dilution water were fed using peristaltic pumps. Experiments were carried out by feeding the MECs at an influent acetate concentration of 1000 mg L (1070 mg L^{-1} as COD). Following MEC operation on synthetic wastewater the influent stream was changed to brewery wastewater. Methane yield (L g^{-1}) was calculated according to the equation 2.1 as described in chapter 2.

4.3 Electrical measurements and numerical methods

The MEC was operated at an applied voltage of 1.5 V using a PW18-1.8AQ power supply (Kenwood Corp, Tokyo, Japan) interfaced with a computer. Current was measured with a 15 Ohm shunt resistance (R_{ext}) according to the diagram shown in Figure 3.1. MEC operation with periodic power supply disconnection (on/off operation) was achieved using a relay controlled by LabJack U3-LV (LabJack Corp., Lakewood, CO, USA) data acquisition board, which was also used to *record* power supply voltage (U_s), and voltage measured across the MEC (U_{MEC}). Voltage across the external resistor (U_R) was calculated as the difference of U_{MEC} and U_S values and then used to calculate MEC current.

Software for on/off MEC operation and data acquisition was written in Matlab R2010a (Mathworks, Natick, MA, USA). After certain (user specified) time, the computer program calculated and recorded the average current (I_{avg}) and power (P_{avg}) per each on/off cycle. These values were calculated as follows:

$$I_{avg} = \frac{1}{T_c}\int_0^{T_c} i dt \qquad (3.1)$$

$$P_{avg} = \frac{1}{T_c}\int_0^{T_c} p dt \,, \qquad (3.2)$$

where T_c is the cycle length, i and p are the current and power at time t. Here, p is calculated as

$$p = iU_s \,, \qquad (3.3)$$

where U_s is the applied voltage at time t.

Numerical solution of the equivalent electrical circuit model was obtained by solving first order differential equation of the model using *ode45* function of Matlab R2010a. Estimation of model parameters was carried out using *fminsearch* function of Matlab R2010a, which minimized the difference between experimental values and model outputs. The objective function (mean square error, MSE) used in presented in Eq. 2.3 in chapter 2.

4.4 Electrochemical techniques

Cyclic voltammetry was performed using an electrochemical analyzer CHI 601A (CH Instruments, Austin, TX). The anode and cathode were used as working and counter electrodes respectively, while an Ag/AgCl electrode was employed as reference. Voltammetry was carried out at different scan rates between 10 and 0.5 mV/s, at amplitudes between –0.9 and 0.4V vs the Ag/AgCl electrode. The cyclic voltammetry test was performed on day 47 (MEC-B) to estimate the double layer capacitance. The test was carried out by using cathode as a working electrode and then also using anode as a working electrode. Another approach of estimating internal capacitance by energy discharge experiment is mentioned in Appendix D (Section A.6).

The internal resistance of the electrode pairs in MECs was estimated using a voltage scan technique (Escapa et al. 2012). Voltage scans were performed by changing the applied voltage between 0.2 and 1.4 V with 10-min intervals after each voltage change to allow the outputs to stabilize. The results were used to estimate MEC internal resistance as a slope of the linear part of voltage vs current curve.

4.5 Results and discussion

4.5.1 Duty cycle optimization and the impact of on/off operation on MEC performance

Operation of MEC-A and MEC-B on synthetic wastewater consisted of four distinctive phases. Phase 1 (start-up) lasted 10 days and was followed by 3 phases of operation under differing conditions for either MEC. Startup phase for both MEC-A and MEC-B was initiated with a fixed applied voltage of 1.5 V and continuous acetate feeding at an influent concentration of 1070 mg

L^{-1} as COD. Once stable current was observed, phase 2 was initiated by subjecting MEC-A to a periodic connection/disconnection of the power supply (on/off operation), while MEC-B continued to be maintained at a fixed applied voltage.

Figure 3.2A illustrates the approach of MEC-A operation in the on/off mode. As can be seen from this graph, the highest current is observed immediately after the power supply is connected to MEC electrodes. During the "on" part of the cycle at a constant applied voltage the current somewhat decreases and then drops to zero once the power supply is disconnected. Interestingly, after each disconnection of the power supply MEC voltage only drops to about 0.9 V and then remains in the vicinity of this value with slight decrease during the off part of the cycle. Such voltage dynamics could be attributed to the significant internal capacitance of the electroactive biofilm (Coronado et al. 2013) and large surface area of GAC electrodes.

To observe the impact of frequency with which power supply is connected to MEC (duty cycle, D) and the length of the connection/disconnection cycle (T_c) on MEC current, MEC-A was operated at several combinations of T_c and D. In particular, T_c was varied between 2 and 10 s. For each T_c value, D values were changed from 10% to 100% with a step of 5%. Figure 3.2B shows the resulting dependencies of average current calculated according to Eq. 2 on T_c and D values. At all values of T_c a near linear increase of current was observed with increasing D (between D = 10 - 40%). Fast increase of average current was followed by a slower increase at D values between 40 – 70% (especially at T_c values of 4 and 5 s) and then a somewhat faster increase at D values above 70%. As the result, at all tested T_c values the highest average current was observed at D = 100%, i.e. the highest average current corresponded to fixed applied voltage. This result is contrary to the observation of a higher power production, i.e. higher current, in MFCs operated with periodic disconnection of external resistance at D values of 90 - 95% (Recio-Garrido, al.2013) or with pulse-width modulated connection of the external resistance (Coronado et al.2013). In case of on/off MFC operation, energy storage in the anodic biofilm (high internal capacitance) results in a burst of power once external resistance is reconnected. Accordingly, the average (per cycle) power output was observed to exceed the power output at a constantly connected R_{ext} (Recio-Garrido, et al.2015).

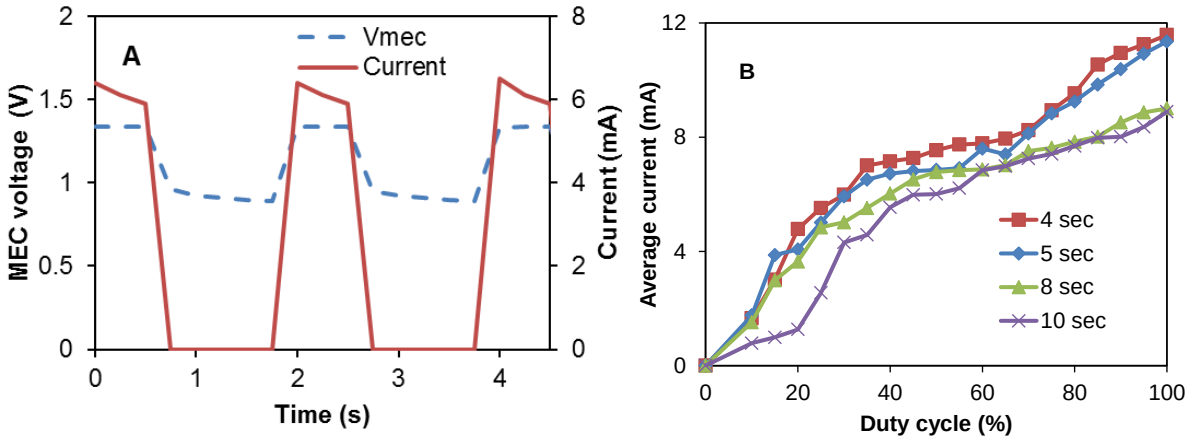

Figure 3.2: (A) MEC-A voltage and current observed at D =12.5% and T_c = 2s, and (B) average (per cycle) current calculated at several D and T_c values.

Second attempt at D optimization involved a Perturb-and-Observe (P/O) algorithm, which was used to maximize the average current by step-wise changes of D starting from a D value of 50%. Detailed description of the algorithm can be found elsewhere (Woodward et al. 2010). Results of this test are shown in Figure 3 (inset). The test was carried out at a T_c = 5 s with each D value maintained for 30 min. Once again, the highest average current was obtained at D = 100% (fixed applied voltage). Interestingly, although the test did not indicate the existence of optimal duty cycle, progressive increase of the current towards the end of the test in which D fluctuated between 95% and 100% was observed, as can be seen from the graph (Fig 3.3 inset). The optimization test was repeated over a period of several days. Overall, the duty cycle tests continued for 5 days (between days 10-15). Although each test indicated that the highest average current corresponds to fixed applied voltage, a pronounced increase in the current of MEC-A was noticed by day 15. At the same time, the current of MEC-B operated at a fixed applied voltage remained unchanged, as can be seen from Figure 3.3.

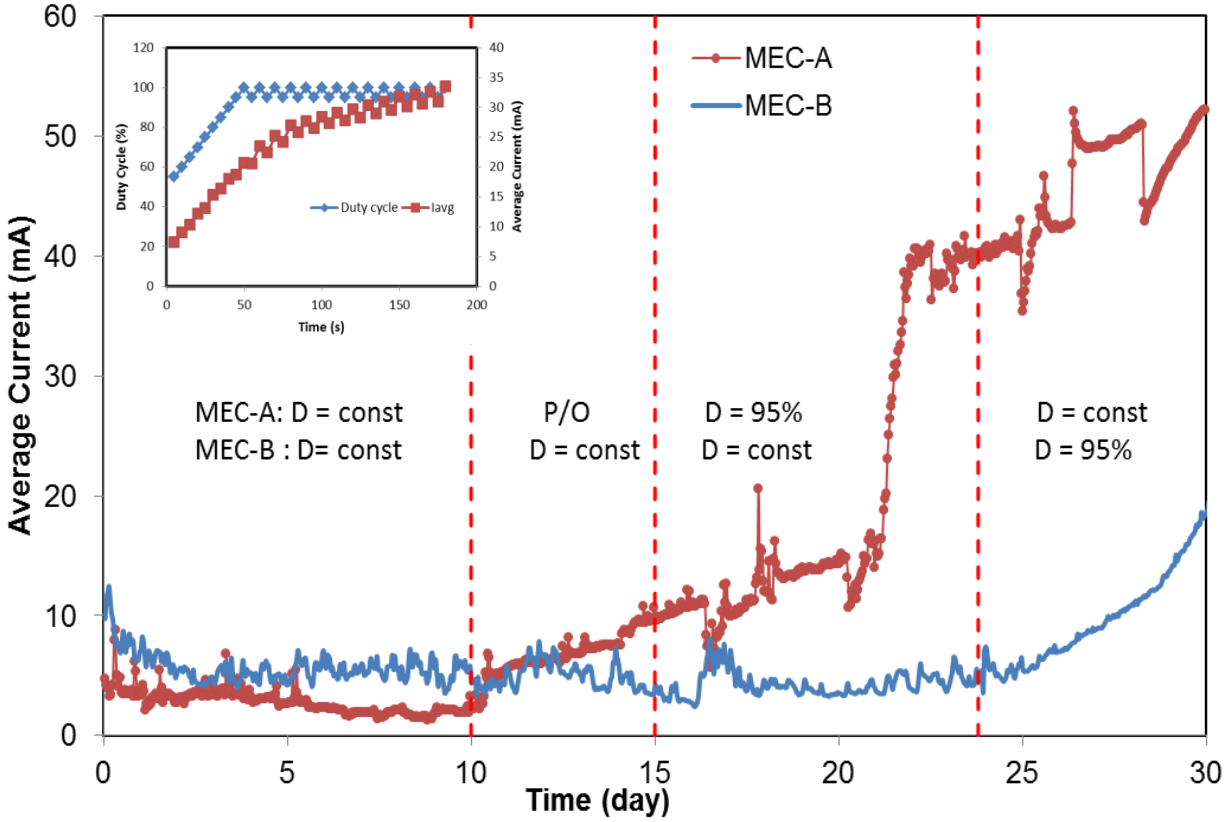

Figure 3.3: Average current observed during MEC-A and MEC-B operation during periodic applied voltage and fixed applied voltage modes of operation. Periodic mode of operation was started at day 10 (MEC-A, periodic operation). Modes of operation were switched at day 24 (MEC-B on/off and MEC-A fixed), as indicated by vertical dashed lines. Inset shows results of the perturbation-and-observation test performed on day 12 to optimize *D*.

As a result of this observation, in phase 3 of the test MEC-A continued to operate in the on/off mode at a *D* of 95% and T_c of 5 s, while maintaining MEC-B at *D* = 100% (fixed applied voltage). The resulting long-term performance of the two MECs in terms of average currents is shown in Figure 3.3 (day 15-24). Clearly, MEC-A operation in the on/off mode led to a

progressively increased average current. At the same time, MEC-B current did not improve, although it was operated at the same applied voltage, flow rate and influent carbon source concentration as MEC-A. While some differences between performances of the two MECs might be expected due to biological nature of this bioelectrochemical system (e.g. variations in biofilm growth rates and/or microbial populations, inhomogeneity of flow through granular carbon electrodes, etc), the observed differences in average currents by the end of the test on day 24 were remarkable. While MEC-A current exceeded 40 mA, MEC-B current remained at around 6 mA, same as on day 10.

Interestingly, a sharp increase in MEC-A average current between days 19-23 was noticeable. It can be hypothesized that this increase was reflected higher density (or activity) of bioelectrochemically active biofilm. In particular, significant delay in the formation of bioelectrochemically active cathodic biofilm during MEC tests with biocathodes was previously observed (Pinto et al. 2010). Accordingly, we can attribute current increase between days 10-19 to the anodophilic biofilm formation at the anode and the increase between days 19-23 to the proliferation of electroactive microbial populations at the cathode.

Additional confirmation of better MEC-A performance was obtained from the analysis of acetate concentration in the effluent and its comparison with MEC-B acetate removal efficiency. As shown in Figure 3.4, shortly after the startup of the on/off operation the effluent acetate concentration of MEC-A considerably decreased, while it remained at the same level in the MEC-B effluent. It can be concluded that MEC-A provided better COD removal efficiency (90% and 78% for MEC-A and MEC-B, respectively). Fast current increase in MEC-A between days 19-23 was not accompanied by a corresponding decrease in the effluent acetate concentration (Fig.3.4). It can be argued that at already low acetate concentration of 103-117 mg L^{-1} corresponding to this period, the kinetics of COD consumption was carbon source - limited for methanogenic microorganisms. The anodophilic microorganisms are known to exhibit higher affinity for acetate (Pinto et al. 2010) and it can be suggested that the increase in average MEC-A current was indicative of the population shift, where a larger part of acetate was consumed by the electroactive microorganisms due to increased current. Columbic efficiency calculations based on current and COD measurements between days 20-23 suggested values of 20-23% and 4-5% for MEC-A and MEC-B, respectively.

To confirm the hypothesis of improved MEC performance due to periodic power supply disconnection, in phase 4 of the test the operation strategies of the two MECs were changed. On day 23 MEC-B was connected to the electronic switch to enable the on/off operation (D = 95%), while MEC-A was connected to fixed applied voltage. This test continued until day 30. Shortly after the startup of the on/off operation for MEC-B the average current improved, reaching 22 mA by the end of the test (Figure 3.3). At the same time, MEC-A current remained nearly constant at 40-43 mA. Although MEC-B current did not reach the level observed in MEC-A, the increase of the average current was accompanied by a decrease of the effluent acetate concentration (Fig. 3.4). Overall, the test strongly suggested a positive link between the improved MEC performance and the on/off mode of operation, at least at a D value of 95%.

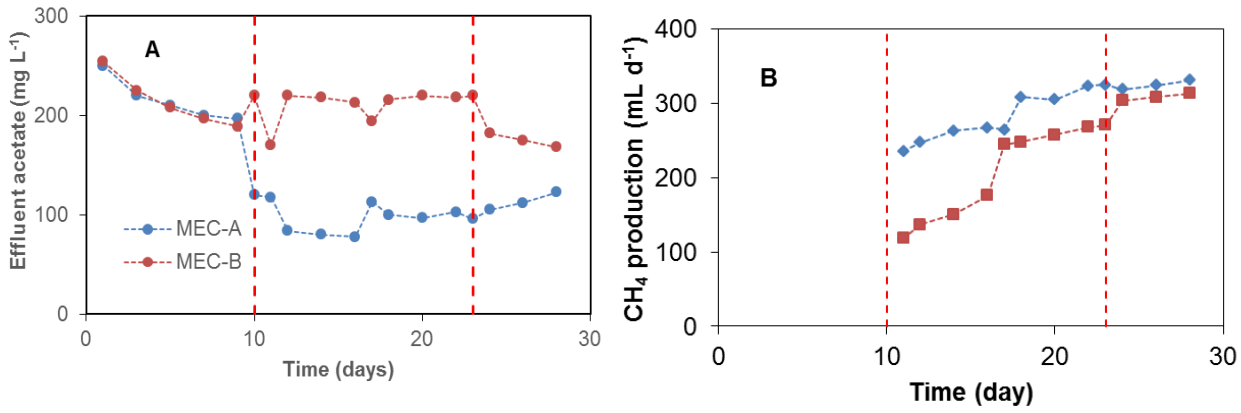

Figure 3.4: (A) Effluent acetate concentration and (B) CH_4 production in MEC-A and MEC-B reactors. MEC-A operated in on/off mode between day 10-23 and MEC-B between day 24-30. CH_4 measurements were started on day 11 of the test.

4.5.2 Online MEC monitoring and electrochemical characterization

To achieve real-time monitoring of key MEC electrochemical parameters, such as internal resistance and capacitance, a recently described model-based monitoring approach was used (Hussain et al. 2018). This approach involves on-line estimation of key electrical internal parameters by using a simple equivalent electrical circuit (EEC) model. The simplicity of the EEC model enables its analytical solution and provides means for estimating the internal resistance components associated with ohmic and activation losses (R_0 and R_1) as well as the

internal capacitance (*C*). Detailed description of the parameter estimation procedure is given in Appendix-A. The on-line monitoring of MEC-A parameters was started on day 16 and continued until the end of the on/off mode of operation for this MEC (day 24). It was carried out simultaneously with on/off operation. On-line monitoring of MEC-B parameters was performed between days 24-30. The parameter estimation procedure was performed with an interval of 3 h and required approximately 3 min, i.e. it was non-disruptive.

Figure 3.5 shows results of MEC-A real-time monitoring during its operation at D = 95%. As might be expected from the average (per cycle) current values shown in Figure 3.3, both R_0 and R_1 estimations decreased over time with a total internal resistance estimation ($R_{int} = R_1 + R_2$) changing from 1.2 to 0.7 Ohm. At the same time, the estimated internal capacitance increased from 7.5 to 9.7 F. Several MFC studies suggested a link between the internal capacitance and the anodophilic biofilm thickness (Coronado et al. 2013) i.e. an increase in the estimated *C* could be attributed to the growth of electroactive biofilm, both at the anode and cathode.

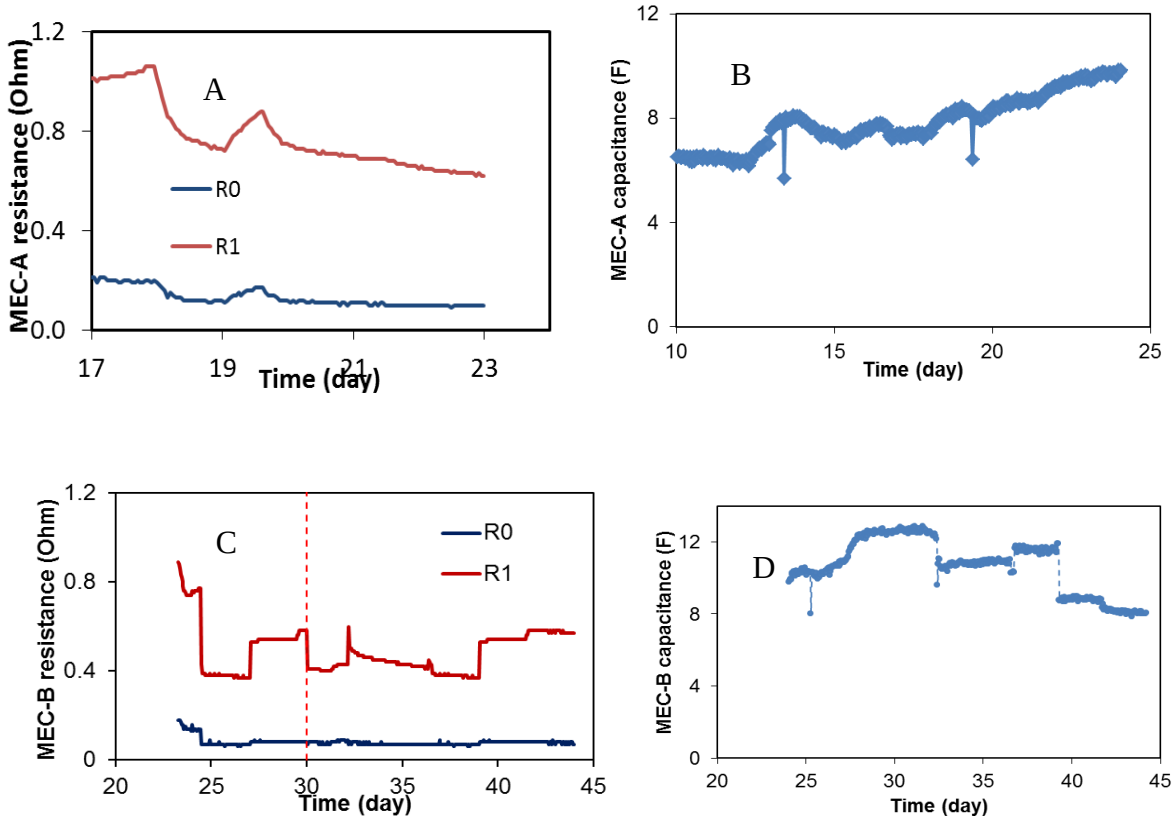

Figure 3.5: **(**A &C) Real time monitoring of internal resistance, and (B & D) capacitance values in MEC-A (days 17-23) and MEC-B (day 24-44) respectively. Red dotted line marks the change in influent concentration from acetate feed from day 1 to day 30 and brewery wastewater feed from day 31 to day 45.

Brewery wastewater with influent concentration of (2000 mg/L) was used in MEC-A and MEC-B from day 30 to day-45. MEC-B was operated at 95% duty cycle of applied voltage whereas, MEC-A with continuous power supply. Figure A.3 in appendix D presents the results.

The EEC model-based parameter estimation was also carried out during the on/off mode of MEC-B operation on acetate (day 24-30). Furthermore, starting from day 31 of the experiment the influent feed composition of both MECs was changed from synthetic to brewery wastewater and the experiment was continued for another 15 days. During this time, the on/off mode of operation of MEC-B was continued with MEC-A maintained at a fixed applied voltage. Figure 3.6B shows average current values obtained during operation on brewery wastewater. As can be seen from this graph, by the end of the test MEC-B current almost approached that of MEC-A, which remained nearly at a constant value (current fluctuations are related to operational problems, such is feed pump failure). Figure 3.6A shows the effluent concentrations of MEC-A & MEC-B with influent fees as brewery wastewater.

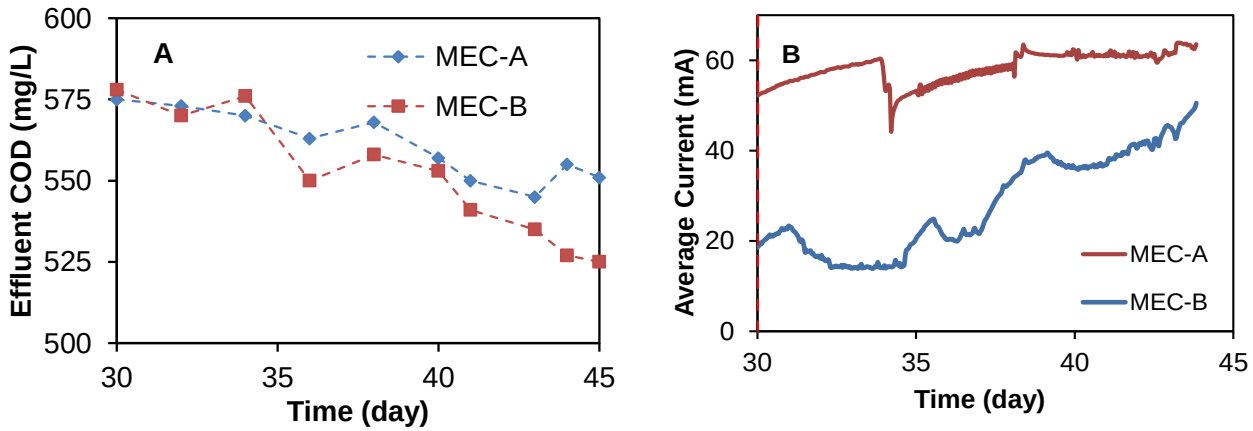

Figure 3.6: (A) MEC-A and MEC-B effluent COD concentrations and (B) current during operation on brewery wastewater. MEC-B was operated in the on/off mode, while MEC-A was operated at a fixed applied voltage.

During MEC-B operation with periodic disconnection of the power supply, both R_0 and R_1 components of the total internal resistance estimated with the real time monitoring algorithm decreased from 1.1 to 0.7 Ohm (Figure 3.5B). Also, the internal capacitance increased (Fig. 3.5D), which is similar to R_{int} and *C* behavior in MEC-A during on/off operation. Once the feed composition was changed from acetate to brewery wastewater (day 30), R_{int} values of MEC-B remained almost unchanged, while *C* somewhat decreased (Fig. 3.5) in spite of a significantly higher current. It can be hypothesized that by this time electroactive biofilms in the anode and cathode compartments were well developed. Although brewery wastewater had higher COD content (2 g L^{-1}), it also had lower conductivity (3-5 mS cm^{-1}). Thus, the electroactive biofilm thickness remained unchanged, while its metabolic activity increased, as indicated by the increased current in MEC-B. Columbic efficiency calculations based on measurements collected between days 43-45 suggested values of 28% and 22% for MEC-A and MEC-B, respectively, i.e. the contribution of electroactive microorganisms declined in MEC-A, while it increased in MEC-B as compared to day 30.

In addition to real-time parameter estimation, R_{int} and *C* were estimated using conventional electrochemical techniques (voltage scan test and cyclic voltammetry for estimating R_{int} and *C*, respectively). Voltage scan tests were conducted on day 20, during MEC operation on acetate and then repeated during the brewery wastewater part of the test, on day 45 as shown in figure 3.7. The estimated total internal resistance values are given in Table 3.1. Clearly, the on/off mode of operation helped to reduce R_{int} of MEC-A during its operation on acetate. Also, R_{int} of MEC-B was substantially decreased by the end of the test, as compared to its initial R_{int} value. Real-time model-based parameter estimation procedure resulted in somewhat lower R_{int} values as compared to the values estimated using voltage scans. However, the on-line estimation procedure correctly estimated the trends, was non-disruptive, and did not involve broad variations in MEC applied voltage needed for the voltage scans (0.2 – 1.6V). Also, each voltage scan required 80 min, as opposed to only 3 min for the model-based estimation.

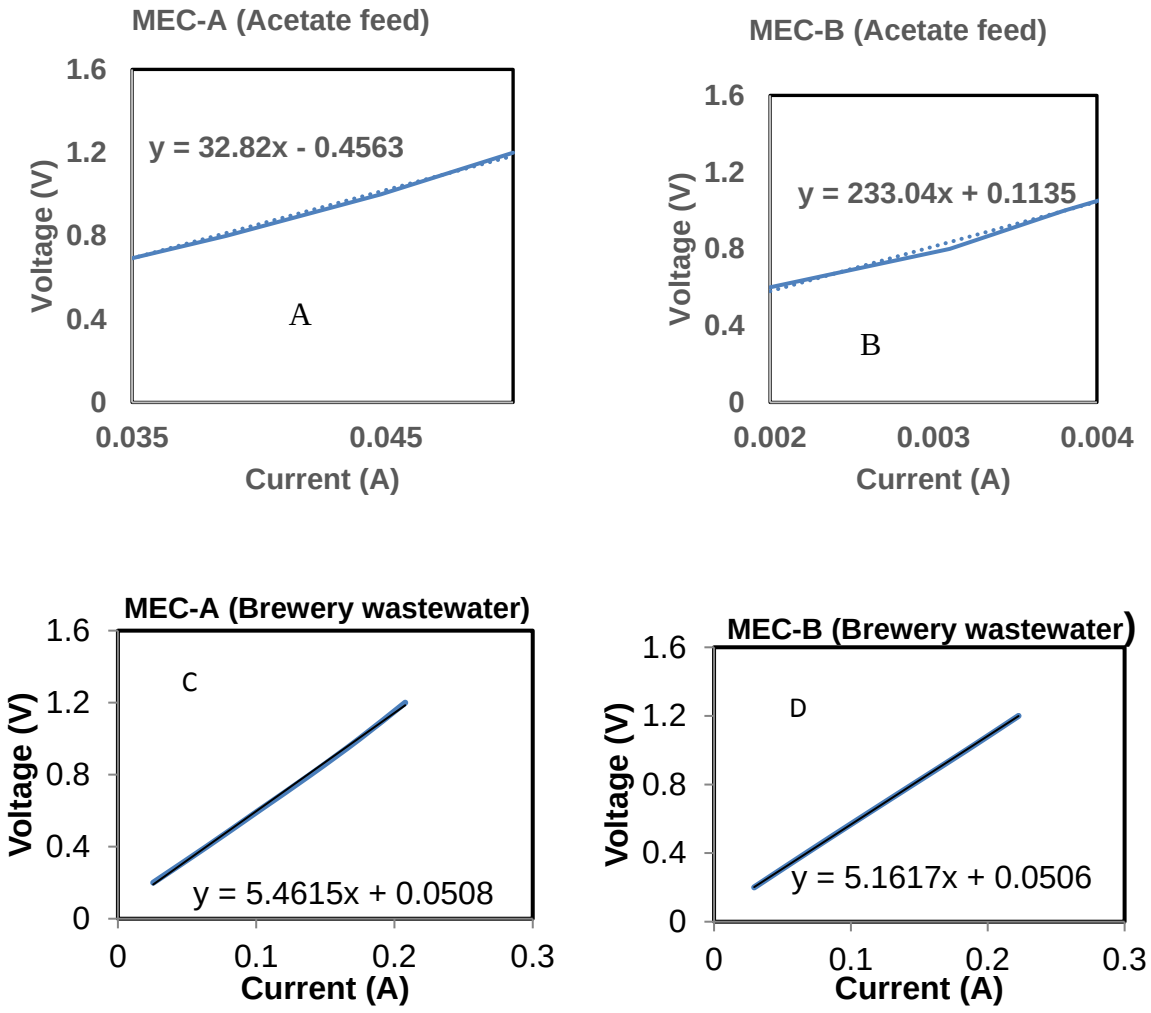

Figure 3.7: (A&B) Voltage scan test MEC-A & MEC-B with acetate feed. (C&D) Voltage scan test MEC-A & MEC-B with brewery wastewater.

Table 3.1: Internal resistance and capacitance of MEC-A and MEC-B. Estimations are based on voltage scan tests and cyclic voltammetry respectively

Feed	**MEC-A**		**MEC-B**	
	R_{int} (Ω)	C (F)	R_{int} (Ω)	C (F)
Acetate	32.3[a]	n/a	233[a]	n/a
Brewery WW	5.5[b]	n/a	5.2[b]	2.9[c]

a – Test on day 20

b – Test on day 45

c – Test on day 47

It should be noticed that internal capacitance estimations by the cyclic voltammetry technique were even more lengthy and disruptive, as electrode polarity had to be changed to estimate both anode and cathode double layer capacitance. While the model-based procedure appeared to overestimate internal capacitance, most likely the estimated trends of C changes were correctly captured. Graphs shown in Figure 3.8 show the relation between different scan rates and current, which was used for the calculation of internal capacitance.

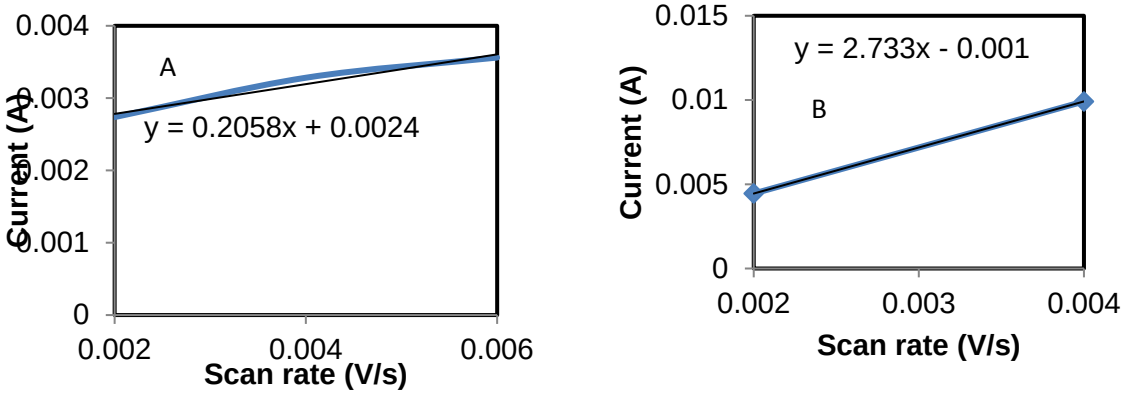

Figure 3.8: (A&B) Cyclic voltammetry on MEC-B day-47 with anode and cathode as working electrodes respectively.

Overall, while some discrepancy was observed between the estimations obtained through electrochemical tests and using the on-line estimation procedure, it is important to underline that the electrochemical tests are highly disruptive and laborious. For example, one voltage scan required approximately 1 h and during this period MEC operation was disrupted, e.g. lower COD removal might be expected at applied voltages below 1 V. Furthermore, a voltage increase above 1.4 V could result in the onset of water electrolysis, which is harmful for the strictly anaerobic andodophilic bacteria. Similarly, cyclic voltammetry requires MEC operation at several applied voltages and scan rates, which can damage the electroactive biofilm at the anode and cathode or require long recovery time. In contrast, the on-line estimation approach enables non-disruptive MEC monitoring and can be used as an indicator of MEC performance and the state of the electroactive biofilm, e.g. for MEC state diagnostics and as a method for timely detection of significant changes in the influent carbon source concentration and/or MEC performance due to the presence of toxic substances in wastewater.

4.5.3 Conceptual biofilm model

The observation of improved long-term performance in a MEC operated with periodic disconnection of applied voltage can be attributed to multiple factors, including process electrochemistry and microbiology. Indeed, improved performance of an MFC operated with periodic disconnection from electrical load was hypothesized to be related to reduced activation losses (Coronado et al., 2013), a hypothesis, which requires a thorough electrochemical investigation. Changes in microbial populations due to a complex non-linear dynamics of a biological system subjected to periodic operation could be another plausible explanation. Indeed, periodic disconnection of applied voltage might affect dynamics of carbon source consumption by electroactive (anodophilic) microorganisms at the anode. Considering the coexistence of anodophilic and methanogenic populations in the biofilm (Pinto et al., 2010, Torres et al., 2009), the methanogenic populations might be also affected. Furthermore, periodic variations in the anodophilic activity might also affect electroactive microbial populations at the cathode.

To discuss implications of the on/off mode of MEC operation, a conceptual biofilm model can be proposed. The conceptual model considers the electroactive and methanogenic microbial populations are considered. While these populations can be evenly distributed in the biofilm, it is more likely to expect biofilm stratification, with the electroactive species predominantly present

in the electrode (anode) vicinity, as shown in Figure 3.9. Although both direct and mediator-based electron transfer mechanisms were experimentally confirmed in anodophilic species, direct electron transfer has the advantage of lower internal resistance. The methanogenic microorganisms might be expected to populate the remaining biofilm. Moreover, a more complex multi-layer biofilm structure can be expected in MEC fed with complex carbon sources, i.e. fermentative bacteria could proliferate at the biofilm surface (Tartakovsky and Guiot, 1997).

The proposed layered structure of the electroactive biofilm also agrees with the known kinetics of carbon source consumption by the anodophilic and methanogenic species. As compared to anodophilic bacteria, acetoclastic methanogens have lower specific growth rate and lower affinity to acetate, i.e. these species require relatively high carbon source concentration for growth (Martin et al., 2010). In a two-layer biofilm shown in Figure 3.9, a gradient of carbon source within the biofilm is expected, as shown in several previous works (Arcand et al., 1994, Flora et al., 1995, Tartakovsky and Guiot, 1997).

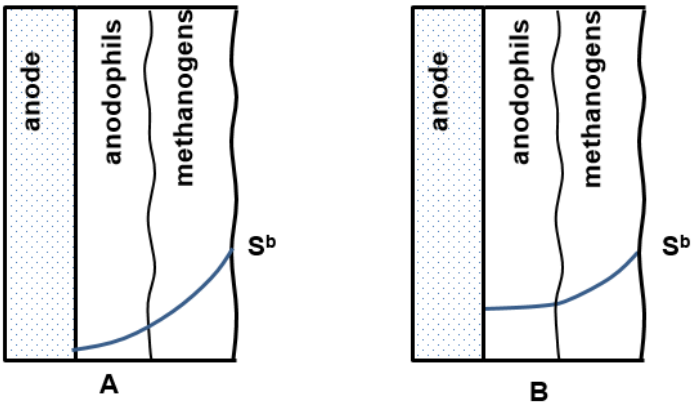

Figure 3.9: Conceptual model of carbon source distribution in a two layer electroactive anodic biofilm with anodophilic and methanogenic microbial populations. A – connected power supply, $U_s > 0$; B – disconnected power supply, $U_s = 0$.

The two-layer biofilm structure enables both microbial populations to coexist, with methanogenic microorganisms exposed to higher acetate concentrations and anodophilic microorganisms growing at lower levels of acetate. In fact, such two-layer structure could explain higher COD

removal rates experimentally observed in MECs as compared to conventional anaerobic reactors (Asztalos and Kim, 2015, Liu et al., 2016).

Periodic disconnection of applied voltage does not affect metabolism of methanogenic populations. However, as proposed in the conceptual biofilm model (Figure 3.9) methanogens are expected to grow in the outer biofilm layer, thus creating carbon-limiting conditions for the growth and metabolic activity of the anodophilic populations and preventing carbon source consumption in the anodophilic part of the biofilm. Only a very thin layer of anodophilic biofilm can be developed and this biofilm contributes to a small fraction of COD removal. At the same time, low affinity of methanogenic microorganisms to acetate implies that at acetate concentrations below approximately 100-200 mg/L the methanogens are not efficiently removing acetate. High current observed immediately after the power supply is reconnected can be explained both by internal (double layer) capacitance of the biofilm (charge accumulation and storage in the biofilm) and by higher carbon source availability in the anodophilic biofilm layer shown in the conceptual model diagram (Figure 3.9). Considering higher growth rates of anodophilic microorganisms as compared to the methanogens in the presence of a carbon source, it can be hypothesized that the on/off mode of operation provided long-term advantages and increased the fraction of the electroactive anodophilic species in the biofilm. Confirmation of this hypothesis could be achieved by direct analysis of anodophilic and methanogenic microorganisms using biomolecular tools.

4.6 Conclusion

This study proposes a novel approach of MEC operation in which the applied voltage is periodically disconnected. Although the on/off mode of operation does not appear to increase the average MEC current as compared to operation at a fixed applied voltage, it was observed to substantially improve MEC performance. Monitoring of key electrical parameters (MEC internal resistance and capacitance) was accomplished by estimating parameters of a simple EEC model in real time. This monitoring procedure confirmed decreased R_{int} and increased C values during on/off operation. Furthermore, long-term MEC performance characterized by the COD removal efficiency and current was observed to increase. Although the proposed approach for MEC operation requires a more comprehensive study, e.g. to optimize duty cycle based on long-term

MEC operation, it can be already considered for practical applications where stability and high COD removal are of importance.

CHAPTER 5 DYNAMIC MODELING OF A MICROBIAL ELECTROLYSIS CELL

This chapter describes two models of a microbial electrolysis cell (MEC). (i) Dynamic model of flow-through MEC, and (ii) one dimensional anodophilic biofilm model. The MEC model takes into account anodic and cathodic compartments of a flow-through MEC and simulates the two compartments as CSTR connected in series. The resulting model is able to simulate key MEC performance parameters such as the effluent carbon source concentration and the current. To calibrate the model, simulations are compared with the experimental data. The second modeling approach uses a simple one dimensional biofilm model to describe carbon source profile in the anodic compartment biofilm. Model simulations are used to predict current of an MEC operated with periodic power supply disconnection.

5.1 MEC design and operation

A horizontal flow-through MEC was used in the experiments. Design of this MEC is provided in Chapter 3. The MEC was fed with acetate stock solution and dilution water at a combined flow rate of 2 L d^{-1}, corresponding to a hydraulic retention time of one day based on the total reactor volume. Composition of the feed solution is provided in Chapter 2. To provide carbon source mixing, external re-circulation line was added. The recirculation returned part of the effluent to the influent stream at a flow rate of 9.6 mL min^{-1} (13.8 L/day). The acetate solution and the dilution water were fed to the reactors by using peristaltic pumps. Experiments were carried out by feeding MEC at an acetate concentration of 500 mg/L for first 13 days, then influent acetate concentration was increased to 1000 mg/L for the following 5 days. The reactor was operated at a room temperature of 21-22 °C. The experimental setup is shown in Figure 3.1.

5.2 Electrical measurements and numerical methods

The MEC was operated at an applied voltage of 1.5 V using a PW18-1.8AQ power supply (Kenwood Corp, Tokyo, Japan) interfaced with a computer. Current was measured with a 15 Ohm shunt resistance (R_{ext}) according to the diagram shown in Figure 3.1. MEC operation with periodic power supply disconnection (on/off operation) was achieved using a computer-controlled relay. Data acquisition board LabJack U3-LV (LabJack Corp., Lakewood, CO, USA) was used to control the relay and record power supply voltage (U_s), and voltage measured across

MEC (U_{MEC}). Voltage across the resistor (U_R) was calculated as the difference of U_s and U_{MEC} values.

Mathematical calculations for online monitoring of MEC current and simulation for modelling were performed in *Matlab R2015a* (Mathworks, Natick, MA, USA). For 1-D biofilm modeling simulations were carried out with different duty cycles (0-100%) and cycle length (10, 8 and 4 sec) to simulate various operating conditions during on/off MEC operation. For MEC simulations using dynamic model of a continuous flow-through MEC fixed applied voltage was assumed.

Numerical parameter estimation procedure of the model parameters is explained in Chapter 2. Objective function is defined by Eq. 2.3.

Sensitivity analysis was carried out by considering the following model equation:

$$\frac{dx}{dt} = f(t, x, u, \theta) \tag{4.1}$$

The output equation is

$$y(t) = g(t, x, u, \theta) \tag{4.2}$$

where t is the time, x represents the vector of state variables, u is the input vector, y is the output vector and $\boldsymbol{\theta}$ is the parameter vector. In order to find parameters with the maximum influence on the model outputs, normalized sensitivity functions of the outputs with respect to each parameter were calculated as described by Kravaris et al. 2013:

$$\frac{d}{dt}\left(\frac{\partial x}{\partial \bar{\theta}}\right) = \frac{\partial f}{\partial x}\left(\frac{\partial x}{\partial \bar{\theta}}\right) + \frac{\partial f}{\partial \bar{\theta}} \tag{4.3}$$

$$\frac{\partial \bar{y}}{\partial \bar{\theta}} = \frac{d\bar{y}}{dy}\left[\frac{\partial g}{\partial x}\left(\frac{\partial x}{\partial \bar{\theta}}\right) + \frac{\partial g}{\partial \bar{\theta}}\right] \tag{4.4}$$

The correlation between the sensitivity functions was calculated for the selected parameters. The confidence intervals were obtained using covariance matrix by taking the inverse of Fisher information matrix F.

$$F = \bar{S}^T \sum \bar{S} \ , \tag{4.5}$$

where $\bar{S}$ is the sensitivity matrix for each output and $\sum$ is the matrix containing scale factors, $1/\sigma^2$ for each output. σ^2 is the mean square error for each model output.

5.3. RESULTS AND DISCUSSION

5.3.1 Dynamic Model of a Continuous Flow Microbial Electrolysis Cell

5.3.1.1 Model description and model assumptions

The proposed model assumes two MEC compartments. In the first (anodic) compartment main microbial activities consist of carbon source hydrolysis and degradation, either by methanogenic or anodophilic microorganisms. In the second (cathodic) compartment the hydrolytic and methanogenic activities are also present, but bioelectrochemical hydrogen production also results in methane production from carbon dioxide and hydrogen. The same set of differential equations describing the dynamics of microbial populations and carbon source transformations is used in both compartments. Each compartment is modeled as a CSTR, i.e carbon source and biomass distribution within each compartment are neglected. Nevertheless, this simple model captures the principal dynamics of a flow-through MEC and can be used for qualitative studies of this complex system. Figure 4.1 presents the schematic diagram of MEC.

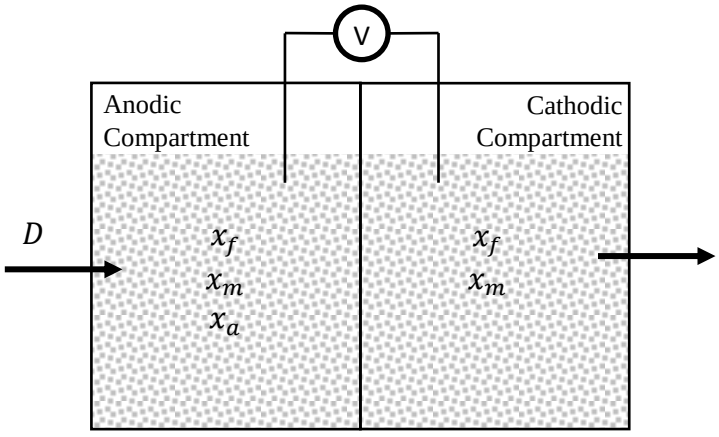

Figure 4.1: Schematic diagram of MEC

The following equations describe kinetics and state variables of the model. Description of the symbols is given in Table 4.1

A. Kinetic dependencies

Fermentative biomass growth:

$$\mu_f^i = \mu_{max,f}^i \left(\frac{X_S^i}{K_{S,f}+X_S^i}\right). \quad (4.6)$$

Anodophilic biomass growth

$$\mu_{ma}^i = \mu_{max,ma}^i \left(\frac{S_S^i}{K_{S,m}+S_S^i}\right) \quad (4.7)$$

Methanogenic biomass growth

$$\mu_{mh}^i = \mu_{max,mh}^i \left(\frac{S_{H2}^i}{K_{H2,m}+S_{H2}^i}\right) \quad (4.8)$$

Anodophilic biomass growth

$$\mu_a^i = \mu_{max,a}^i \left(\frac{S_S^i}{K_{S,a}+S_S^i}\right)\left(\frac{V_{app}^i}{K_V+V_{app}^i}\right) \quad (4.9)$$

Hydrolysis of solids

$$b_h = k_{h,f} \left(\frac{X_S^i/X_{B,f}^i}{K_X+X_S^i/X_{B,f}^i}\right) \quad . \quad (4.10)$$

B. Biofilm detachment (α^i)

A standard logistic function is used to describe biofilm detachment:

$$X_{B,tot} = X_{B,f}^i + X_{B,m}^i + X_{B,a}^i \quad (4.11)$$

$$\alpha^i = \frac{1}{1+e^{\left(X_{max}^i - X_{B,tot}\right)}} \quad (4.12)$$

C. Fermentative biomass ($X_{B,f}^i$)

$$\frac{dX_{B,f}^i}{dt} = \left(\mu_f^i - b_f - D\alpha^i\right)X_{B,f}^i + D\alpha^{i-1}X_{B,f}^{i-1} \quad (4.13)$$

D. Acetoclastic and hydrogenotrophic methanogenic biomass ($X_{B,m}^i$)

$$\frac{dX_{B,m}^i}{dt} = \left(\mu_{ma}^i + \mu_{mh}^i - b_m - D\alpha^i\right)X_{B,m}^i + D\alpha^{i-1}X_{B,m}^{i-1} \quad (4.14)$$

E. Anodophilic biomass ($X_{B,a}^{i}$)

$$\frac{dX_{B,a}^{i}}{dt} = \left(\mu_a^i - b_a - D\alpha^i\right)X_{B,a}^{i} + D\alpha^{i-1}X_{B,a}^{i-1} \tag{4.15}$$

F. Slowly biodegradable particulate substrate (X_S^i)

$$\frac{dX_S^i}{dt} = \underbrace{(1-f_P)\left(b_f X_{B,f}^i + b_m X_{B,m}^i + b_a X_{B,a}^i\right)}_{\text{Decay of biomass}} - \underbrace{b_h X_{B,f}^i}_{\text{Hydrolysis}} + \underbrace{D\left(X_S^{i-1} - X_S^i\right)}_{\text{Flow term}} \tag{4.16}$$

G. Readily biodegradable soluble substrate (S_S^i)

$$\frac{dS_S^i}{dt} = \underbrace{-\frac{\mu_f^i}{Y_{S,f}}X_{B,f}^i - \frac{\mu_{ma}^i+\mu_{mh}^i}{Y_{S,m}}X_{B,m}^i - \frac{\mu_a^i}{Y_{S,a}}X_{B,a}^i}_{\text{Growth of biomass}} + \underbrace{b_h X_{B,f}^i}_{\text{Hydrolysis}} + \underbrace{D\left(S_S^{i-1} - S_S^i\right)}_{\text{Flow term}} \tag{4.17}$$

Equations for sensitivity analysis are given below

$$\frac{\partial S_S^i}{\partial \mu_{max,a}^i} = -\frac{X_{B,a}^i}{Y_{S,a}}\left(\frac{S_S^i}{K_{S,a}+S_S^i}\right)\left(\frac{V_{app}^i}{K_V+V_{app}^i}\right) \tag{4.18}$$

$$\frac{\partial S_S^i}{\partial K_{S,a}} = \frac{X_{B,a}^i}{Y_{S,a}}.\mu_{max,a}^i.S_S^i\left(K_{S,a}+S_S^i\right)^{-2}\left(\frac{V_{app}^i}{K_V+V_{app}^i}\right) \tag{4.19}$$

Parameter Estimation

Three model parameters (*Ka*, *μmax*, and ***∂***) were estimated by minimizing the mean square error in the objective function (Eq-1) between the model outputs and the experimental data for current and effluent substrate concentration by using *fminsearch* in Matlab 2015a. Estimated values for *Ka*, *μmax*, and ***∂*** are 145, 0.3178, 0.0421 respectively (units are mentioned in table-1). With a 95 % confidence level, the intervals of confidence were 1%, 0.03% and 56.3% for *μmax, Ka* and respectively

Sensitivity Analysis

Sensitivity analysis was carried out to reduce the number of model parameters for parameter estimation procedure. The three model parameters (*Ka*, *μmax*, and delta (***∂***)) with the highest impact factor were selected for parameter identification. Procedure of sensitivity analysis is already explained in section 4.2 as given by the equations (4.1- 4.5). The magnitude of the effect of *Ka*, and *μmax* and ***∂*** on the model outputs (current and effluent substrate concentration) are shown in the figure 4.2. According to the sensitivity analysis, K_a shows the highest effect on

substrate concentration and also on current. Figure 4.2 shows the sensitivity profiles of the three parameters (*Ka*, *μmax*, and *∂*).

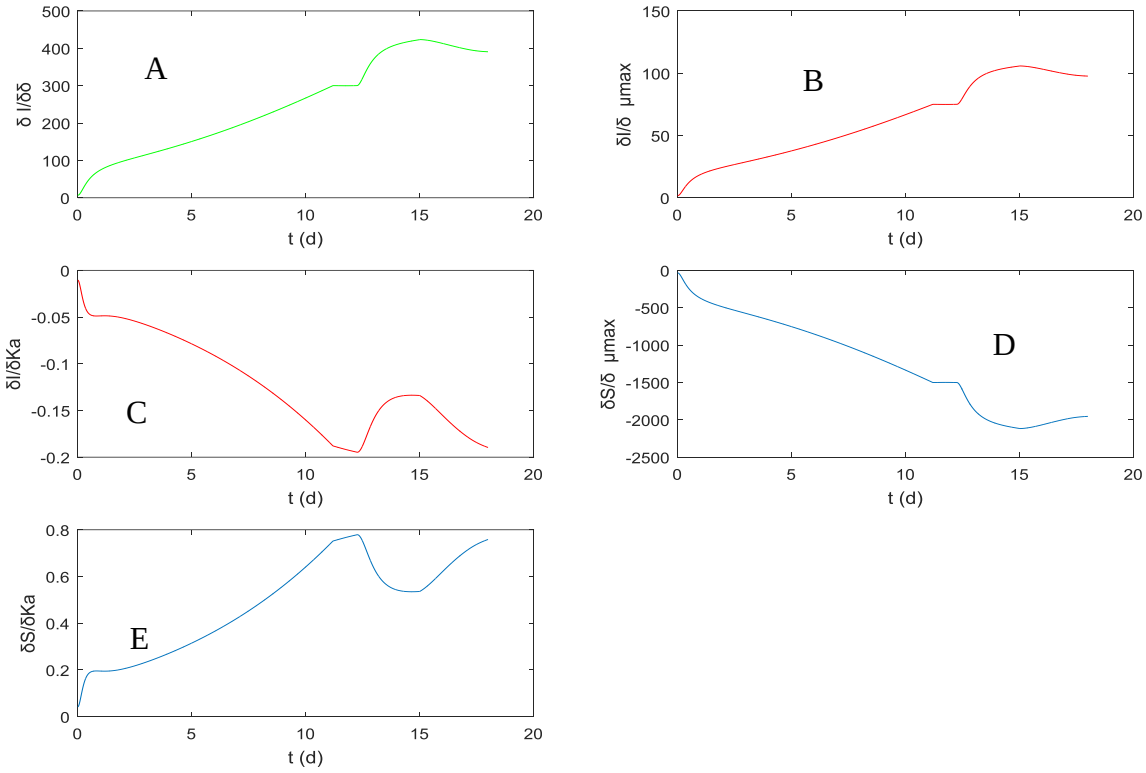

Figure 4.2: sensitivity analysis of: (A) current with respect to delta (δ), (B) current with respect to maximum specific growth rate of anodophilic bacteria (μ_{max}), (C) current with respect to half-saturation coefficient of soluble substrate for anodophilic bacteria(K_a), (D) effluent substrate concentration with respect to maximum specific growth rate of anodophilic bacteria and, (E) effluent substrate concentration with respect to half-saturation coefficient of soluble substrate for anodophilic bacteria.

Values of current are more sensitive to maximum specific growth rate of anodophilic bacteria (μ_{max}), and to the to half-saturation coefficient of soluble substrate for anodophilic bacteria (*Ka*) as shown in figure 4.2 (B & C) whereas effluent substrate concentration changes greatly with the change in half-saturation coefficient of soluble substrate for anodophilic bacteria (*Ka*).

5.3.1.2 Simulation results

Figures (4.3) and (4.4) show MEC simulation results based on model equations (4.7-4.19).

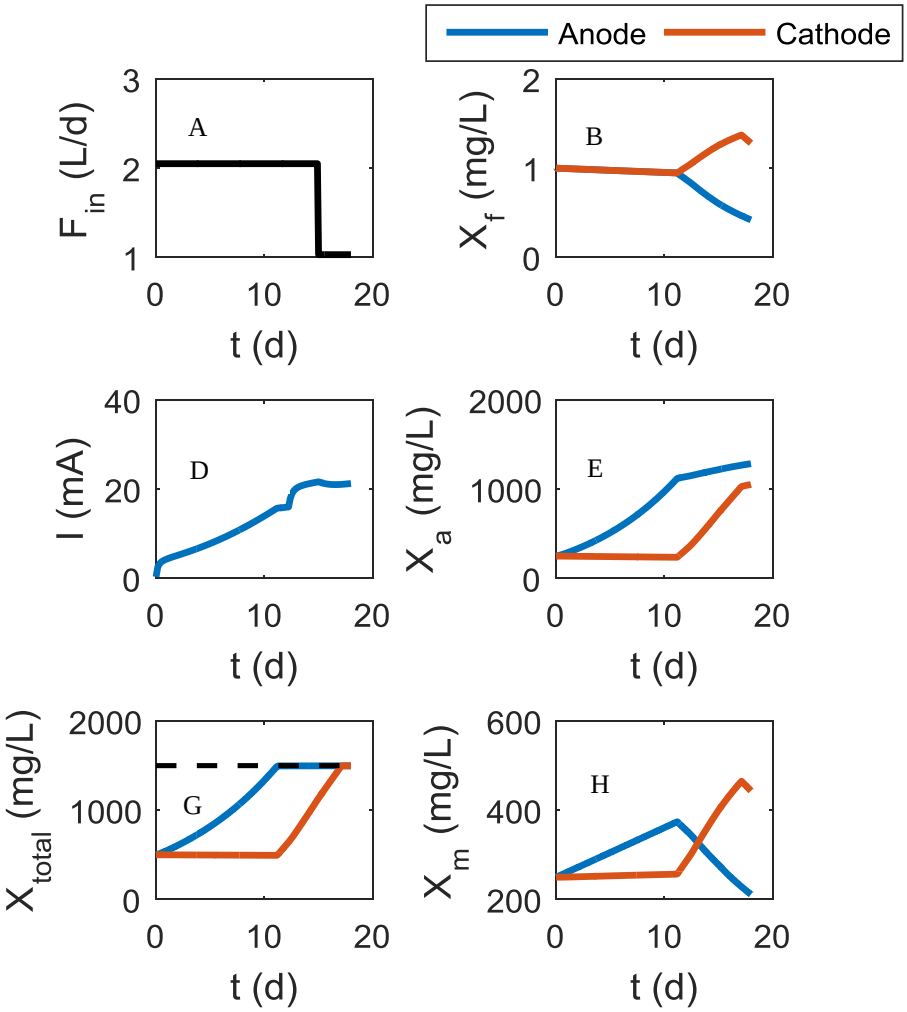

Figure 4.3: (A) Influent flow rate, (B&C) concentration of Fermentive bacteria and Concentration of biodegradable particulate substrate respectively, (D) simulation of current flowing through MEC, (E) concentration of anodophilic bacteria, (F) concentration of biodegeradable soluble substrate, (G) Total microbial concentration, (H) concentration of methanogenic bacteria and, (I) concentration of soluble hydrogen

Influent acetate concentration was 500 mg/L for 15 days and later it was increased to 1000 mg/L. There is no particulate substrate in the influent and effluent streams.

Figure 4.4 compares model outputs with the experimental values of current (*I*) and effluent concentration (*Ss*). Figure 4.4 (D) shows the comparison between experimental and simulated current values. The graph shows a reasonable fit. The increase in current from day 13 to day 15 can be explained by the increase in influent acetate concentration. Model is also able to correctly describe carbon source consumption, as can be seen from Figure 4.4(D), which shows good fit between the experimental data and simulated values for effluent acetate concentration.

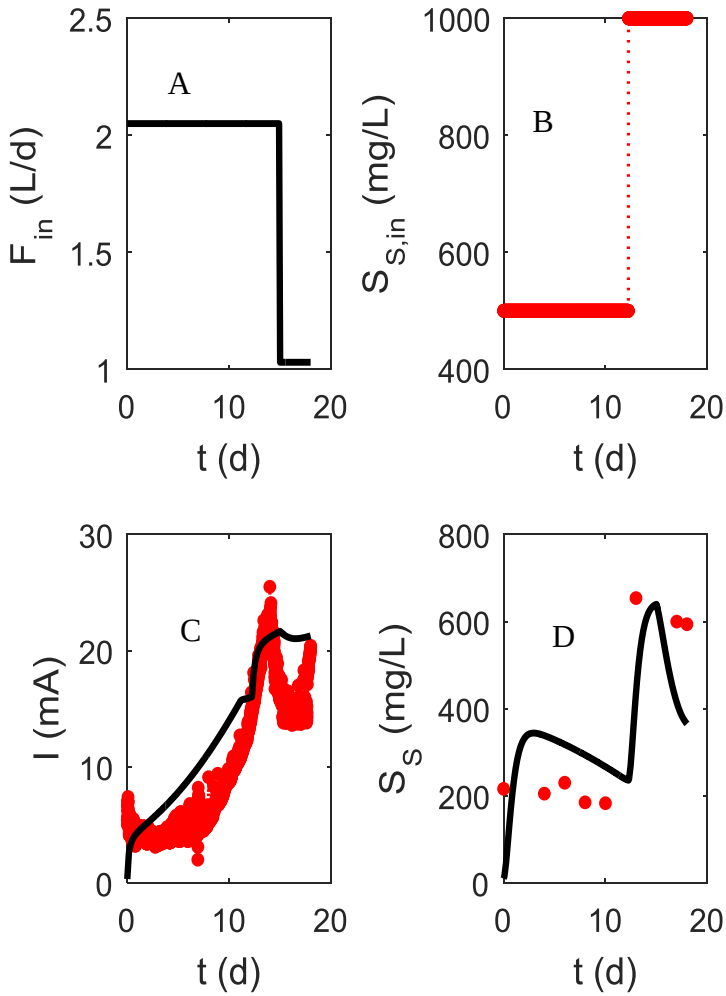

Figure 4.4: (A) Influent flowrate, (B) influent concentration, (C) current and, (D) effluent concentration.

As depicted in the Figure (4.4), the model provides a good fit between the experimentally measured and simulated current values. Model parameters are given in Table 4.1.

Table 4.1: Model parameters

Parameter	Description	Value	Units	Note	Source
Kinetic parameters					
$\mu_{max,a}$	Maximum specific growth rate of $X_{B,a}$	5	d^{-1}	Calibrated	Batstone et al. (2002)
$\mu_{max,f}$	Maximum specific growth rate of $X_{B,f}$	5	d^{-1}	Calibrated	Batstone et al. (2002); Henze et al. (2000)
$\mu_{max,ma}$	Maximum specific growth rate of acetoclastic $X_{B,m}$	5	d^{-1}	Calibrated	Batstone et al. (2002); Henze et al. (2000)
$\mu_{max,mh}$	Maximum specific growth rate of hydrogenotrophic $X_{B,m}$	5	d^{-1}	Calibrated	Batstone et al. (2002); Henze et al. (2000)
b_a	Decay rate of $X_{B,a}$	0.01	d^{-1}	Assumed	Coronado et al. (2013)
b_f	Decay rate of $X_{B,f}$	0.01	d^{-1}	Assumed	Coronado et al. (2013)
b_m	Decay rate of $X_{B,m}$	0.01	d^{-1}	Assumed	Coronado et al. (2013)
$K_{S,a}$	Half-saturation coefficient of S_S for $X_{B,a}$	20	mg-S_S L^{-1}	Assumed	
$K_{S,f}$	Half-saturation coefficient of S_S for $X_{B,f}$	30	mg-S_S L^{-1}	Assumed	
$K_{S,m}$	Half-saturation coefficient of S_S for $X_{B,m}$	100	mg-S_S L^{-1}	Assumed	
$K_{H2,m}$	Half-saturation coefficient of S_{H2} for $X_{B,m}$	100	mg-S_S L^{-1}	Assumed	
K_V	Half-saturation/Inhibition coefficient of V_{app}	0.25	V	Assumed	
K_X	Half-saturation coefficient of X_S for $X_{B,f}$	0.75	-	Assumed	
$k_{h,f}$	Maximum specific hydrolysis rate for $X_{B,f}$	20	d^{-1}	Assumed	
Stoichiometric parameters					
$Y_{H2,a}$	Yield factor of S_{H2} for $X_{B,a}$	0.05	mg-S_{H2} mg-X_B^{-1}	Assumed	
$Y_{H2,f}$	Yield factor of S_{H2} for $X_{B,f}$	0.05	mg-S_{H2} mg-X_B^{-1}	Assumed	
$Y_{S,a}$	Yield factor of S_S for $X_{B,a}$	0.05	mg-S_S mg-X_B^{-1}	Assumed	
$Y_{S,f}$	Yield factor of S_S for $X_{B,f}$	0.05	mg-S_S mg-X_B^{-1}	Assumed	
$Y_{S,m}$	Yield factor of S_S for $X_{B,m}$	0.05	mg-S_S	Assumed	

			mg-X_B^{-1}		
f_P	Fraction of dead X_B yielding inert particulates	0.08	%	Assumed	
Other parameters					
F	Faraday's constant	96480	C mol-e^{-1}	-	
m	Number of electrons exchanged per mole of S_S (acetate)	8	mol-e^-	-	
δ	Current conversion factor from S_S consumed by $X_{B,a}$	0.1	mA L mg-X_B^{-1}	Assumed	
γ	Molecular weight of S_S (acetate)	60.05	Mg-S_S mol-S_S^{-1}	-	

Overall, this modeling approach can be used to predict MEC current, carbon source effluent concentration. Such model application requires prior knowledge of model parameters listed in Table 4.1.

5.3.2 1-Dimensional anodophilic biofilm model

5.3.2.1 Model formulation

The one dimensional biofilm model described in this section portrays biofilm expected to be formed at the MEC anode. This biofilm consists of anodophilic microorganisms consuming carbon source (e.g. acetate). The model is used to simulate substrate concentration and substrate consumption rate across the biofilm of an MEC operated with periodic disconnection of power supply (on/off operation). The model is capable of simulating current in the MEC based on substrate consumption rate at different duty cycles and cycle lengths of applied voltage.

Carbon source concentration across the biofilm is mainly dependent on the diffusivity and the reaction rate. The model is simplified by considering constant biomass concentration and only simulating carbon source distribution. The concentration of carbon source is the highest in the bulk liquid and gradually decreases as it is consumed in the biofilm as represented in Figure 4.5.

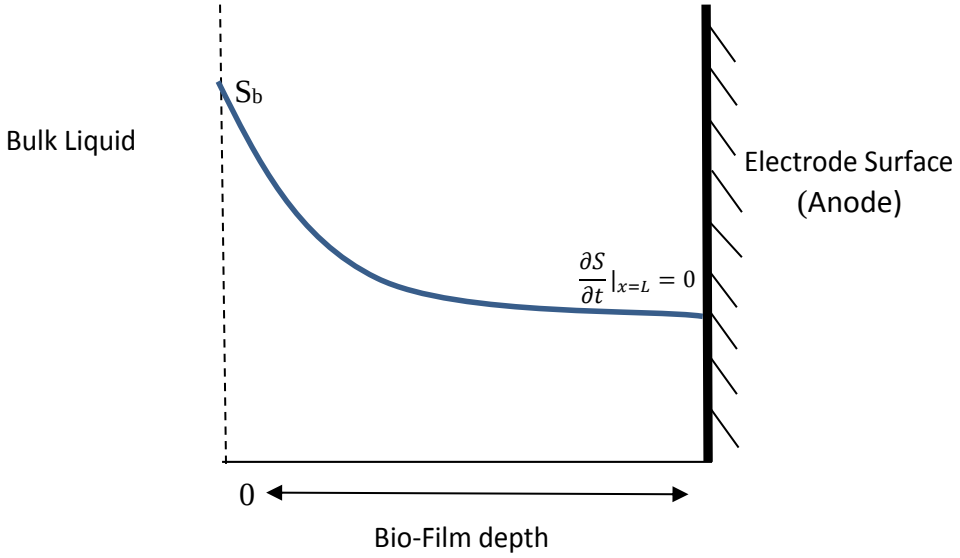

Figure 4.5: One-dimensional biofilm

The biofilm on the electrode surface is composed of anodophilic microorganisms. Current was calculated using algebraic expression of columbic efficiency (assuming 100% efficiency) and using change in substrate concentration. Reaction rate (r) is described by the multiple Monod terms. Reaction rate is dependent on (i) substrate concentration (S), (ii) voltage applied (V_{app}), and (iii) internal resistance (R_{int}).

$$r = f\left(S, R_{int}, V_{app}\right)$$

Internal resistance is expressed as the function of biofilm depth, i.e. it increases with increasing distance (x) from the electrode surface. MEC internal resistance is given by following equation.

$$R_{\text{int}} = R_0 + x * K_{\text{int}} \tag{4.20}$$

Where, R_0 is the internal resistance at the bulk, "x" represents the thickness of biofilm and K_{int} is the constant (Ohms/length)

Based on the above description, MEC model equation for substrate consumption is presented below:

$$\frac{\partial S}{\partial t} = D_s \frac{\partial^2 S}{\partial x^2} - \mu_{max} \frac{S}{(K_s + S)} X \cdot \left(\frac{V}{K_v + V}\right) \cdot \left(\frac{K_r}{R_{int} + K_r}\right) \tag{4.21}$$

The boundary conditions are defined below:

Substrate concentration in the bulk liquid = S_b

$$\frac{\partial S}{\partial t}|_{x=L} = 0 \qquad (4.22)$$

In equation (4.21) applied voltage (V) changes from 0 to U_{app} based on the duty cycle.

Current is calculated by using columbic efficiency.

$$I_{MEC} = \eta_{CE} * F * n * \Delta S \qquad (4.23)$$

Current was integrated over cycle length to calculate the average current.

$$I_{av} = \frac{1}{T_{total}} \int I_{mec}\, dt\,, \qquad (4.24)$$

where T_{total} represents the total cycle length (one period).

The proposed model is capable of describing current at different duty cycle and cycle lengths in order to study the effect of different parameters on the current.

Partial differential equation was solved by using *pdpe* function of Matlab. Integartion of current and time was done using *trapz* function.

5.3.2.2 Model output

Change in substrate concentration across the biofilm in MEC operated at 50% duty cycle is plotted in figure 4.6.

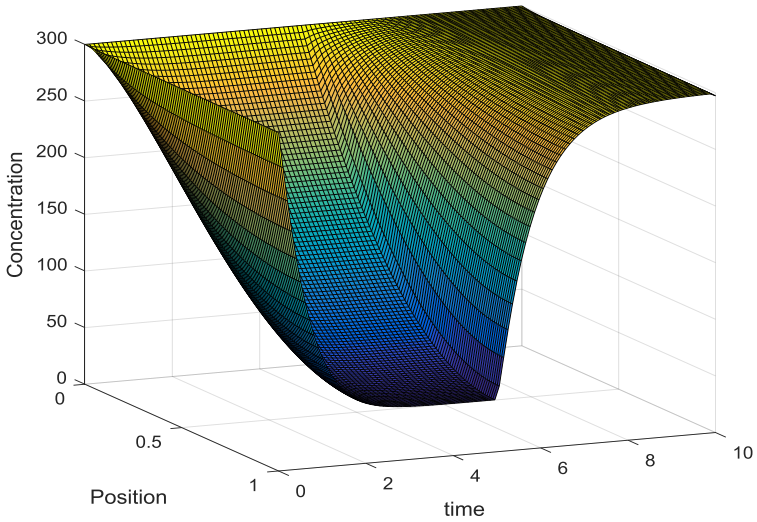

Figure 4.6: Substrate consumption across the biofilm in a MEC operated with 50% duty cycle.

Figure 4.6 shows that the carbon source is consumed in the biofilm when power supply is connected ($U_{MEC} = U_{app}$). Once power supply is disconnected, carbon source is not consumed and its concentration in the biofilm increases. Table 4.2 shows model parameters used for the simulation.

Table 4.2: Model parameters for 1-D biolfim model

Parameter	**Description**	**Value**	**Units**	**Note**
X	Bio-film depth	1	µm	Assumed
D	Duty cycle	50	%	Assumed
D_s	Diffusivity	0.5	$\mu m/s^2$	Assumed
S_b	Concentration in Bulk liquid	300	mg/L	Assumed
μ_{max}	Maximum growth rate	2	1/s	Assumed
K_s	Substrate half growth rate	20	mg/L	Assumed
X	Concentration of microorganisms	500	mg/L	Assumed
V	Voltage supplied	1.4	V	Assumed
Kv	Monod term of voltage	0.3	V	Assumed
$Kint$	Resistance per unit length	2	$\Omega/\mu m$	Assumed
Kr	Monod term of resistance	0.03	Ω	Assumed
Ro	Resistance at the electrode	1	Ω	Assumed
ηCE	Coloumbic efficiency	50	%	Assumed
F	Farady's constant	96480	C/mol	-
N	Number of electrons	8	-	-
$Vfilm$	Volume of bio-film	$3*10^{-15}$	L	Assumed

Figure 4.7 presents the concentration of substrate across the biofilm in the presence of applied voltage. Simulation is based on the parameters specified in table 4.2.

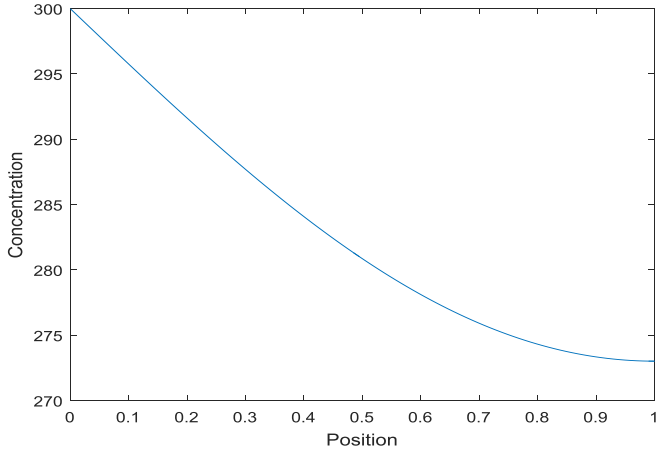

Figure 4.7: Change in concentartion across the biofilm at U_{app} = const.

For the sake of simplicity, all simulation results presented below show one on/off cycle. following figures describe the change in carbon source concentration and consumption rate across the biofilm with respect to time. The simulations also show the change in current with respect to time and the dependence of internal resistnace.

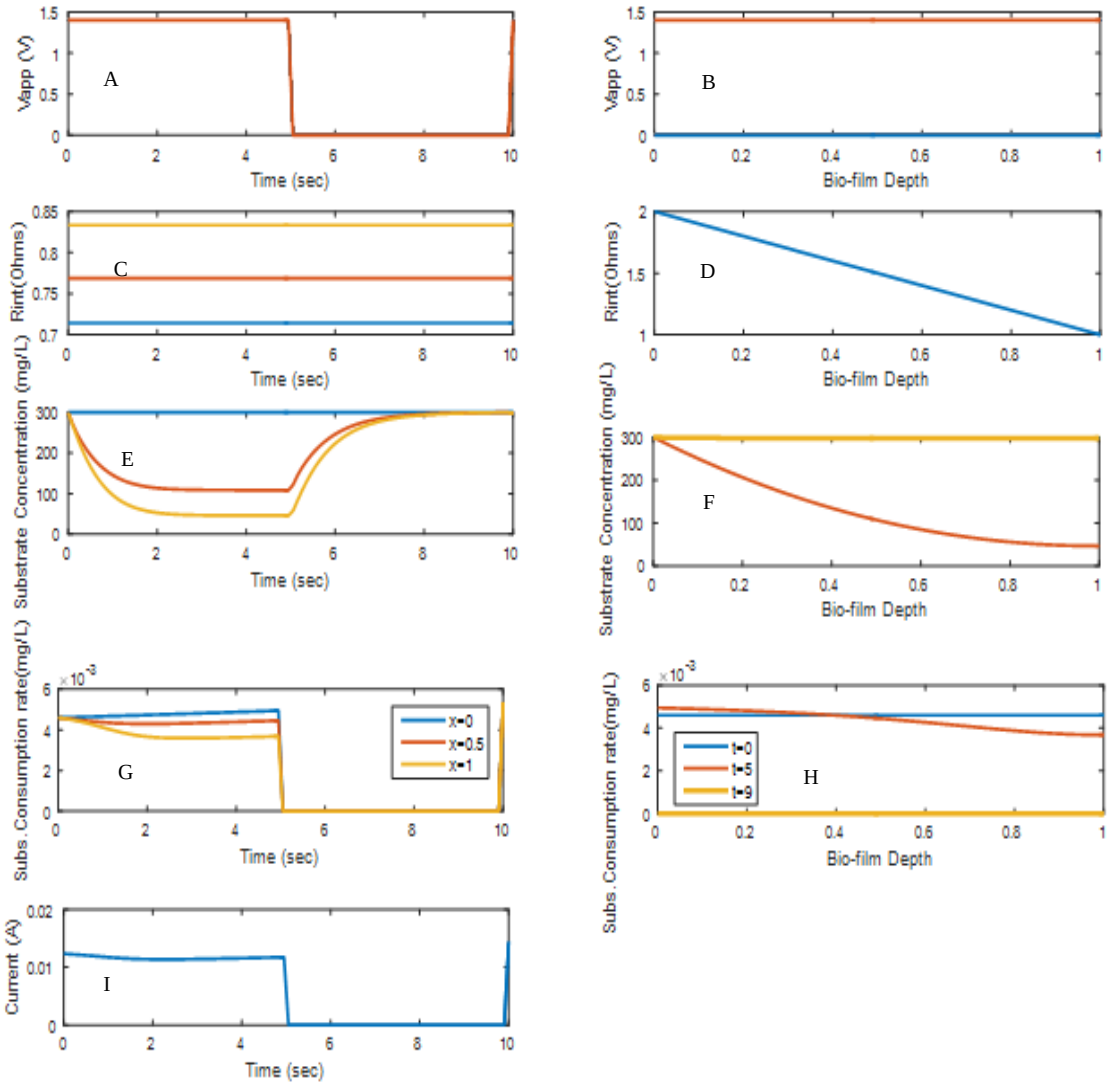

Figure 4.8. (A, B) voltage applied with time and across biofilm depth respectively, (C, D) internal resistance with respect to time and biofilm depth respectively, (E, F) change in substrate concentration with time and biofilm depth, (G, H) substrate consumption rate with respect to time and biofilm depth respectively and, (I) average current.

Although quantitative comparison of model outputs and experimental results is difficult to achieve in the absence of carbon source distribution measurements, it is important to compare the simulated and experimentally measured current values. Figure 3.2A shows the experimental data of current across the MEC and compares these values with the model outputs obtained for the on/off mode of operation.

Simulation results (Figure 4.8) suggest that internal resistance decreases from bulk liquid to the surface of the electrode. Substrate consumption is augmented when power supply is connected. When power supply is disconnected, substrate consumption rate goes to zero. The difference in the current simulated by the model equation and the current obtained from the experimental data (figure 3.2A) can be explained by the absence of capacitance term in the model, since the biofilm model does not take into account the internal capacitance of the biofilm.

The effect of model parameters on average current was also studied. Two cases were considered. Case-1 studies the effect of *Ks* on average current, and Case-2 demonstrates the effect of internal resistance on average current.

Case-1.

Three different values of Ks were considered to study the effect of Ks on average current. Other model parameters are same as in Table 4.2. In this simulation maximum current occurs at the shortest cycle length. Figure 4.9 shows the average current at cycle length 10 sec at different chosen values of Ks (0.5, 20 and 100 mg/L).

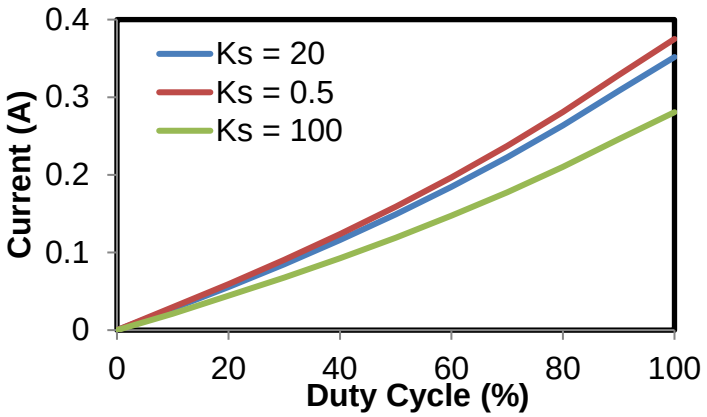

Figure 4.9: Effect of Ks on current at different duty cycles

As expected, with the increasing value of Ks, the average current decreases. Also, the maxir current is predicted to correspond to 100% duty cycle.

Case-2:

In order to study the effect of internal resistance, this category is further classified into 3 different sub-categories. (i) To Study the effect of *Kr* in the Monod term on average current (ii) To analyze the effect of K_{int} (constant of proportionality i.e. ohm/µm) as described in equation (4.20) on average current and (iii) To demonstrate the effect of *Ro* (internal resistance at the electrode surface). All parameters are same as given in Table 4.2, unless specified.

Effect of K_r: Three different values of K_r were considered to study the effect of K_r on average current. Maximum current occurs at the shortest cycle length. Figure (4.10) shows the average current at cycle length 10 sec at different chosen values of K_r (0.5, 5 and 20 ohms).

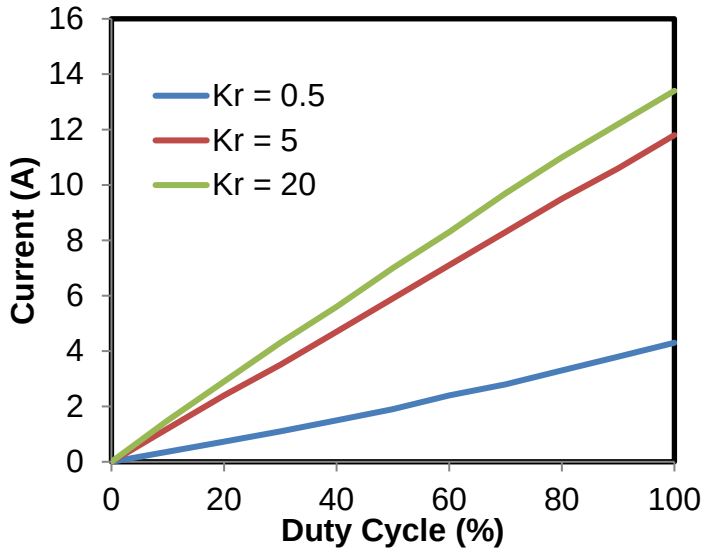

Figure 4.10: Effect of K_r on current at different duty cycle

It is clear from the figure that as the *Kr* increases, average current increases as well because appear in the denominator of the Monod term (Eq 4.21). Figure presents the effect of Kr at cycle length 10 sec.

ii) Studying the effect of Ro on average current.

R_o in the equation (4.20) represents the internal resistance at the surface of electrode. The term Ro represents the minimum internal resistance. If this term is assigned a higher value, it

result in high internal resistance of the MEC and vice versa. Figure 4.11 shows the effect of different values of R_o (1, 20 and 50 ohms) on the average current in the MEC.

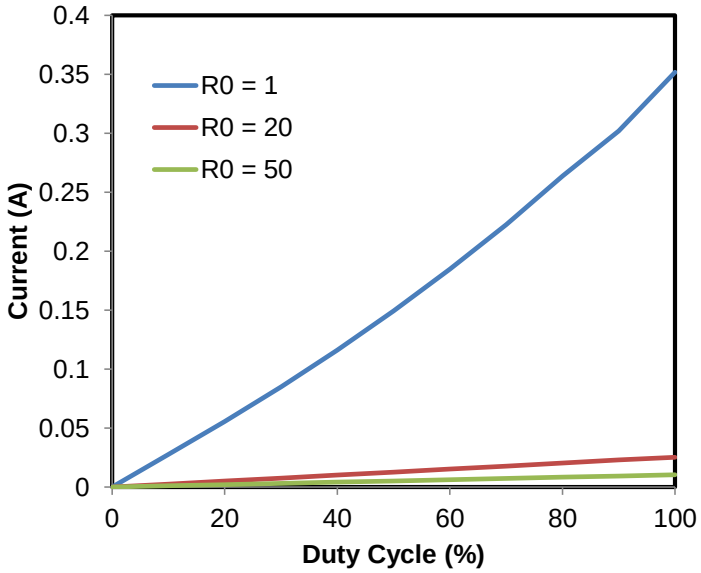

Figure 4.11: Effect of R_o on MEC current

iii) Analyizng the effect of K_{int} on the average current.

Kint is constant of proprotionality (Ohms/µm). This model defines internal resistance as a function of biofilm depth. $R_{int} \alpha\ L$

$$R_{int=}\ K_{int}.\ L \qquad (4.25)$$

Kint is the resistnace per unit length in the biofilm. It is an important parameter that influnces the total inetrnal resistance as defined by eqaution (4.20). Following figure (4.12) depicts the average current calculated at time period 10 sec and at different duty cycles (10%-100%) with K_{int} = 1, 5 and 20 Ohm/μm.

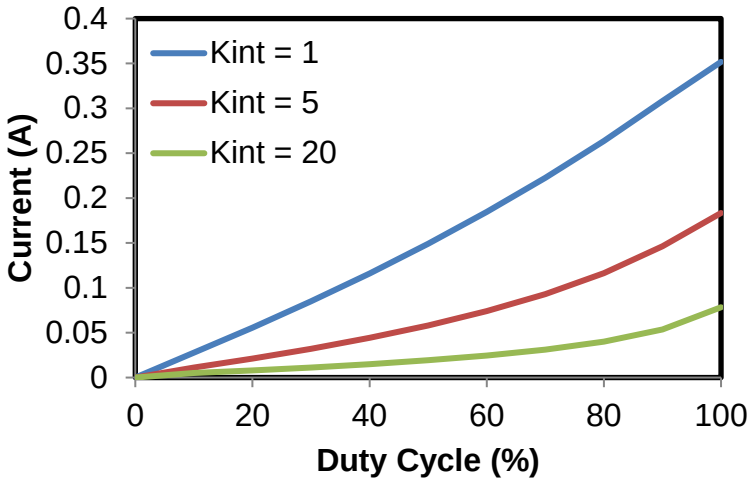

Figure 4.12. Effect of K_{int} on MEC current

Average current in the MEC is inversely related to the internal resistance. It is concluded from the above graphs that as the total internal resistance increases, the current decreases. Effect of internal resistance on the average current as describe by the simulation graphs and results of the model equation are exactly what is shown by the experimental data.

5.4 Conclusion

The anodophilic biofilm model is capable of simulating average current in the MEC at different duty cycle and cycle lengths. Current is calculated based on the rate of carbon source consumption, which is the function of depth in the biofilm, carbon source concentration, and internal resistance. Current in the MEC obtained by solving the model equations doesn't provide the same trend as of experimental data because model doesn't account the effect of capacitance in the MEC as an electrical parameter. However, model is helpful in locating the maximum current based on different duty cycles and cycle lengths. It is concluded that maximum average current in MEC is only present at 100% duty cycle. The observed significant improvement in the flow-through MEC current and COD removal needs to be better understood. while further experiments, including electrochemical and biomolecular studies of the anode and cathode electrodes might be needed, biofilm modeling can be also used. In particular, a simple 1-D anodic biofilm model can be used to predict the distribution of microbial species and carbon sources in the biofilm and relate this distribution to the observed performance improvement during on/off (applied voltage) MEC operation. While the proposed 1D biofilm model was rather simple

only simulated carbon source distribution inside a mature anodophilic (electroactive) biofilm (e.g. both biofilm growth and the methanogenic population was not considered in the simulations), the model suggested that during the off part of each cycle (zero applied voltage) carbon source concentration inside the biofilm significantly increases (Fig 3.9). Importantly, the part of anodophilic biofilm adjacent to the electrode features the lowest ohmic resistance and is expected to have the highest biodegradation rate. Once the voltage is restored, this inner part of the biofilm has the highest removal efficiency. In a mixed biofilm populated with anodophilic and methanogenic populations the inner part of the biofilm can be expected to be dominated by the anodophilic species. In the absence of on/off operation the competition between anodophilic and methanogenic populations could result in the proliferation of methanogenic microorganisms. The biofilm structure can be studied by improving the 1D model to include growth dynamics. Furthermore, a similar model can be developed to describe biocathode performance.

While this study was focused on anodic biofilm model, a similar model can be developed to describe the electroactive (cathodotrophic) biofilm at the cathode. Such simulation should be important in understanding MECs with biocathodes, since in this case metal catalysts are absent. The cathodic biofilm structure could be hypothesized to be similar to the anodic biofilm with the electroactive bacteria at the cathode producing H_2 and then methanogenic microorganisms in the outer biofilm layer converting H_2 to CH_4 and consuming carbon dioxide.

Dynamic model of MEC as anodic and cathodic compartments connected in series demonstrates the average current and effluent substrate concentration.

CHAPTER 6 CONCLUSION, SCIENTIFIC CONTRIBUTION AND PERSPECTIVES

Conclusion

Firstly, this thesis presents an equivalent electrical circuit model of MEC. Different model equations were considered. First, a simplified EEC model was developed by considering an R - R/C circuit. Several experiments were designed and carried out to estimate the model parameters. Open circuit voltage (OCV) tests demonstrated the existence of an internal electromotive force (EMF) in the MEC, thus requiring to modify the initial EEC model by incorporating an EMF in series with the R - R/C circuit. Numerical and analytical parameter estimation procedures were developed. Model parameters (R_0, R_1, C and EMF) were estimated by minimizing the difference between the experimental data and the model outputs. Also, the model was solved analytically and a parameter estimation procedure based on the MEC reactor operation at high and low frequencies of power supply connection (on/off operation). High frequency (1 Hz) on/off operation was used to estimate R_0, while R_1 was estimated by operating MEC at low frequency (0.01 Hz) of connection/disconnection. Also, internal capacitance (C) was estimated during low frequency operation using least squares method. Finally, to estimate EMF the MEC was operated at open circuit mode (without voltage applied). Another EEC model was developed by considering two R/C circuits. Although this model provided somewhat better fit between the experimental and simulated values, due to simplicity of the single R/C circuit with EMF model it was selected for further online parameter estimation and monitoring tests.

Next step was to study the effects of influent carbon source concentration on MEC performance and the EEC model parameters. Influent carbon source concentration was varied while model parameters were estimated in real time. It was observed that with the decrease in influent substrate concentration there is a decrease in the current and consequently increase in the internal resistances (R_0 and R_1) of MEC as well as decrease in the internal capacitance of the MEC, whereas electromotive force nearly remains constant.

Secondly, this thesis presents a new approach for enhancing MEC performance by intermittent connection/disconnection of power supply. Initially, a perturb-and-observe (P/O) algorithm was developed to locate the maximum average (per cycle) current flowing through the MEC at different duty cycles (0% to 100%). According to the algorithm, once the duty cycle rea 100%, it was set back to 95% duty cycle. This experiment determined that the duty cycle was oscillating between 95% and 100% duty cycle, i.e the maximum current corresponded to constantly connected power supply. Several tests were conducted by considering different duty cycle lengths (3 to 10 s), each time resulting in the highest average current at 100% duty cycle. The optimization tests lasted for several weeks, during which average current and COD removal in the MEC operated in the on/off mode drastically improved (e.g. current improvement from 7mA to 42 mA). At the same time, no improvement was observed in the COD removal or current of the control MEC operated at a fixed applied voltage. To confirm this observation, the operating strategies of the two MECs were reversed, i.e. first MEC was operated at a fixed applied voltage and the second MEC was operated at a duty cycle of 95%. In response, the average current flowing through the second MEC improved from around 7 mA to 22 mA, while the first MEC current remained unchanged. Also, performance of the second MEC improved in terms of COD removal, as evidenced by measuring effluent COD concentrations. It is concluded that long-term performance of MEC is enhanced by on/off mode of operation (connection/disconnection of power supply).

Last but not the least, this thesis presents dynamic model of a flow-through MEC. A general bioelectrochemical model was developed by considering anodic and cathodic compartments connected in series. The model is capable of describing the MEC current and carbon source concentrations in each compartment. The model provides acceptable fit between the experimental values and the simulated data. Sensitivity analysis of the model was carried out to determine the effects of model parameters on current and effluent COD concentration. Current and effluent COD concentration were greatly affected by Ka (half saturation constant for anodophilic microorganisms and μ_{max} (maximum growth rate of anodophilic microorganisms) model parameters. Following the sensitivity analysis, several model parameters namely Ka, μ_{max}, and also ∂ (constant in the current term) were estimated by numerical parameter estimation procedure and confidence intervals were calculated for these parameters.

In addition, an 1D biofilm model of MEC was developed. 1D biofilm model predicted significant changes in carbon source concentration with biolfilm depth under on/off operation of power supply. In particular, when power supply is connected to MEC, there is an increase in the substrate consumption rate resulting in a carbon source – depleted conditions inside the bio
When power supply is switched off, the carbon source consumption rate is slow leadir
increased concentration in the biofilm core. As a result, the on/off operation provides growth advantage to the electroactive microorganisms in the biofilm core.

MEC research related to modeling, monitoring and control is still at the very beginning. Development of the EEC and bioelectrochemical models and well as the proposed approaches for real-time MEC monitoring and power supply control provide significant improvements in the understanding of MEC-based wastewater treatment systems and help to overcome the obstacles in increasing MEC performance so that the potential of this system for wastewater treatment and biogas production can be realized.

Scientific contribution

Scientific contribution of this thesis is summarized as follows:

1) Development of EEC model of MEC capable of describing fast process dynamics.
2) Development of the online monitoring and parameter estimation procedure based on the EEC model and studying the effect of change in influent carbon source concentration on MEC internal parameters.
3) Enhancing long-term MEC performance in terms of COD removal by applying the power supply connection/disconnection (on/off operation) approach.
4) Development of a bioelectrochemical model of MEC capable of predicting current and carbon source concentrations in a flow-through MEC.
5) Development of a 1D biofilm model, which describes carbon source concentration profiles in the electroactive mixed culture biofilm and application of this model to a MEC operated with periodic power supply connection/disconnection.

Scientific publications are as follows:

1) Hussain, S.A., Perrier, M., & Tartakovsky, B. (2018). Real time monitoring of a microbial electrolysis cell using an electrical equivalent circuit *Bioprocess and biosystems engineering*,

2) Hussain, S.A., Perrier, M., & Tartakovsky, B. (2018). Long-term performance microbial electrolysis cell operated with periodic disconnection of power supply (Submitted and accepted).

3) Hussain, S.A., Recio-Garrido, D., Perrier, M., & Tartakovsky, B. (2018). 1-Dimenisonal biofilm model with periodic disconnection of power supply of microbial electrolysis cell. (In progress).

Different conclusions from this thesis were presented in following conferences:

- 6th meeting of International Society for Microbial Electrochemistry and Technology (ISMET 6). Conference was held in Lisbon, Portugal in October 2017. Poster presentation
- 12th Specialized Conference on Instrumentation, Control and Automation (ICA 2017). Conference took place in Québec city, Canada in June 2017. Poster presentation.
- Québec-Ontario Statistics and control meeting held in Québec city, Canada in May 2017. Oral Presentation.

Perspectives and recommendations

MEC represents a novel bioelectrochemical technology, which can be applied for wastewater treatment combined with renewable energy (biomethane) production as well as to the production of other valuable chemicals through bioelectrosythesis. Several pathways leading to better understanding of bioelectrochemical processes at the MEC anode and cathode can be exploited.

1. Research related to MEC modeling, monitoring, optimization, and control is in its early stages. The flow-through MEC design could provide multiple advantages for advanced wastewater treatment and biomethane production. This system can be better understood using an adequate modeling tool. For example, 1-D anodic biofilm model can be extended to also incorporate a cathodic biofilm model. In many ways, such cathodic biofilm model is expected to be similar to the anodic biofilm model. The expanded model then could be used to simulate carbon dioxide

(and CH_4) production at the anode and hydrogen and methane generation at the cathode. Furhtermore, the 1-D anode and cathode biofilm model can be coupled with the material balance of the flow-through MEC that considers anodic and cathodic compartments connected in series. This would enable performance simulation of MEC (including on/off operation of applied voltage) with respect to current, effluent carbon source concentration and biogas production.

2. New optimization and process control strategies can be developed based on the results described in this thesis, in particular using a model-based approach. Intermittent connection of power supply on MEC performance is expected to enhance both COD removal efficiency and biogas production in a flow-through MEC. The approach of intermittent applied voltage can be further improved by investigating MEC operation at low frequency as well as high frequency (cycle length less than 1 sec).

3. A combined bioelectrochemical-electrical (CBE) model of a flow-through MEC can be developed. Such model combines bioelectrochemical equations (e.g. described in the MEC model developed by Pinto et al. 2010 and EEC equations proposed by Hussain et al. 2018). CBE model might be capable of describing slow and fast dynamics of the system.

4. The effect of on/off operation of power supply on the biofilm development and MEC performance can be studied at a biomolecular level. The study will be able to provide insight into biofilm formation, microbial populations growth and decay under on/off operation.

5. Advanced control strategies are envisioned to be developed in order to predict and control effluent concentration and biogas production in a flow-through MEC.

BIBLIOGRAPHY

Amro, H., Freddy, W., Xiaohui, G., Liang. Y., Stephanie, L., and Ling, Q. (2017) Next generation digestion: complementing anaerobic digestion (AD) with a novel microbial electrolysis cell (MEC) design. International Journal of Hydrogen 42, 28681-28689.

Arcand, Y., Chavarie, C., and Guiot, S. (1994) Dynamic modelling of the population distribution in the anaerobic granular biofilm. Wat. Sci. Technol 30, 63-73.

Asztalos, J.R. and Kim, Y. (2015) Integration of microbial electrolysis cells with mesophilic anaerobic digestion forwastewater sludge treatment. PLOS ONE for review.

Batstone, D. J., Keller, J., Angelidaki, I., Kalyuzhnyi, S. V., Pavlostathis, S. G., Rozzi, A., ... & Vavilin, V. A. (2002). The IWA Anaerobic Digestion Model No 1 (ADM1). Water Science And Technology, 45(10), 65-73.

Call, D.F., Merrill, M.D., Logan, B., (2009) High Surface Area Stainless Steel Brushes As Cathodes In Microbial Electrolysis Cells. Environ Sci Technol 43:2179-2183

Call, D; Logan, B.E; 2008. "Hydrogen Production In A Single Chamber Microbial Electrolysis Cell Lacking A Membrane". Environ Sci Technol 42, 3401–6.

Chae, K.J; Choi, M.J; Lee, J; Ajayi, F.F; Kim, IS; 2008. "Biohydrogen Production Via Biocatalyzed Electrolysis In Acetate-Fed Bioelectrochemical Cells And Microbial Community Analysis". Int. J. Hydrogen Energ. 33, 5184-92.

Cheng, S., Logan, B.E., 2007. Sustainable And Efficient Biohydrogen Production Via Electrohydrogenesis. Proc. Natl. Acad. Sci. USA 104, 18871–18873

Cheng, S., Xing, D., Logan, B., (2009) Direct Biological Conversion Of Electrical Current Into Methane By Electromethanogenesis. Env Sci Technol 43:3953-3958

Cheng, S., Logan, B.E., 2011. "High Hydrogen Production Rate Of Microbial Electrolysis Cell (MEC) With Reduced Electrode Spacing". Bioresour. Technol. 102, 3571–3574.

Clauwaert P, Verstraete W (2008) Methanogenesis In Membraneless Microbial Electrolysis Cells. Appl Microbiol Biotechnol 82:829-836

Clauwaert, P., P. Aelterman, H. Pham, L.D. Schamphelaire, M. Carballa, K. Rabaey, W. Verstraete (2008). Minimizing Losses In Bio-Electrochemical Systems: The Road To Applications. Applied Microbiology And Biotechnology 79: 901-903.

Coronado, J., Perrier, M., Tartakovsky, B., (2013) Pulse-Width Modulated External Resistances Increases The Microbial Fuel Cell Power Output. Bioresour Technol 147:65-70

Coronado, J., Tartakovsky, B., Perrier, M., (2015) On-line monitoring of microbial fuel cells operated with pulse-width modulated electrical load. Proc Control 35:59-64

Cougnon, P., D. Dochain, P. Cougnon, M. Guay, M. Perrier (2011). On-Line Optimization Of Fedbatch Bioreactors By Adaptive Extremum Seeking Control. Journal Of Process Control 21(10): 1526-1532.

Dewan, A., H. Beyenal, Z. Lewandowskiet Al. (2009). Intermittent Energy Harvesting Improves The Performance Of Microbial Fuel Cells. Environmental Science & Technology 43(12): 4600-4605

Ding, A; Yang, Y; Sun, G; Wu, D; 2016. “Impact Of Applied Voltage On Methane Generation And Microbial Activities In An Anaerobic Microbial Electrolysis Cell (MEC)”. Chemical Engineering Journal 283, 260–265.

Ditzig, J., Liu, H. and Logan, B.E. (2007) Production of hydrogen from domestic wastewater using a bioelectrochemically assisted microbial reactor (BEAMR). Int. J. Hydrogen Energy 32, 2296-2304.

Dochain, D. (2003). State And Parameter Estimation In Chemical And Biochemical Processes: A Tutorial.Journal Of Process Control 13(8): 801-818.Du, Z., H. Li, T. Gu (2007). "A State Of The Art Review On Microbial Fuel Cells: A Promising Technology For Wastewater Treatment And Bioenergy." Biotechnology Advances 25(5): 464-482

Durr, M., A. Cruden, S. Gair, J.R. Mcdonald (2006). Dynamic Model Of A Lead Acid Battery For Use In A Domestic Fuel Cell System. Journal Of Power Sources 161(2): 1400-1411.

Escapa, A; Gil-Carrera, L; García, V; Morán, A; 2012. Performance Of A Continuous Flow Microbial Electrolysis Cell (MEC) Fed With Domestic Wastewater. Bioresource Technology 117, 55–62.

Escapa, A., Mateos, R., Martinez, E.J., Blanes, J., (2016) Microbial electrolysis cells: An emerging technology for wastewater treatment and energy recovery. From laboratory to pilot plant and beyond Renew Sustainable Energ Reviewa 55:942-956

Fandler, K.R., Kim, J.R., Boghani, H.C., Dinsadle, R.M., Guwy, A.J., Premier GC (2014) The Effect Of Internal Capacitance On Power Quality And Energy Efficiency In A Tubular Microbial Fuel Cell. Proc Biochem 49:973-980.

Feng, Y., 1, Y. Cheng , Y. Du, Q. Teng, H. Li (2014). Hydrogen Production From Acetate In A Sleeve Shape Microbial Electrolysis Cell With A Mipor Cathode. International Journal Of Electrochemical Sciences.

Flora, J.R.V., Suidan, M.T., Biswas, P. and Sayles, G.D. (1995) A modeling study of anaerobic biofilm systems: I. Detailed biofilm modeling. Biotechnology and Bioengineering 46, 43-53.

Gao, L., S. Liu, R.A.Dougal (2002). Dynamic Lithium-Ion Battery Model For System Simulation. Components And Packaging Technologies, IEEE Transactions On 25(3): 495-505.

Gao, H., Scherson, Y.D., Wells GF (2014) Towards energy neutral wastewater treatment: methodology and state of the art. Environ Sci: Processes Impacts 16:1223-1246

Gil-Carrera, L., Escapa, A., Moreno, R., Morán, A., (2013) Reduced Energy Consumption During Low Strength Domestic Wastewater Treatment in A Semi-Pilot Tubular Microbial Electrolysis Cell. J Environ Management 122:1-7

Grondin, F., Perrier, M., Tartakovsky, B., (2012) Microbial Fuel Cell Operation With Intermittent Connection Of The Electrical Load. Power Sources 208:18-23

Hamelers, H. V. M., A. Ter Heijne, N. Stein, R. A. Rozendal, C. J.N. Buisman (2011). Butler–Volmer–Monod Model For Describing Bio-Anode Polarization Curves. Bioresource Technology 102(1): 381-387.

Henze, M., Gujer, W., Mino, T., & Van Loosdrecht, M. C. M. (2000). Activated Sludge Model ASM1, ASM2, ASM2d And ASM3. IWA Publishing.

Hou, Y., Zhang, R., Luo, H., Liu, G., Kim, Y., Yu, S., Zeng, J., (2015) Microbial electrolysis cell with spiral wound electrode for wastewater treatment and methane production. Process Biochem 50:1103-1109

Hu, H., Fan, Y., Liu, H., 2009. Hydrogen Production In Single-Chamber Tubular Microbial Electrolysis Cells Using Non-Precious-Metal Catalysts". Int. J. Hydrogen Energy 34, 8535–8542.

Hu, H; Fan, Y; Liu, H; 2008. Hydrogen Production Using Singlechamber Membrane-Free Microbial Electrolysis Cells. Water Res. 42, 4172–8.

Hussain, A., Manuel, M.F., Tartakovsky, B., (2016) A comparison of simultaneous organic carbon and nitrogen removal in microbial fuel cells and microbial electrolysis cells. J Environ Management 173:23-33

Hussain, S.A., Perrier, M. and Tartakovsky, B. (2018) Real-time monitoring of a microbial electrolysis cell using an electrical equivalent circuit model. Bioprocess and Biosystems Engineering in press.

Hyung, S.L., Bruce., (2009) Characterization Of Energy Losses In An Up Flow Single Chamber Microbial Electrolysis Cell . International Journal of Hydrogen Energy 35: 920–927

Jafary, T., Daud, W.R.W., Ghasemi, M., Kim, B.H., (2015) Biocathode In Microbial Electrolysis Cell; Present Status And Future Prospects Renewable And Sustainable Energy Reviews 47(2015)23-33 47:23-33

Jeppsson, U., (1996). Modelling Aspects of Wastewater Treatment Processes. IEA, LTH, Box 118, SE-221 00 Lund, Sweden.

Jeremiasse, A.W., Hamelers, V.M., Buisman, C.J.N., (2010) Microbial electrolysis cell with a microbial biocathode. Bioelectrochemistry 78:39-43

Kim, H. J., H. S. Park, M. S. Hyun, I. S. Chang, M. Kim, B. H. Kim (2002). A Mediator-Less Microbial Fuel Cell Using A Metal Reducing Bacterium, Shewanella Putrefaciens. Enzyme And Microbial Technology 30(2): 145-152.

Kravaris, C., J. Hahn, Y. Chu (2013). Advances And Selected Recent Developments In State

And Parameter Estimation. Computers &Amp; Chemical Engineering 51(0): 111-123.

Larminie. J; Dicks, A; 2003. Fuel Cell Systems Explained. Chichester, England: John Wiley & Sons.

Liang, P., W. Wu, J. Wei, L. Yuan, X. Xia, X. Huang (2011). Alternate Charging And Discharging Of Capacitor To Enhance The Electron Production Of Bioelectrochemical Systems. Environmental Science &Amp; Technology 45(15): 6647-6653.

Lee, H.S; Rittmann, B.E., (2010). Characterization Of Energy Losses In An Upflow Single-Chamber Microbial Electrolysis Cell. International Journal Of Hydrogen Energy 35, 920 –927.

Lee, H.S; Torres, C.I; Parameswaran, P; Rittmann, B.E; (2009). Fate Of H_2 In An Upflow Single-Chamber Microbial Electrolysis Cell Using A Metal-Catalyst-Free Cathode. Environ Sci Technol 43, 7971–6.

Linji, X; Wenzong, L; Yining, W; Aijie, W; Shuaia, L; Wei, J; (2013). "Optimizing External Voltage For Enhanced Energy Recovery From Sludge Fermentation Liquid In Microbial Electrolysis Cell". International Journal Of Hydrogen Energy 38, 15801-5806.

Liang, D.W; Peng, S.K; Lu, S.F; Liu,Y; Lan, F; Xiang, Y; (2011). Enhancement Of Hydrogen Production In A Single Chamber Microbial Electrolysis Cell Through Anode Arrangement Optimization. Bioresource Technology 102, 10881–10885

Liu, H., Hu, H., Chignell, J., Fan, Y., (2010). Microbial Electrolysis Novel Technology For Hydrogen Production From Biomass. Biofuels 1, 129–142.

Liu, H., Grot, S., Logan, B.E., (2005) Electrochemically assisted microbial production of hydrogen from acetate. Env Sci Technol 39 (11):4317-4320

Liu, W., Cai, W., Guo, Z., Wang, L., Yang, C., Varrone, C., Wang, A., (2016) Microbial Electrolysis Contribution To Anaerobic Digestion Of Waste Activated Sludge, Leading To Accelerated Methane Production. Renew Energ 91:334-339

Logan, B.E., Call, D., Cheng, S., Hamelers, H.V.M., Sleutels, T.H.J.A., Jeremiasse, A.W., Rozendal, R.A., (2008). "Microbial Electrolysis Cells For High Yield Hydrogen Gas Production From Organic Matter. Environ". Sci. Technol. 42, 8630–8640.

Logan, B. (2010). Scaling Up Microbial Fuel Cells And Other Bioelectrochemical Systems.

Applied Microbiology and Biotechnology 85(6): 1665-1671.

Logan, B. E., and Regan, J. M., (2006). Microbial Fuel Cells: Challenges and Applications. Environmental Science &Amp; Technology 40(17): 5172-5180.

Merill, M.D., Logan, B.E., (2009) Electrolyte effects on hydrogen evolution and solution resistance in microbial electrolysis cells. J Power Sources 191:203-208

Manuel. M-F., Neburchilov, V., Wang, H., Guiot, S.R., Tartakovsky, B., (2010) Hydrogen production in a microbial electrolysis cell with nickel-based gas diffusion cathodes. Power Sour 195 (5514-5519)

Martin, E., Savadogo, O., Guiot, S.R., Tartakovsky, B., (2013) Electrochemical characterization of anodic biofilm development in a microbial fuel cell. Appl Electrochem 43:533-540

Marcus, A. K., C. I. Torres,B. E. Rittmann (2007). Conduction-Based Modeling of The Biofilm Anode of A Microbial Fuel Cell. Biotechnology and Bioengineering 98(6): 1171-1182.

Moreno, R; San-Martín, M-I; Escapa, A; Moran, A; (2016). Domestic Wastewater Treatment In Parallel With Methane Production In A Microbial Electrolysis Cell. Renewable Energy 93, 442-448.

Noren, D. A., And M. A. Hoffman (2005). Clarifying The Butler-Volmer Equation And Related Approximations For Calculating Activation Losses In Solid Oxide Fuel Cell Models. Journal Of Power Sources, 152(1-2), 175-181

O'Hayre, R., S.-W. Cha And F.B. Prinz (2006). Fuel Cell Fundamentals (1 Ed.). : Hoboken, N.J.: John Wiley And Sons.

Oh, S. (2010). Trend Of Mathematical Models In Microbial Fuel Cell For Environmental Energy Refinery From Wastewater. EKC 2009 Proceedings Of The EU-Korea Conference On Science And Technology 135: 25-30.

Oh, S. T., J. R. Kim, G. C. Premier T. H. Lee, C. Kim, W. T. Sloan (2010). Sustainable Wastewater Treatment: How Might Microbial Fuel Cells Contribute. Biotechnology Advances 28(6): 871-881.

Oliveira, V. B., M. Simoes, L. F. Melo, A.M.F.R. Pinto (2013). Overview On The Developments Of Microbial Fuel Cells. Biochemical Engineering Journal 73(0): 53-64.

Pathapati, P. R., X. Xue, J. Tang (2005). A New Dynamic Model For Predicting Transient Phenomena In A PEM Fuel Cell System. Renewable Energy 30(1): 1-22.

Picioreanu, C., I. M. Head, K. P. Katuri , M. C.M. V. Loosdrecht , K. Scott (2007). A Computational Model For Biofilm-Based Microbial Fuel Cells. Water Research 41(13): 2921-2940.

Picioreanu, C., K. P. Katuri, K. Scott, I. M. Head, C. Picioreanu, T. P. Curtis (2008). Mathematical Model For Microbial Fuel Cells With Anodic Biofilms And Anaerobic Digestion. Water Science And Technology 57(7): 965-972.

Picioreanu, C., K. P. Katuri, M. C. M. V. Loosdrecht, I. M. Head, K. Scott (2010). "Modelling Microbial Fuel Cells With Suspended Cells And Added Electron Transfer Mediator." Journal Of Applied Electrochemistry 40(1): 151-162.

Picioreanu, C., J.-U. Kreft, M. C. M. V. Loosdrecht (2004). "Particle-Based Multidimensional Multispecies Biofilm Model."Applied And Environmental Microbiology 70(5): 3024-3040.

Picioreanu, C., M. C. M. Van Loosdrecht, T. P. Curtis, Keith Scott (2010). Model Based Evaluation Of The Effect Of Ph And Electrode Geometry On Microbial Fuel Cell Performance. Bioelectrochemistry 78(1): 8-24.

Pinto, R. P., Srinivasan, B., Guiot, S.R., Tartakovsky, B., (2011). The Effect Of Real-Time External Resistance Optimization On Microbial Fuel Cell Performance. Water Research 45(4): 1571-1578.

Pinto, R. P., B. Srinivasan, Manuel, M-F., Tartakovsky, B., (2010). A Two Population Bio- Electrochemical Model Of A Microbial Fuel Cell. Bioresource Technology 101(14): 5256-5265

Pinto, R. P., B. Tartakovsky, M. Perrier , B. Srinivasan (2010). "optimizing Treatment Performance Of Microbial Fuel Cells By Reactor Staging. Industrial &Amp; Engineering Chemistry Research 49(19): 9222-9229.

Pinto, R. P., Srinivasan, B., Escapa, A., & Tartakovsky, B. (2011). Multi-Population Model of a Microbial Electrolysis Cell. Environmental Science & Technology, 45(11), 5039-5046.

Pinto, R.P., Srinivasan, B., Guiot, S.R., Tartakovsky, B., (2011) The Effect of Real-Time External Resistance Optimization on Microbial Fuel Cell Performance. Wat Res 45:1571-1578

Rabaey, K., Rozendal, R.A., (2010) Microbial Electrosunthesis Revisiting The Electrical Route For Microbial Production. Nature Reviews Microbiology 8, 706-716

Recio-Garrido, D., Perrier, M., Tartakovsky, B., (2015) Combined Bioelectrochemical-Electrical Model of a Microbial Fuel Cell. Bioprocess Biosyst Eng 39:267-276

Rivera, I; Buitron, G., Bakony, P., Nemestothy. N; Bako. K; (2015). Hydrogen Production In A Microbial Electrolysis Cell Fed With A Dark Fermentation Effluent. J. Appl Electrochem 45, 1223–1229.

Rozendal, R.A; Hamelers, H.V.M; Euverink, G.J; Metz, S.J; Buisman, C.J.N; (2006). Principle And Perspectives Of Hydrogen Production Through Biocatalyzed Electrolysis" Int. J. Hydrogen Energy 31, 1632–40.

Rozendal, R.A; Hamelers, H.V.M; Molenkmp, R.J; Buisman, C.J.N; (2007). Performance Of Single Chamber Biocatalyzed Electrolysis With Different Types Of Ion Exchange Membranes". Water Res. 41, 1984–94.

Rozendal, R.A., Hamelers, H.V.M., Euverink, G.J.W., Metz, S.J., Buisman, C.J.N (2006) Principle and perspectives of hydrogen production through biocatalyzed electrolysis. International Journal of Hydrogen Energy 31:1632-1640

Rozendal, R.A., Jeremiasse, A.W., Hamelers, H.V.M., Buisman, C.J.N., (2008) Hydrogen production with a microbial biocathode. Environ Sci Technol 42:629-634

Schrott, G.D, Bonanni, P.S, Robuschi, L., Esteve-Nuñex, A., Busalmen, J.P., (2011) Electrochemical Insight Into The Mechanism Of Electron Transport In Biofilms Of Geobacter Sulfurreducens. Electrochim Acta 56(28):10791-10795

Selembo, P.A., Merrill, M.D., Logan, B.E., (2009)., The Use Of Stainless Steel And Nickel Alloys As Low-Cost Cathodes In Microbial Electrolysis Cells. J. Power Sources 190, 271–278.

Sleutels, T.H.J.A; Hamelers, H.V.M; Rozendal, R.A; Buisman, C.J.N; (2009). Ion Transport Resistance In Microbial Electrolysis Cells With Anion And Cation Exchange Membranes. Int. J. Hydrogen Energy 34, 3612–20.

Tartakovsky. B; Manuel, M-F; Wang, H; Guiot, S.R; (2009). High Rate Membrane-Less Microbial Electrolysis Cell For Continuous Hydrogen Production". Int. J. Hydrogen Energy 34, 672–7.

Tartakovsky, B., Mu, S.J., Zeng, Y., Wu, P., Lou, S.J., (2008). Anaerobic Digestion Model No. 1- Based Distributed Parameter Model Of An Anaerobic Reactor: II. Model Validation.Bioresource Technology 99(9): 3676-3684.

Tartakovsky, B., Manuel, M.F., Neburchilov, V., Wang, H., Guiot, S.R., (2008) Biocatalyzed hydrogen production in a continuous flow microbial fuel cell with a gas phase cathode. Power Sour 182:291-297

Tartakovsky, B., Mehta, P., Santoyo, G., Guiot, S.R., (2011) Maximizing Hydrogen Production In A Microbial Electrolysis Cell By Real-Time Optimization Of Applied Voltage. International Journal Of Hydrogen Energy 36(2011):10557-10564

Tartakovsky B, Kleiner Y, Manuel M-F (2017) Bioelectrochemical anaerobic sewage treatment technology for Arctic communities. Environ Sci Pollut Res in press

Tartakovsky, B. and Guiot, S.R. (1997) Modeling and analysis of layered stationary anaerobic granular biofilms. Biotechnology and Bioengineering 54, 122-130.

Torres, C. I., Marcus, R.K., Parameswaran, P., Rittmannet, B.E (2008). Kinetic Experiments For Evaluating The Nernst-Monod Model For Anode-Respiring Bacteria (ARB) In A Biofilm Anode. Environmental Science &Amp; Technology 42(17): 6593-6597

Torres, C.I., Krajmalnik-Brown, R., Parameswaran, P., Marcus, A.K., Wanger, G., Gorby, Y.A. and Rittmann, B.E. (2009) Selecting Anode-Respiring Bacteria Based on Anode Potential: Phylogenetic, Electrochemical, and Microscopic Characterization. Eviron. Sci. Technol. 43, 9519-9524.

Verea, L; Savadogo, O; Verde, A; Campos, J; Ginez, F; Sebastian, P.J; (2014). Performance Of A Microbial Electrolysis Cell (MEC) For Hydrogen Production With A New Process For The Biofilm Formation. International Journal Of Hydrogen Energy 3 9, 8938-8946.

Villano, M., Aulenta, F., Ciucci, C., Ferri, T., Giuliano, A., Majone, M., (2010) Bioelectrochemical Reduction Of CO_2 To CH_4 Via Direct And Indirect Extracellular Electron Transfer By A Hydrogenophilic Methanogenic Culture. Bioresource Technol 101:3085-3090

Villano, M., Monaco, G., Aulenta, F., Majone, M., (2011) Electrochemically assisted methane production in a BIOfiLM reactor. J Power Sources 196:9467-9472

Wagner, R.C., Regan, J.M., Oh, S.E., Zuo, Y., Logan, B.E., (2009) Hydrogen and methane production from swine wastewater using microbial electrolysis cells. Wat Res 43:1480-1488

Wang, K; Sheng, Y; Cao, H; Yan, K; Zhang, Y; (2017). Impact Of Applied Current On Sulfate-Rich Wastewater Treatment And Microbial Biodiversity In The Cathode Chamber Of Microbial Electrolysis Cell (MEC) Reactor. Chemical Engineering Journal 307, 150–158.

Wang, A.J; Liu, W.Z; Cheng, S.A; Xing, D.F; Zhou, J.H; Logan, B.E; (2009). Source Of Methane And Methods To Control Its Formation In Single Chamber Microbial Electrolysis Cells. Int. J. Hydrogen Energy 34, 3653–8.

Wagner, N. (2002). Characterization Of Membrane Electrode Assemblies In Polymer Electrolyte Fuel Cells Using A.C. Impedance Spectroscopy. Journal Of Applied Electrochemistry 32(8): 859-863.

Wanner, O., Eberl, H., (2006). Mathematical Modeling Of Biofilms (IWA Task Group On Biofilm Modeling, Scientific And Technical Report No. 18), London: IWA Publishing.

Woodward, L., M. Perrier, B. Srinivasan, B. Tartakovsky, R.Pinto (2010). Comparison Of Real- Time Methods For Maximizing Power Output In Microbial Fuel Cells. AICHE Journal 2742-2750.

Woodward, L., B. Tartakovsky, M. Perrier, B. Srinivasan, R. Pinto (2009). "Maximizing Power Production In A Stack Of Microbial Fuel Cells Using Multiunit Optimization Method." Biotechnology Progress 25(3): 676-682.

Woodward ,L., Perrier, M., Srinivasan, B., Pinto, R.P., Tartakovsky B (2010) Compariosn Of Real-Time Methods For Maximizing Power Output In Microbial Fuel Cells. Aiche J 56(10):2741-2750.

Yang, F., Zhang, D., Shimotori, T., Wang, K-C., Huang, Y., (2012) Study Of Transformer-Based Power Management System And Its Performance Optimization For Microbial Fuel Cells. J Power Sources 205:86-92.

APPENDIX A –ELECTRICAL EQUIVALENT CIRCUIT MODEL

Current at the internal capacitors shown in Figure 2.4 (equivalent circuit Model #1 with two R/C circuits) can be described as

$$i_1 = C_1 \frac{dU_{C1}}{dt} \tag{A1}$$

$$i_2 = C_2 \frac{dU_{C2}}{dt} \tag{A2}$$

By applying Kirchhoff's current and voltage laws to the EEC model diagram in Figure 2.4 and expressing voltages using Ohm's law the following model equation can be written:

$$U_s + U_{emf} = i_0 R_0 + i_1 R_1 + i_2 R_2 + i_0 R_{ext} \tag{A3}$$

After substituting the currents and rearranging the terms in Eq. A3 voltages across internal capacitors can be expressed as:

$$\frac{dU_{C1}}{dt} = \frac{U_s + U_{emf}}{C_1\left(R_0 + R_{ext}\right)} - \frac{U_{C1}\left(R_0 + R_1 + R_{ext}\right)}{C_1 R_1\left(R_0 + R_{ext}\right)} - \frac{U_{C2}}{C_1\left(R_0 + R_{ext}\right)} \tag{A4}$$

and,

$$\frac{dU_{C2}}{dt} = \frac{U_s + U_{emf}}{C_2\left(R_0 + R_{ext}\right)} - \frac{U_{C2}\left(R_0 + R_2 + R_{ext}\right)}{C_1 R_2\left(R_0 + R_{ext}\right)} - \frac{U_{C1}}{C_2\left(R_0 + R_{ext}\right)} \quad \text{(A5)}$$

Once again, voltage across MEC can be expressed by applying Kirchhoff's laws and rearranging terms as

$$U_{MEC} = U_s - (U_s - U_{C1} - U_{C2} - U_{emf})\frac{R_{ext}}{R_0 + R_{ext}} \quad \text{(A6)}$$

Furthermore, a single R/C circuit model (Model #2) can be obtained by assuming $R_2 = 0$, and $U_{C2} = 0$. In this case the dynamic model equations are simplified to

$$\frac{dU_{C1}}{dt} = \frac{U_s + U_{emf}}{C_1\left(R_0 + R_{ext}\right)} - \frac{U_{C1}\left(R_0 + R_1 + R_{ext}\right)}{C_1 R_1\left(R_0 + R_{ext}\right)} \quad \text{(A7)}$$

and

$$U_{MEC} = U_s - (U_s - U_{C1} - U_{emf})\frac{R_{ext}}{R_0 + R_{ext}} \quad \text{(A8)}$$

Finally, Eqs A7-A8 can be further simplified by assuming $U_{emf} = 0$ (Model #3).

APPENDIX B- ANALYTICAL SOLUTION OF SINGLE R/C CIRCUIT EEC MODEL #2

Analytical solution of the EEC Model #2 with one R/C circuit described by Eqs A7-A8 can be obtained by the variable separation method. For simplicity, let's define the following variables:

$$K = \frac{U_s + U_{emf}}{C(R_0 + R_{ext})} \ , \ L = \frac{R_0 + R_1 + R_{ext}}{CR_1(R_0 + R_{ext})} \tag{B1}$$

Then Eq. A7 can be written as

$$\frac{dU_{C1}}{dt} = K - U_{C1}L \tag{B2}$$

Isolating the variables and integrating both sides of the equation we obtain

$$\int_{U_0}^{U} \left(K - U_{C1}L\right)^{-1} dU_{C1} = \int_{t_0}^{t} dt \tag{B3}$$

Solving Eq B3 we obtain

$$\frac{K - U_{C1}L}{K - U_0 L} = e^{(t_0 - t)L} \tag{B4}$$

Substituting the values of *K* and *L* into Eq. B4 and simplifying the algebraic expression:

$$\left(U_s + U_{emf}\right)R_1 - U_{C1}\left(R_0 + R_1 + R_{ext}\right) = e^{(t_0 - t)\frac{R_0 + R_1 + R_{ext}}{C_1 R_1 (R_0 + R_{ext})}}\left(\left(U_s + U_{emf}\right)R_1 - U_0\left(R_0 + R_1 + R_{ext}\right)\right) \quad \text{(B5)}$$

Isolating U_{C1}:

$$U_{C1} = \frac{(U_{emf} + U_s)R_1}{R_0 + R_1 + R_{ext}} + e^{(t_0 - t)\frac{R0 + R_1 + R_{ext}}{CR_1 (R_0 + R_{ext})}}\left(U_0 - \frac{(U_s + U_{emf})R_1}{R_0 + R_1 + R_{ext}}\right) \quad \text{(B6)}$$

The above equation can be written as

$$U_{C1} = U_{final} + \left(U_0 - U_{final}\right)e^{-\frac{t - t_0}{\tau}} \quad \text{(B7)}$$

where

$$U_{final} = \frac{(U_{emf} + U_s)R_1}{R_0 + R_1 + R_{ext}},\ \tau = \frac{C_1 R_1 (R_0 + R_{ext})}{R_0 + R_1 + R_{ext}} \quad . \quad \text{(B8)}$$

Here, U_{final} and time constant τ can be determined from an experiment.

APPENDIX C- SYMBOLS AND NOTATIONS

Symbol	Description	Units
b_a	Decay rate of $X_{B,a}$	d^{-1}
b_f	Decay rate of $X_{B,f}$	d^{-1}
b_h	Hydrolysis rate of X_S by $X_{B,f}$	d^{-1}
b_m	Decay rate of $X_{B,m}$	d^{-1}
CSTR	Continuous stirred tank reactor	-
D	Dilution rate	d^{-1}
F	Faraday's constant	C mol-e^{-1}
f_P	Fraction of X_B yielding X_S	%
I_{MEC}	Current drawn from the MEC	mA
$K_{S,a}$	Half-saturation coefficient of S_S for $X_{B,a}$	mg-S_S L^{-1}
$K_{S,f}$	Half-saturation coefficient of S_S for $X_{B,f}$	mg-S_S L^{-1}
$K_{S,m}$	Half-saturation coefficient of S_S for $X_{B,m}$	mg-S_S L^{-1}
$K_{H2,m}$	Half-saturation coefficient of S_{H2} for $X_{B,m}$	mg-S_S L^{-1}
K_V	Half-saturation/Inhibition coefficient of V_{app}	V
K_X	Half-saturation coefficient of X_S for $X_{B,f}$	mg-X_B L^{-1}
$k_{h,f}$	Maximum specific hydrolysis rate for $X_{B,f}$	d^{-1}
q_{in}	Input flow rate	L d^{-1}
S_S	Concentration of biodegradable soluble substrate	mg-S_S L^{-1}
S_{H2}	Concentration of soluble hydrogen	mg-S_{H2} L^{-1}

$X_{B,a}$	Concentration of anodophilic bacteria	mg-X_B L^{-1}
$X_{B,f}$	Concentration of fermentative bacteria	mg-X_B L^{-1}
$X_{B,m}$	Concentration of methanogenic bacteria	mg-X_B L^{-1}
X_S	Concentration of biodegradable particulate substrate	mg-X_S L^{-1}
$Y_{S,a}$	Yield factor of S_S for $X_{B,a}$	mg-S_S mg-X_B^{-1}
$Y_{S,f}$	Yield factor of S_S for $X_{B,f}$	mg-S_S mg-X_B^{-1}
$Y_{S,m}$	Yield factor of S_S for $X_{B,m}$	mg-S_S mg-X_B^{-1}
$Y_{H2,a}$	Yield factor of S_{H2} for $X_{B,a}$	mg-S_{H2} mg-X_B^{-1}
$Y_{H2,f}$	Yield factor of S_{H2} for $X_{B,f}$	mg-S_{H2} mg-X_B^{-1}

Greek letters

α	Biofilm detachment function	-
γ	Molecular weight of S_S (acetate)	Mg-S_S mol-S_S^{-1}
$\mu_{max,a}$	Maximum specific growth rate of $X_{B,a}$	d^{-1}
$\mu_{max,f}$	Maximum specific growth rate of $X_{B,f}$	d^{-1}
$\mu_{max,ma}$	Maximum specific growth rate of acetoclastic $X_{B,m}$	d^{-1}
$\mu_{max,mh}$	Maximum specific growth rate of hydrogenotrophic $X_{B,m}$	d^{-1}

Indices

a	Related to anaerobic microbial population	-
B	Related to biomass	-
f	Related to fermentative microbial population	-
$H2$	Related to soluble hydrogen	-
m	Related to methanogenic microbial population	-

i	Current compartment	-
S	Related to soluble substrate	-

APPENDIX D- ADDITIONAL EXPERIMENTAL RESULTS

A.1 Online Monitoring of MEC and parameter estimation

Influent acetate concentration in MEC was changed from 1334 mg/Ld to 667 mg/Ld (Fig A.1) and the its effect was observed on the internal electrical parameters of MEC.

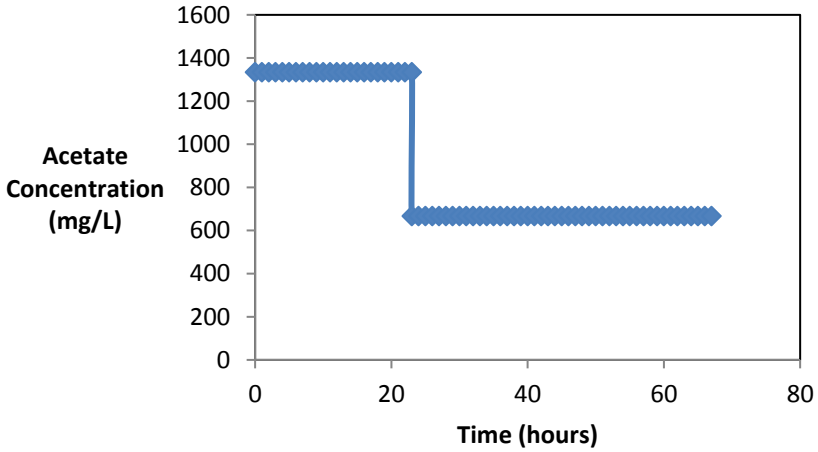

Figure A.1: Influent acetate concentration

Following graphs show the change in internal electrical parameters with the change in influent acetate concentration. Online monitoring of MEC was carried out by analytical solution.

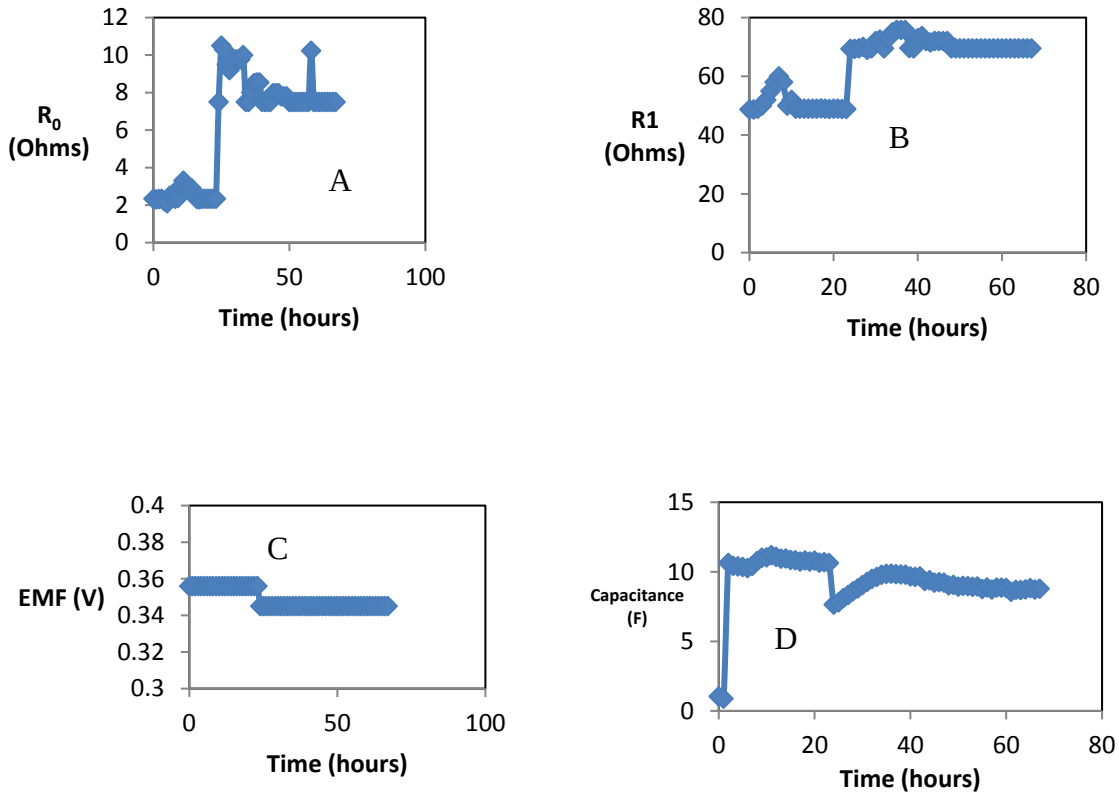

Figure A.2: (A &B) MEC Internal resistance, (C) MEC internal EMF and (D) MEC capacitance.

A.2 MEC performance under intermittent connection of power supply with different influent concentration

MECs were operated with acetate influent feed (1000 mg/L) as the carbon source from day 0 to day 30. From day 30 to day 45, MECs were real wastewater with influent concentration of 2000 mg/L. MEC-B was operated under on/off operation of power supply (duty cycle 95%) and MEC-A was operated with constant duty cycle from day 30 to day 45 as presented in figure A.3.

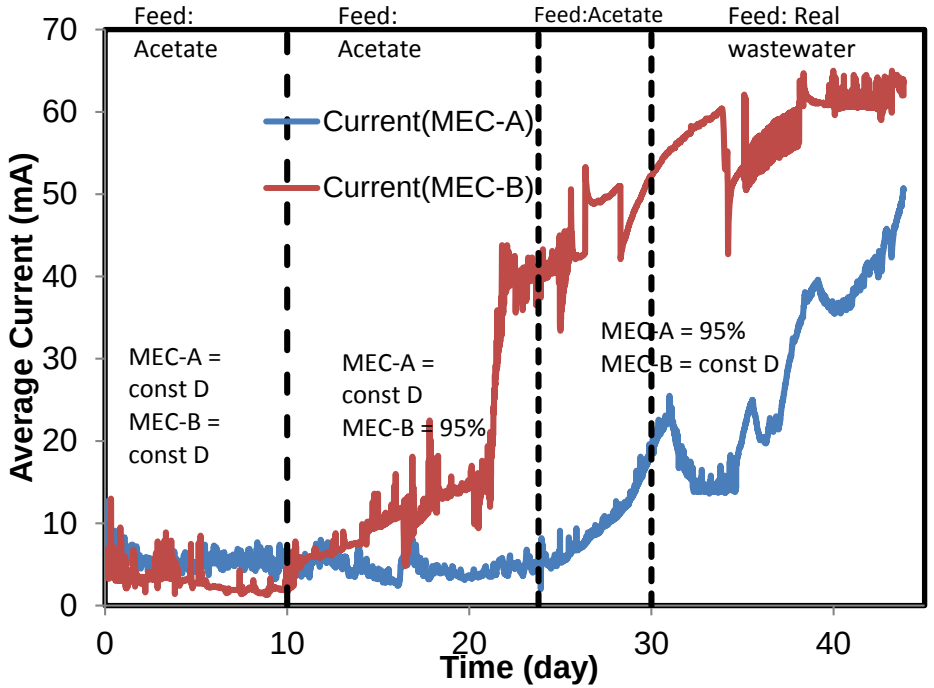

Figure A.3: On/off operation of MEC with different influent carbon source.

A4. Cyclic Voltammetry

Following figure presents cyclic voltammetry result to estimated double layer capacitance in MEC with influent acetate concentration of 500 mg/L.

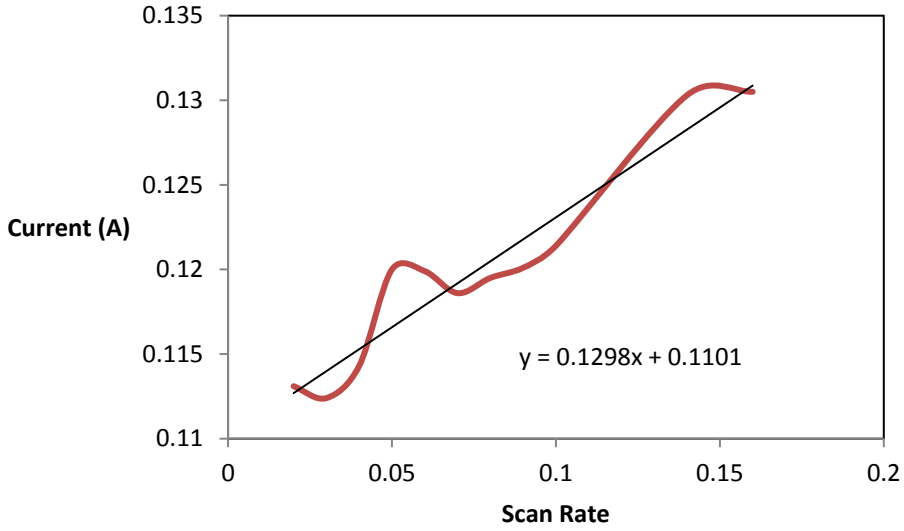

Figure A.4: Cyclic voltammetry

Double layer capacitance was estimated to be 0.13 F.

A.5 Voltage Scan test

Voltage scan tests were performed to estimate total internal resistance in MEC. Following figure presents the results for voltage scan tests performed at influent concentration of 500 mg/L and 1000 mg/L.

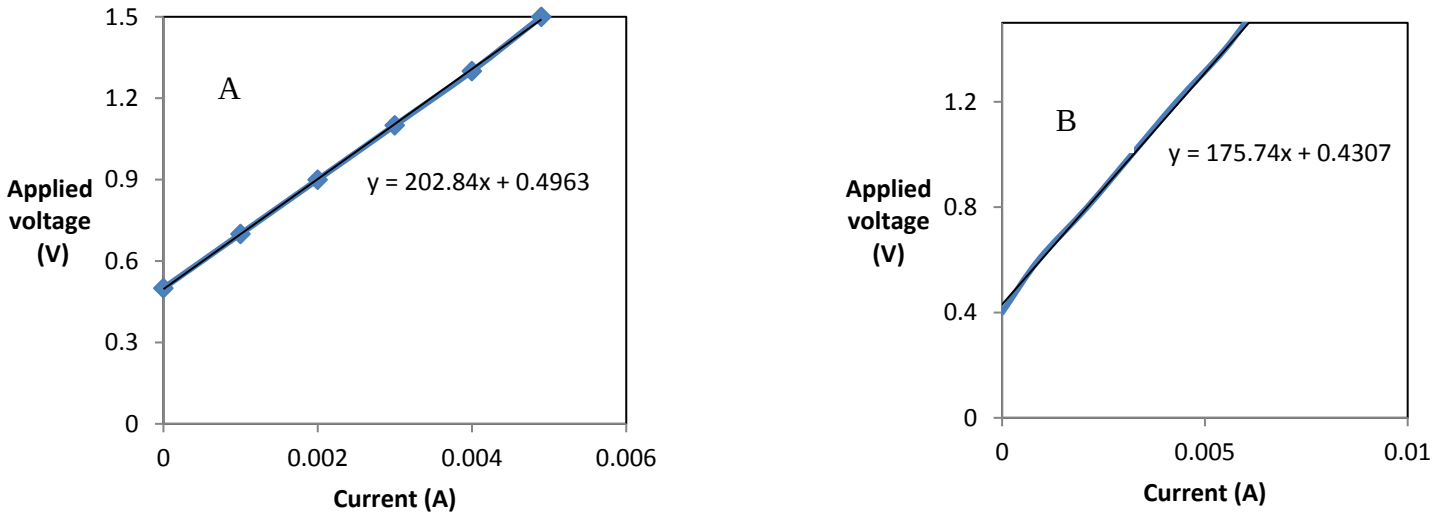

Figure A.5: Voltage Scan test with influent acetate concentration of 500 mg/L (A) and 1000 mg/L (B).

R_{int} ~203 Ω when acetate concentration was 500 mg/L.

R_{int} ~175 Ω when acetate concentration was 1000 mg/L.

A6. Energy discharge experiment

A different approach used to estimate the capacitance of the reactor when they were fed with real waste water. An external resistor (R_{ext}) of 1480 Ω was connected in parallel to the reactor and power supplied was switched off. The internal energy of the reactor was discharged through the external resistance and voltage across the resistance was recorded which is same as the voltage across the MEC (V_{MEC}) as they are connected in parallel.

Ohms law was used to calculate the current.

$$I = \frac{Vmec}{Rext} \quad \text{(D1)}$$

Power was calculated by following Eq 5.

Energy stored by MEC was calculated by integrating Power and time in MATLAB by using in-built *trapz* command.

$$E = \int_0^t Pmec \ dt \quad \text{(D2)}$$

Different cycles were recorded for better estimation of the energy stored in the MEC. Capacitance (C) was calculated by following equation.

$$C = \frac{1}{2} E \ Vmec^2 \quad \text{(D3)}$$

Energy discharge experiment was performed to estimate the capacitance of the reactor. When power supply is switched off, energy across the reactor is drained through an external resistance connected in parallel to the reactor. Integration of power and time gives

energy as shown in figure A.6. By using equation (D3), Capacitance of reactor-B was estimated by this method when the carbon source was real waste water with influent concentration of 7000 mg/L and hydraulic retention time (HRT) was reduced to 12 hours but in reality due to the porosity of activated granular carbon it was 6 hours. Different cycles were recorded for better results. Integration of Power and time gives energy, which is used to calculate the capacitance. Following graph shows decreases in power Vs. time.

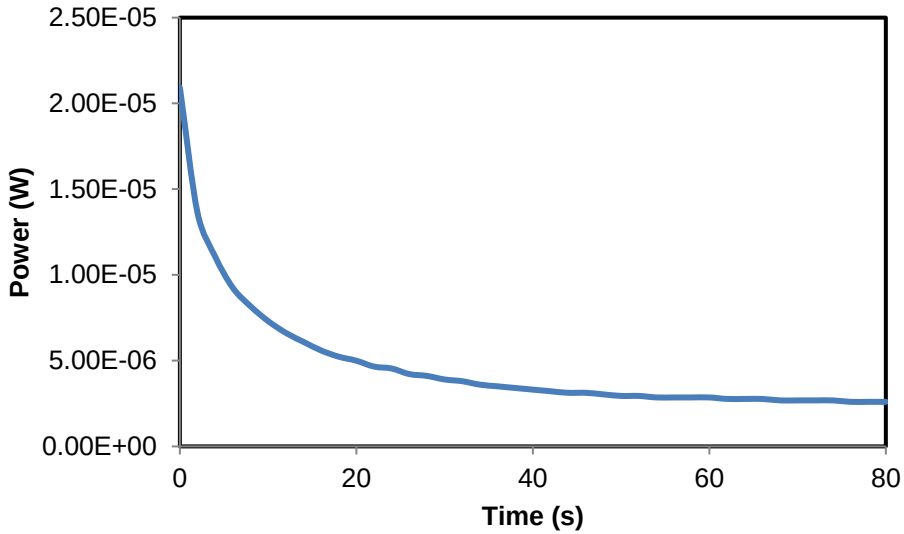

Figure A.6: Energy discharge experiment

Capacitance was estimated to be ~ 0.05 F.